

INFORMATION TO USERS

This manuscript has been reproduced from the microfilm master. UMI films the text directly from the original or copy submitted. Thus, some thesis and dissertation copies are in typewriter face, while others may be from any type of computer printer.

The quality of this reproduction is dependent upon the quality of the copy submitted. Broken or indistinct print, colored or poor quality illustrations and photographs, print bleedthrough, substandard margins, and improper alignment can adversely affect reproduction.

In the unlikely event that the author did not send UMI a complete manuscript and there are missing pages, these will be noted. Also, if unauthorized copyright material had to be removed, a note will indicate the deletion.

Oversize materials (e.g., maps, drawings, charts) are reproduced by sectioning the original, beginning at the upper left-hand corner and continuing from left to right in equal sections with small overlaps. Each original is also photographed in one exposure and is included in reduced form at the back of the book.

Photographs included in the original manuscript have been reproduced xerographically in this copy. Higher quality 6" x 9" black and white photographic prints are available for any photographs or illustrations appearing in this copy for an additional charge. Contact UMI directly to order.

UMI

A Bell & Howell Information Company
300 North Zeeb Road, Ann Arbor MI 48106-1346 USA
313/761-4700 800/521-0600

NOTE TO USERS

This reproduction is the best copy available

UMI

University of Alberta

1-(β -L-Fucosyl)-5-fluorouracil; A Novel Antimetabolite Prodrug

by

Barry P. Williams



A thesis submitted to the Faculty of Graduate Studies and Research in partial
fulfillment of the requirements for the degree of Master of Science

in

Pharmaceutical Sciences (Bionucleonics)

Faculty of Pharmacy and Pharmaceutical Sciences

Edmonton, Alberta

Fall 1998



**National Library
of Canada**

**Acquisitions and
Bibliographic Services**

**395 Wellington Street
Ottawa ON K1A 0N4
Canada**

**Bibliothèque nationale
du Canada**

**Acquisitions et
services bibliographiques**

**395, rue Wellington
Ottawa ON K1A 0N4
Canada**

Your file Votre référence

Our file Notre référence

The author has granted a non-exclusive licence allowing the National Library of Canada to reproduce, loan, distribute or sell copies of this thesis in microform, paper or electronic formats.

The author retains ownership of the copyright in this thesis. Neither the thesis nor substantial extracts from it may be printed or otherwise reproduced without the author's permission.

L'auteur a accordé une licence non exclusive permettant à la Bibliothèque nationale du Canada de reproduire, prêter, distribuer ou vendre des copies de cette thèse sous la forme de microfiche/film, de reproduction sur papier ou sur format électronique.

L'auteur conserve la propriété du droit d'auteur qui protège cette thèse. Ni la thèse ni des extraits substantiels de celle-ci ne doivent être imprimés ou autrement reproduits sans son autorisation.

0-612-34433-9

University of Alberta

Library Release Form

Name of Author: Barry Paul Williams

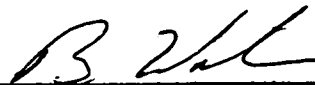
Title of Thesis: 1-(β -L-Fucosyl)-5-fluorouracil; A Novel Antimetabolite Prodrug

Degree: Master of Science

Year This Degree Was Granted: Fall 1998

Permission is hereby granted to the University of Alberta Library to reproduce single copies of this thesis and to lend or sell such copies for private, scholarly, or scientific research purposes only.

The author reserves all other publication and other rights in association with the copyright in the thesis, and except as hereinbefore provided, neither the thesis nor any substantial portion thereof may be printed or otherwise reproduced in any material form whatever without the author's prior written permission.

x  x

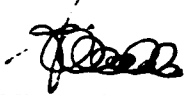
15421 - 55 Street
Edmonton, Alberta
Canada
T5Y 2S4

July 30, 1998

University of Alberta

Faculty of Graduate Studies and Research

The undersigned certify that they have read, and recommend to the Faculty of Graduate Studies and Research for acceptance, a thesis entitled 1-(β -L-Fucosyl)-5-fluoruracil; A Novel Prodrug submitted by Barry Paul Williams in partial fulfillment of the requirements for the degree of Master of Science in Pharmacy and Pharmaceutical Sciences.

• 

Dr. Leonard Wiebe

• 

Dr. Edward Knaus

• 

Dr. A. J. B. McEwan

Date: July 30, 1998

ABSTRACT

5-Fluorouracil (5FU) is an antimetabolite used in cancer chemotherapy, its mechanism of action related to metabolic activation to FdUMP (blocking the enzyme TS) and FUTP. The therapeutic use of 5FU is limited by frequent dosing at toxic levels to achieve therapeutic effectiveness.

1-(β -L-Fucosyl)-5-fluorouracil (FUF), has been developed for the treatment of hepatomas to provide high levels of 5FU in the liver. L-Fucose is known to concentrate in the liver and it is postulated that it retains this property when attached to 5FU as FUF. FUF would act as a prodrug of 5FU by concentrating in the liver.

Two biodistribution studies of FUF in B₆D₂F₁ mice bearing implanted Lewis lung carcinomas were undertaken. The first, using neutron activation analysis (NAA) measurement of fluorine, (dose limited) fluorine concentrations were not within the NAA detection range for fluorine. The second dual labelled study, provided information on the chemical nature of the metabolites, using 6-[³H]-5FU and 1-[¹⁴C]-fucose. Results indicated that nucleoside cleavage occurred, but the limited nature of the study precluded any statistically significant conclusions.

Dedication

To my very special immediate family for their support and encouragement. In particular, to Patti, Ryan and Ashlee for their patience, understanding and helping organize and cover for me to allow me to put in the tremendous time required to complete this project. This dedication is to my wife, Patti-Jane Marie Williams, my children, Ryan and Ashlee, my Mother, Annamary (Meg) Williams and to the memory of and inspiration from, my late Father, Mr. John F. Williams.

All part of a very special Williams Family!

Thank you

Acknowledgements

Many people contributed to assist me in the completion of this project in many different ways. One person, in particular, contributed far beyond any mandatory, professional responsibility, or even personal courtesy or friendship. Without the constant rescues from Dr. Leonard Wiebe, I would have ended up with nothing to show for all of the work put in. Beyond Dr. Wiebe's professional contribution, as a supervisor, his direction and encouragement to bring me up to speed (after falling a DECADE behind) were unwavering and without question. Dr. Wiebe's professional integrity is such that, in the years of infinite patience taken to complete this project, I always felt from Dr. Wiebe that the successful completion of my work was a priority.

Other people who contributed at some point throughout the project were; Gord Haverland, John Mercer, Pete Ford, John Duke, Joyce, Carolyn, V. J. Somayaji, Daria Stepinski and Kirsten Wiebe.

TABLE OF CONTENTS

I) INTRODUCTION	1
II) LITERATURE REVIEW	4
A) APPROACHS TO CANCER CHEMOTHERAPY.....	4
I) HISTORIC	4
II) CURRENT APPROACH TO CANCER CHEMOTHERAPY	5
III) PREVENTION AND ONCOGENES	6
B) IMPORTANT TUMOR CELL CHARACTERISTICS.....	10
I) TUMOR GROWTH.....	11
II) CELL CYCLE	11
III) TUMOR CELL KINETICS	13
C) CLASSIFICATION OF CHEMOTHERAPEUTIC AGENTS.....	14
I) BASED ON CELL GROWTH	14
II) CLINICAL CHEMOTHERAPEUTIC AGENTS	16
D) BIOCHEMISTRY OF PYRIMIDINE NUCLEOSIDES.....	18
I) INTRODUCTION.....	18
II) NATURALLY OCCURRING PYRIMIDINE NUCLEOSIDES.....	22
III) NUCLEOSIDE ANALOGUES AS ANTIMETABOLITES	24
IV) 5-FLUOROURACIL.....	25
V) MECHANISM OF ACTION AS A FUNCTION OF TOXIC METABOLITES	33
a) 5-Fluoro-2'-deoxyuridine-5'-monophosphate (FdUMP)	33
b) 5-Fluorouridine 5'-Triphosphate (FUTP)	36
c) 5-Fluorodeoxyuridine-5'-triphosphate (FdUTP)	37
E) APPROACHES TO INCREASE THERAPEUTIC EFFECTIVENESS OF 5FU	38
I) TOXICITY AND EFFECTIVENESS	38
II) ADJUNCTIVE RADIATION THERAPY	39
III) INFUSIONAL 5FU ADMINISTRATION	40
IV) BIOMODULATION OF 5FU	40
V) PRODRUG DELIVERY TO TARGET 5FU.....	43
a) Considerations For 5FU Prodrug Development	43
b) 5-Fluorouracil Prodrugs.....	44
F) RATIONALE FOR THE DEVELOPMENT OF FUF	46

G) DETECTION AND ANALYSIS OF FLUOROPYRIMIDINES	47
III) EXPERIMENTAL	49
A) SYNTHESIS OF FUCOSYL 5-FLUOROURACIL.....	49
B) ANIMAL STUDIES.....	49
I) ANIMAL AND TUMOR MODEL.....	49
II) ADMINISTRATION OF 5FU & FUF	51
III) BIOLOGICAL SAMPLE COLLECTION	51
C) NAA.....	52
D) DUAL LABEL STUDY USING ³H AND ¹⁴C LABELLED FUF.....	54
IV) RESULTS AND DISCUSSION	56
A) SYNTHESIS OF 1-(β-L-FUCOSYL)-5-FLUOROURACIL (FUF)	56
I) RADIOLABELLED FUF (¹⁴ C LABELLED) FUCOSYL-5-FLUOROURACIL.....	56
II) SYNTHESIS OF [6- ³ H] LABELLED FUF	57
B) NEUTRON ACTIVATION ANALYSIS (NAA) STUDY.....	58
I) STANDARD CURVES.....	58
II) FLUORINE ANALYSIS AFTER DOSING WITH 5FU OR FUF	66
a) Dosage & Detection of 5FU & FUF by NAA Relative to Calibration Results	67
b) NAA Results for 5FU Animal Studies.....	68
c) Biodistribution of FUF in Mice	72
d) Relative Comparison of 5FU and FUF Animal Data.....	76
C) DUAL LABELLED FUF BIODISTRIBUTION STUDY	79
V) SUMMARY & CONCLUSIONS	85
A) ANALYSIS OF FUF BY INAA	85
B) DUAL LABEL FUF RESULTS RELATIVE TO METABOLISM.....	86
VI) BIBLIOGRAPHY	87
A) APPENDIX 1: DATA INTERPRETATION CALCULATIONS	100
I) DUAL LABEL COUNTING TECHNIQUE.....	100
II) OPTIMUM DOSE FOR DETECTION USING NAA.....	101
III) NAA DATA CALCULATIONS.....	102
a) Standard Curve Equation For µg F	102
1) Half Geometry.....	102

2) $\mu\text{g F}$ FULL GEOMETRY	102
b) STANDARD CURVE EQUATION FOR SODIUM INTERFERENCE	103
1) Half Geometry	103
2) FULL GEOMETRY	104
c) NAA SUMMARY OF EQUATIONS DERIVED FROM STANDARD CURVE DATA	104
d) NAA ANIMAL DATA CONVERSION	105
1) Determination of F in animal samples	105
e) NAA CORRECTION FOR TAIL LOSS	106
IV) DUAL LABELLED DATA CONVERSIONS ...	ERROR! BOOKMARK NOT DEFINED.
B) APPENDIX 2. SYNTHESIS	106
I) SYNTHESIS OF FUCOSYL-5-FLUOROURACIL (V.J. SOMAYAJI)	106
1) 1-(2',3',4'-tri-O-acetyl- β -L-fucopyranosyl)-5-fluorouracil (3)	108
2) 1-(β -L-fucopyranosyl)-5-fluorouracil (4)	109
II) RADIOLABELLED FUF SYNTHESIS	109
1) ^{14}C LABELLED FUF	109
2) TRITIUM LABELLED FUF	111
C) APPENDIX 3 DISTRIBUTION RESULTS	112
I) NAA STANDARD DATA RESULTS	112
a) Fluorine	112
b) Sodium	113
II) 5FU ANIMAL DATA RESULTS	114
a) Liver	114
III) FUF NAA ANIMAL DATA RESULTS	119
IV) DUAL LABELLED ANIMAL STUDY RESULTS	122

LIST OF TABLES

Table 1 Cell cycle phase-specific chemotherapeutic agents	15
Table 2 Cell cycle-specific and non-specific chemotherapeutic agents	15
Table 3 LSC of TLC analysis of ¹⁴ C labelled FUF	57
Table 4 LSC of TLC analysis of ³ H labelled FUF to determine radiochemical purity.....	58
Table 5 Fluorine Standard Curve Data.....	112
Table 6 Sodium Standard Curve Data.....	113
Table 7 Liver Results For 5FU.....	114
Table 8 Kidney Results For 5FU.....	114
Table 9 Tumor Results For 5FU.....	115
Table 10 GIT Results For 5FU.....	116
Table 11 Tail Results For 5FU.....	116
Table 12 % Injected Dose Of 5FU Per Organ.....	117
Table 13 5FU data corrected for tail, % injected dose per organ	117
Table 14 FUF NAA Animal Results For Tail.....	119
Table 15 FUF NAA Results For Liver	119
Table 16 NAA FUF GIT Data.....	120
Table 17 FUF NAA Tumor Data, % Injected Dose Vs Time.....	120
Table 18 FUF NAA Kidney Data.....	121
Table 19 FUF NAA Data Corrected For Tail Loss, % Injected Dose Per Organ Vs Time.....	122
Table 20 Dual Label Liver	122
Table 21 Dual Label FUF Tumor	123
Table 22 Dual Label FUF Kidney, % Injected Dose Vs Time.....	123
Table 23 Dual Label Blood	123

LIST OF FIGURES

Figure 1 Proto-oncogene regulation of proliferation. G = G or N regulatory proteins; R = receptor, p-ser = phosphoserine; p-tyr = phosphotyrosine; Ptdl = phosphatidylinositol; PKC = protein kinase C.	7
Figure 2 Cell Cycle Diagram.	12
Figure 3 General NA acid structure showing the phosphate-ester linkage with the base attached to the sugar back bone(adapted from fig.6-7, p. 77, Frobisher, 1974).	19
Figure 4 Chemical structure of the nucleic acid sugars β -D-ribose and β -D-2-deoxyribose (adapted from p.74, Frobisher, 1974).	20
Figure 5 The general structures for the two bases found in nature (Frobisher, fig.6-6, 1974)	20
Figure 6 Pyrimidine bases thymine and uracil (Frobisher, fig. 6-6, 1974).	20
Figure 7 Cytosine and 5-methylcytosine pyrimidine bases (Frobisher, fig. 6-6, 1974).	21
Figure 8 Purine bases adenine and guanine (Frobisher, fig.6-6, 1974).	21
Figure 9 Anabolic interconversions of naturally occurring pyrimidine nucleosides and nucleotides (adapted from Weckbecker, 1991 and Mercer, 1985).	22
Figure 10 Anabolic conversions of 5FU (Adapted from Weckbecker, 1991, Fig.2, p.370 and Mercer, 1985).	27
Figure 11 Fate of F-nucleotide triphosphates.	30
Figure 12 Catabolic pathways of 5FU (adapted from Malet-Martino, 1988; Malet-Martino, 1986; Weckbecker, 1991 and Mercer, 1985).	32
Figure 13 Conversion of deoxypyrimidine nucleotide monophosphate (FdUMP).	34
Figure 14 Activation of tegafur to 5-fluorouracil via liver microsomes.	44
Figure 15 Possible activation routes for doxifluridine.	45
Figure 16 Method of sample vial arrangement for immobilizing samples for NAA.	53
Figure 17 F standard curve, a linear regression plot of mean counts at 1634 keV with error bars representing standard deviation from the mean vs μg F for Half Geometry samples (— represents the 95% confidence limits). Derived from this plot, Coefficients are: $b[0] = 28.23$, $b[1] = 4.64$ and $r^2 = 0.93$.	59
Figure 18 F standard curve, a linear regression plot of counts at 1634 keV vs μg F for Full Geometry samples ($r^2 = 0.94$ — represents the 95% confidence limits). Derived from this plot, Coefficients: $b[0] = 36.20$, $b[1] = 5.68$ and $r^2 = 0.94$.	60
Figure 19 Na standard curve, a linear regression plot of counts at 1634 keV vs μg Na for Half Geometry (— represents 95% confidence limits). Derived from this plot, Coefficients: $b[0] = 23.83$, $b[1] = 0.02$, $r^2 = 0.77$.	61
Figure 20 Na standard curve, a linear regression plot of counts at 1368 keV vs μg Na for Half Geometry (— represents 95% confidence limits). Derived from this plot, Coefficients: $b[0] = 60.15$, $b[1] = 0.111$, $r^2 = 0.989$.	62
Figure 21 Na standard curve, a linear regression plot of counts at 1634 keV vs μg Na for Full Geometry (— represents 95% confidence limits). Derived from this plot, Coefficients: $b[0] = 6.384$, $b[1] = 0.033$, $r^2 = 0.95$.	63
Figure 22 Na standard curve, a linear regression plot of counts at 1368 keV vs μg Na for Full Geometry (— represents 95% confidence limits). Derived from this plot, Coefficients: $b[0] = 58.26$, $b[1] = 0.096$, $r^2 = 0.9904$.	64
Figure 23 Na standard curve half geometry linear regression plot relating the activity detected at the two γ energies for incremental standards of Na via counts 1634 keV vs 1368keV. (—	

represents 95% confidence limits). Derived from this plot, Coefficients: $b[0] = 9.065$, $b[1] = 0.2157$, $r^2 = 0.80918$.	65
Figure 24 Na standard curve full geometry linear regression plot relating the activity detected at the two γ energies for incremental standards of Na via counts 1634 keV vs 1368keV. (— represents 95% confidence limits). Derived from this plot, Coefficients:	66
Figure 25 5FU distribution to the liver expressed as mean of % injected dose (—solid line, vertical bars representing the standard deviation from the mean) vs time (minutes).	69
Figure 26 5FU distribution to the liver (black line with standard deviation (stdv) positive) and kidney (dashed line with stdv negative) tissue expressed as the mean of % injected dose vs time	70
Figure 27 Distribution of 5FU to GIT over time expressed as mean (solid line) of % injected dose (vertical bars representing stdv) vs. time.	71
Figure 28 Tumor distribution for 5FU expressed as mean (vertical bar) of % injected dose (with vertical lines representing stdv) vs time.	72
Figure 29 Distribution of FUF to liver expressed as mean of % injected dose (vertical bar with vertical line representing stdv) vs time.	73
Figure 30 Distribution of FUF to GIT expressed as mean of % injected dose (vertical bars with vertical lines representing stdv) vs. time.	74
Figure 31 FUF distribution to kidney expressed as mean of % injected dose (vertical bars with vertical lines representing stdv) vs time.	74
Figure 32 FUF distribution to the tumor expressed as mean % injected dose (vertical bars with vertical lines representing stdv) vs time.	75
Figure 33 Comparison of 5FU (dashed line with open circle and negative vertical line representing stdv) and FUF (solid line with filled circle and positive vertical line representing stdv) distribution to the liver using the mean of the % injected dose vs time.	77
Figure 34 Comparison of 5FU (dashed line with open circle and negative vertical line representing stdv) and FUF (solid line with filled circle and positive vertical line representing stdv) distribution to the GIT using the mean of the % injected dose vs time.	77
Figure 35 Comparison of 5FU (dashed line with open circle and negative vertical line representing stdv) and FUF (solid line with filled circle and positive vertical line representing stdv) distribution to the kidney using the mean of the % injected dose vs time.	78
Figure 36 Comparison of 5FU (dashed line with open circle and negative vertical line representing stdv) and FUF (solid line with filled circle and positive vertical line representing stdv) distribution to the tumor using the mean of the % injected dose vs time.	79
Figure 37 Distribution of labelled FUF to the liver (dashed line with open circle represents 5FU with negative vertical line representing stdv and solid line with filled circles representing fucose with positive vertical line representing stdv) expressed as the mean and stdv of the % injected dose vs time.	81
Figure 38 Distribution of labelled FUF to the tumor (dashed line with open circle represents 5FU with negative vertical line representing stdv and solid line with filled circles representing fucose with positive vertical line representing stdv) expressed as the mean and stdv of the % injected dose vs time.	82
Figure 39 Distribution of labelled FUF to the kidney (dashed line with open circle represents 5FU with negative vertical line representing stdv and solid line with filled circles representing fucose with positive vertical line representing stdv) expressed as the mean and stdv of the % injected dose vs time.	83

Figure 40 Distribution of labelled FUF to the blood (dashed line with open circle represents 5FU (^3H) with negative vertical line representing stdv and solid line with filled circles representing fucose (^{14}C) with positive vertical line representing stdv) expressed as the mean and stdv of the % injected dose vs time.....	84
Figure 41 Unquenched pulse height spectra of ^3H and ^{14}C indicating possible window settings for dual label counting.....	100
Figure 42 Synthesis of fucosyl-5-fluorouracil.....	108
Figure 43 Synthesis of radiolabelled L-[1- ^{14}C]fucosyl-5-fluorouracil.....	110
Figure 44 Synthesis of tritium labelled FUF.....	111
Figure 45 5-FU animal results expressed as % injected dose Vs time.....	118

LIST OF ABBREVIATIONS

- 5FU5-fluorouracil
- ACTHadrenocorticotrophic hormone
- ATPadenosine triphosphate
- CDP cytidine diphosphate
- CMP cytidine monophosphate
- c-onc oncogene
- CTP cytidine triphosphate
- dCDP deoxycytidine diphosphate
- dCMPdeoxycytidine monophosphate
- dCTPdeoxycytidine triphosphate
- 5'-dFUdR 5-fluoro-5'-deoxyuridine
- DHPS dihydropyrimidinase
- DNA..... deoxyribonucleic acid
- DTD..... deoxyuridine triphosphate diphosphohydrolase
- dUDP deoxyuridine diphosphate
- dUMP deoxyuridine monophosphate
- dUrddeoxyuridine
- dUTP deoxyuridine triphosphate
- F-DNA DNA containing F substituted NA's
- FdUDP 5-fluoro-2'-deoxyuridine diphosphate
- FdUMP5-fluoro-2'-deoxyuridine-5'-monophosphate
- FdUrd 5-fluoro-2'-deoxyuridine
- FdUTP 5-fluorodeoxyuridine triphosphate
- F-RNA RNA containing F substituted NA's
- FUDP5-fluorouridine diphosphate
- 5'-FUdR 5-fluoro-5'-deoxyuridine
- FUF 1-(β -L-fucosyl)-5-fluorouracil
- FUMP 5-fluorouridine monophosphate
- FUPA..... α -fluoro- β -ureidopropanoic acid
- FUR..... 5-fluorouridine

- FUrGluc..... 5-fluorouracil glucuronide
- FUTP..... 5-fluorouridine triphosphate
- g..... gram
- G₀..... resting state
- G₁..... phase of post mitotic growth period (or "G1" as above)
- G₂..... cell cycle premitotic phase of cell growth (or "G2" as above)
- GI..... gastro-intestinal tract
- HPLC..... high performance liquid chromatography
- IFN- α alpha interferon
- IUdR..... Idoxuridine(1-iodo-2'-deoxyuridine)
- keV..... kilo-electron volts
- LLC..... Lewis lung carcinoma
- M..... mitosis phase of cell cycle
- mg..... milligram
- mL..... millilitre
- MS..... mass spectrometry
- NA..... nucleic acid
- NAA..... neutron activation analysis
- NADP..... nicotinamide-adenine dinucleotide phosphate
- N-Carboxy-FBAL..... N-Carboxy- β -fluoro- β -alanine
- NMR..... nuclear magnetic resonance
- PALA..... N-(phosphonacetyl)-L-Asparate
- PNMK..... pyrimidine nucleoside monophosphate kinase
- PRPP..... 5-phosphoribosyl-1-pyrophosphate
- RNA..... ribonucleic acid
- RR..... ribonucleotide reductase
- stdv..... standard deviation
- S..... synthesis phase of cell growth
- TK..... thymidine kinase
- TLC..... thin layer chromatography
- TMP..... thymidine monophosphate
- TP..... thymidine phosphorylase

- TS..... thymidylase
- μCi micro Curries
- U-DNA-Guracil-DNA-glycolase
- UDP.....uridine diphosphate
- μg micrograms
- UKuridine kinase
- UMPuridine monophosphate
- Ur uracil
- Urd uridine
- UrP uridine phosphorylase
- UTPuridine triphosphate

I) INTRODUCTION

1-(β -L-FUCOSYL)-5-FLUOROURACIL (FUF) is studied here as a novel prodrug of the antitumor agent 5-fluorouracil (5FU). 5FU is an antimetabolite with known antitumor activity, used clinically in cancer chemotherapy. 5FU's mechanism of action is related to its metabolic activation. Metabolic conversion of 5FU results in activation to the nucleotides 5-fluoro-2'-deoxyuridine-5'-monophosphate (FdUMP) and 5-fluorouridine-5'-triphosphate (FUTP). These nucleotides of 5FU are active in DNA and RNA metabolism.

FdUMP exerts its antimetabolic effect through its ability to act as a substrate for a vital enzyme. As a metabolic analog for deoxyuridylate (deoxyuridine monophosphate; dUMP), FdUMP acts as a competitive inhibitor of thymidylase (TS). Under normal circumstances, TS converts dUMP to thymidylate (TMP). This conversion is the ultimate source of thymidine (for reasons explained in detail in the literature review), making this a vitally strategic conversion. TS, being the sole enzyme responsible for the metabolic conversion of the ultimate source of thymidine, is of key significance. As an analog of dUMP, FdUMP acts as a competitive inhibitor of TS. By becoming metabolically involved in the TS mediated pathway (instead of dUMP), FdUMP blocks the activity of TS. The ultimate result of blocking the TS mediated pathway is to starve the cells of TMP. Thymidine is a vital building block in nucleic acid synthesis, being essential for DNA synthesis.

Another mechanism of action of 5FU is via metabolic conversion of the 5-fluorouridylate. After incorporation of 5FU as FUTP into RNA, the mechanism is exerted by affecting RNA synthesis and causing point mutations which interfere with protein synthesis.

The problems encountered with the therapeutic use of 5FU are related to its collateral toxicity to healthy cells, its half life or duration of action and its general distribution or lack of targeting or absence of tumor specificity. These factors are all interrelated in a way that tends to compound the toxic side effects of 5FU. The toxicity of 5FU increases in cells which reproduce rapidly, such as tumor cells but not excluding naturally rapidly growing tissues such as epithelial cells and bone marrow.

Since 5FU is rapidly cleared from the body, therapeutic levels of the drug at the site of the carcinoma are transient. High, frequent doses are therefore required to maintain therapeutic effectiveness of 5FU at the site of action and this results in a low margin of safety. This all combines to produce significantly toxic side effects at minimal antitumor activity.

1-(β -L-Fucosyl)-5-fluorouracil (FUF), has been developed to provide high 5FU concentrations in the liver, specifically, for the treatment of hepatomas. By concentrating (to a great enough degree) in a hepatoma containing liver, the antimetabolic containing drug would cause minimal toxic side effects (low extra-hepatic levels), while providing chemotherapy for the purpose of destroying the hepatoma.

The sugar L-Fucose is known to concentrate in the liver via hepatic immunorecognition sites. It is postulated that, after conversion to a nucleoside, it may retain this property. Specifically, when attached to the antimetabolite (uracil analog), 5FU, the resulting 5FU-Fucose nucleoside retains the properties allowing immunorecognition of the fucose moiety by hepatocytes to act as a mechanism of prodrug concentration. The purpose of concentrating FUF in the liver, in addition to delivering 5FU to the hepatoma for destruction, is to reduce the whole-body dose of

5FU. Dosage reduction would decrease the toxicity to healthy tissues without decreasing effective concentration in the hepatoma.

Once at the site of action, the liver, this nucleoside (FUF) would act as a prodrug by then releasing 5FU to exert its antimetabolic effect. Therefore the subsequent catabolism of the nucleoside bond is necessary to activate FUF to 5FU. Ideally, this FUF catabolism would also serve to prolong the effects of 5FU to the hepatoma while maintaining low whole body dose and therefore minimizing toxic side effects.

In order for the hypothesis to be true, certain criteria for the biodistribution of FUF must first be true. In designing the studies, the important factors pertaining to the postulated FUF properties are that FUF;

- stays intact until reaching the liver in order to act as a prodrug
- is concentrated in the liver via the retained fucose immunorecognition
- is cleaved in the liver to its corresponding 5FU and fucose.

II) LITERATURE REVIEW

A) APPROACHS TO CANCER CHEMOTHERAPY

i) HISTORIC

The advent of the modern era of cancer chemotherapy occurred just before the Second World War. Reviews by Elkerbout (1971) and Livingston and Carter (1970) provide a chronology of the discovery of early chemotherapeutic agents, the subsequent development of additional agents and eventual proliferation leading to various classes of agents. The era of the 5-fluoropyrimidine antimetabolites started in the late 1950s (Heidelberger, 1957; Heidelberger, 1965). The following chronological summary is a comparison of earlier chemotherapy (Elkerbout, 1971; Livingston, 1970) with a more recent overview (Skeel, 1991; Weckbecker, 1991).

It was discovered that a group of chemical compounds derived from a chemical weapon, mustard gas, had a strongly cytotoxic effect (Elkerbout, 1971). Among the cells highly sensitive to these compounds were blood cells, especially the leukocytes, lymphatic tissue, bone marrow and the mucous membrane of the gastro-intestinal tract (GIT). Favorable results were obtained with nitrogen mustard on patients with Hodgkin's disease and in 1947 S. Farber (Livingston and Carter, 1970), reported the use of chemo-therapeutics in the treatment of leukemia's in children. These agents were antagonists of folic acid, an essential metabolite for the development of red and white blood cells.

These agents were followed by the development of mercaptopurine and 5-fluorouracil (5FU) in the 1950's. Other alkylating substances such as thio-tepa and busulfan followed. Agents found to be effective against acute leukemia, lymphosarcoma and Hodgkin's disease were adrenocorticotrophic hormone (ACTH) and corticosteroids. Inhibitors of the metaphase of cell mitosis were developed, including

the derivatives of vinca-rosea. Antibiotics, such as dactinomycin (Elkerbout 1971), could also be used as cytostatics.

The conviction grew, in the 1960's, that long remissions, if not a cure, could be effected with the use of chemotherapeutic agents. This was true especially for rapidly growing malignant processes. In particular, progress was noted with acute lymphatic leukemia, Hodgkin's disease, Burkitt's tumor, choriocarcinoma, Wilm's tumor and testicular carcinoma (Elkerbout, 1971).

Early efforts did not address the fundamental cause of abnormal cell growth or the possibility of many unique triggers. Due to cancer cells having in common an unbridled infiltrative growth of cells capable of metastasis, the ability of the cancer chemotherapeutic agents to inhibit rapid growth appears to account for both the effectiveness and side effects of many of the early agents. They influence cell metabolism most by disturbing the biosynthesis of nucleic acids (Elkerbout, 1971). Their effect on the ordinary dividing cell and the cancer cell, in principal, would be the same. Any selectivity would be chiefly based on differences in cell activity with respect to cell division. This would also apply to undesirable side effects. More actively dividing normal tissue, such as, bone marrow, lymph, gonad, fetus, gastrointestinal epithelial cells, etc, are the most profoundly effected by these antimetabolites. Conversely, their effect on resting cells, malignant or normal, is negligible

ii) CURRENT APPROACH TO CANCER CHEMOTHERAPY

Today the objective of treating cancer with chemotherapeutic agents remains as primarily to prevent cancer cells from multiplying, invading, metastasizing and ultimately killing the host (Skeel, 1991). The agents still in use for this purpose exert their effect primarily on cell multiplication. Since cell multiplication is a characteristic of

normal cells, this activity leads directly to toxic side effects, in particular, to cells with rapid growth rates.

Recent progressive thinking is to develop chemotherapeutic agents with marked growth inhibitory or controlling effect on the cancer cell, with minimal toxic effect to the host. By designing an agent, based on knowledge of the molecular biology of cancer and the host, to capitalize on the differences. This differs from past reality, where the effectiveness of an agent was discovered by treating a subject, after which an attempt was made to discover why the agent works. To date, the mechanisms governing the effectiveness of an agent, and the differences between the normal and cancerous cells, are poorly understood (Skeel, 1991).

iii) PREVENTION AND ONCOGENES

A brief overview of the concepts of the causes of cancer at the cellular level is relevant as a starting point for developing an anticancer agent. Results to explain the nature of the changes in normal cells which lead to uncontrolled growth and spread of cancer cells have been achieved through gene technology (Freeman, 1989) with a strong case for the *oncogene theory*. According to the oncogene theory, a limited number of normal genes involved in cell division or differentiation, contribute to the neoplastic phenotype when altered in their function or expression (Freeman, 1989). The four main types of genetic damage that contribute to the changes in normal cells leading to uncontrolled cell division and later, malignancy, are;

- point mutations of DNA,
- deletions of DNA,
- amplifications of DNA and

- large rearrangements of DNA (Freeman, 1989).

The *proto-oncogene*, a normal cellular gene, becomes an *oncogene (c-onc)*, a transforming cellular gene, after some form of genetic alteration in the DNA (Freeman, 1989). Genetic damage to several classes of proto-oncogenes which are involved in the process of signal transduction for cell division or differentiation result in *C-oncs*

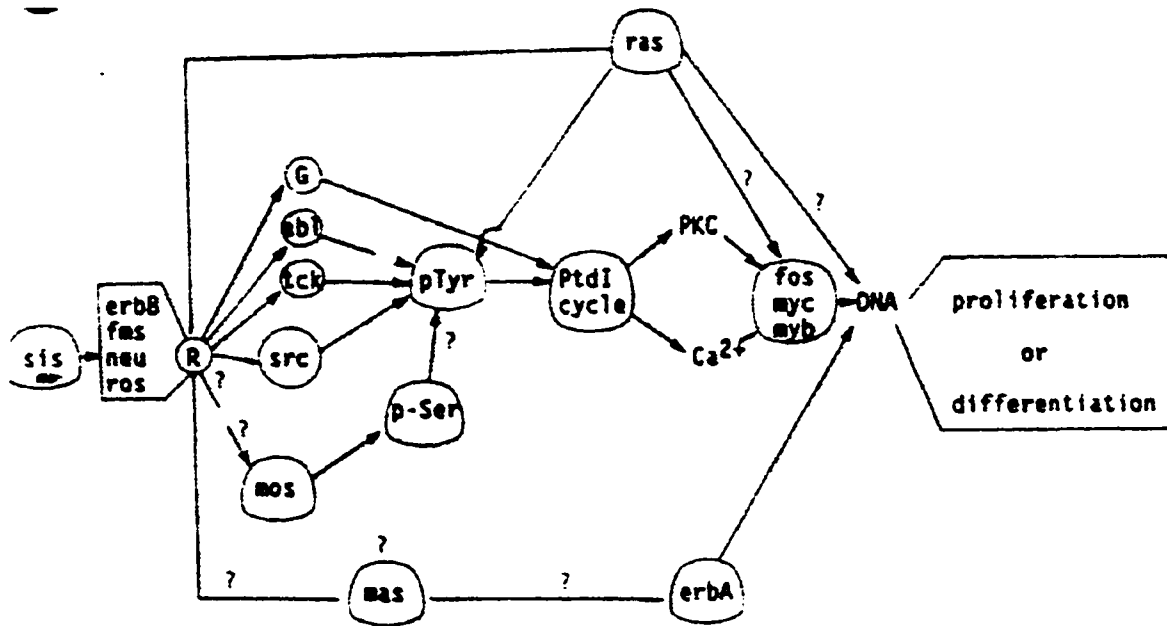


Figure 1 Proto-oncogene regulation of proliferation. G = G or N regulatory proteins; R = receptor; p-ser = phosphoserine; p-tyr = phosphotyrosine; PtdI = phosphatidylinositol; PKC = protein kinase C. (Copied from Figure 1, Freeman, et. al, C., "An Overview of Tumor Biology.", *Cancer Invest.*, 7 247 (1989))

Viral forms of oncogenes are known where mammalian viruses have acquired aberrant forms of proto-oncogenes because of their ability to insert into the host cell DNA. Upon excision they take all or parts of the proto-oncogenes with them (Freeman, 1989). Over time this repeated process has lead to the evolution of another form of oncogene, the *v-onc*. Although v-oncs are homologous with c-oncs and proto-oncogenes, they contain specific differences in DNA sequences due to evolution via

separate genetic pathways. Therefore, v-oncs and c-oncs may transform cells by different biochemical mechanisms (Duesberg, 1987).

There are six major classes of growth transforming *c-oncs* (Freeman, 1989)

See figure 1;

- i) *c-sis* act as protein growth factors
- ii) *c-erbA*, *c-fms* & *c-neu* act as receptors for growth factors and exhibit cytoplasmic tyrosine kinase activity
- iii) *c-abl*, *c-src* & *c-tck* exhibit tyrosine kinase activity associated with the inner side of the plasma membrane
- iv) *c-H-ras* , *c-N-ras* and *c-K-ras* exhibit guanosine triphosphate and diphosphate (GTP/GDP) binding and GTPase activities associated with the inner side of the plasma membrane (*c-H-ras* , *c-N-ras* and *c-K-ras*)
- v) *c-fos*, *c-myb* and *c-myc* have DNA binding activity and are located in the nucleus
- vi) *c-mos* and *c-raf* located in the cytoplasm and exhibit serine kinase activity

These ($\cong 40$) proto-oncogenes and oncogenes proteins appear to act by one of three biochemical mechanisms (Bishop, 1987). They are;

- i) protein phosphorylation
- ii) metabolic regulation via GTP similar to G or N proteins and
- iii) participation in the replication or transcription of DNA (Freeman et al, 1989)

The key to the action of transforming oncogene proteins, leading to abnormal cell proliferation, lies in the process of signal transduction. To illustrate the importance

of the signal transduction process consider the action of transforming oncogene proteins. Physiological changes are induced and occur within seconds of the binding of ligands to their cell surface receptors. This is followed within minutes by changes in gene expression and changes in DNA synthesis within hours (Marshall, 1987). Understanding how oncogene products biochemically activate the signal transduction process will provide the information that will help develop the most effective ways of intervening in the process to inhibit or prevent cancer growth and progression (Freeman, 1989). .

A key to drug delivery targeted to a particular carcinoma could involve employing the signal transduction process as a tool. That is, to use a prodrug to target an anticancer drug that is specific to a c-onc receptor. In doing so the drug would be preferentially taken into the transformed cell to exert its toxicity. For example, a prodrug designed to possess a protein growth factor recognized by the "ii)" class of c-onc receptor, could serve several purposes. First, being a substrate for the protein growth factor receptor, would allow for a targeting mechanism. The receptors of the protein growth factors, *c-erbA*, *c-fms* & *c-neu*, would act to concentrate the prodrug in the genetically damaged cell by substrate recognition. Secondly, with a prodrug designed as relatively stable tyrosine conjugate, a mechanism for activation would also exist. Since the c-oncs, *c-erbA*, *c-fms* & *c-neu*, also exhibit cytoplasmic tyrosine activity (Freeman, 1989), the prodrug would be activated at the site of action via tyrosine cleavage, releasing the drug to exert its cytotoxicity. This illustrates an example of how the changes to a cell by transforming oncogenes that can lead to abnormal cell proliferation and malignancy, can be used as a tool to target, deliver and activate an anti metabolite prodrug.

B) IMPORTANT TUMOR CELL CHARACTERISTICS

Most chemotherapeutic agents act by causing some type of inhibition of cell multiplication. How effective an agent is can depend on the level at which the inhibition of cell multiplication takes place and the characteristics of tumor growth, both of which can be directly related to the cell cycle. A generally accepted method of classifying chemotherapeutic agents is based on the cell cycle specificity of an agent (e.g. cell cycle-nonspecific), its chemical source (e.g. natural product, alkylating agent) and general chemical type (e.g. nitrogen mustard, metal salt, etc). The following is a summary based on information taken from Skeel (Skeel, 1991).

Inhibition of cell multiplication takes place at several levels within the cell. The mechanisms responsible act at the following levels of cell development or function:

1. Macromolecular synthesis and function.
2. Cytoplasmic organization.
3. Cell membrane synthesis function.

With the exception of some biologic response modifiers and immunotherapeutic agents, most agents have their primary effect on either macromolecular synthesis or function, by interfering with either the synthesis or function of DNA, ribonucleic acid (RNA) or related proteins of the neoplastic cells cause a proportion of the cells to die. Ideally, a predictable number of repeated doses should kill all of the cancer cells

This, however, is rarely the case. Since the mechanisms involved are related to cell growth, variables related to tumor cell growth and kinetics must also be considered. Tumor growth, cell cycle, cell phase and cell cycle specificity are parameters that can be used to develop a workable classification system for chemotherapeutic agents.

i) TUMOR GROWTH

Since the antitumor effects of the agents of interest are dependant on metabolic activation, the kinetics of tumor growth are directly interrelated with any antitumor effect. The relative tumor cell kinetic factors are:

- Cell cycle time, the average time for a cell that has just completed mitosis to grow and again divide and pass through mitosis.
- Growth fraction are cells undergoing division and are sensitive to drugs whose major effect is exerted on actively dividing cells.
- Total cell population, determined at some arbitrary time, provides an index of how advanced the cancer is. This number is clinically significant as the cell growth dynamics may change as the tumor size increases. As the dynamics change, factors which affect treatment approach and effectiveness also change. The number of resistant cells increases with increased total cells. The larger the tumor becomes, the greater the compromise of blood supply and drug delivery to the tumor cells resulting in reduced sensitivity to both chemotherapy and radiotherapy.
- Intrinsic cell death rate, rate of death of tumor cells relative to growth of new cells. This rate increases as the tumor grows due to a greater compromise of blood supply causing an increased cell death rate. As a solid tumor gets larger, the intrinsic cell death rate increases, slowing the growth of solid tumors.

ii) CELL CYCLE

Normal cells and cancer cells qualitatively have the same cell cycle. Growth begins during a post-mitotic period, called phase G_1 . During this phase, enzymes necessary for DNA production, other proteins and RNA are produced.

grouped according to whether they depend on the cell being in cycle (i.e. not in G_0), (cell cycle specific) and the cell being in a specific phase of the cycle (Phase Specific).

iii) TUMOR CELL KINETICS

As a tumor grows changes occur in the growth rate due to the size and kinetics of the tumor itself and due to the tumor burden eventually effecting the normal functioning of the host. These changes affect the strategies of chemotherapy from the standpoint of the following factors;

- Stages of Tumor Growth

The stages of tumor growth have been determined and recognized as the following (Skeel, 1991) phases of growth.

The *lag phase* occurs immediately after inoculation. Little growth occurs as the tumor cells become accustomed to the new environment.

The *log phase* follows, as a period of rapid growth with repeated doubling of the cell numbers. The growth fraction approaches 100; with a low cell death rate, resulting in doubling the cell number over one cell cycle.

The *plateau phase* follows the log phase as the tumor becomes macroscopic with the increased cell numbers. The cell death rate increases, causing a decreased growth fraction and prolonging the doubling time of the cell population. By the time most human cancers are clinically measurable they are usually in the plateau phase. The smaller growth fraction is due to increased intrinsic cell death rate due to decreased nutrients and growth promotion factors, increased inhibitory metabolites and inhibition of growth by other cell-cell interactions.

- Growth Rate and the Effectiveness of Chemotherapy

Antimetabolites are effective during the S-phase or the period of logarithmic growth. Tumor discovery in the plateau phase precludes the opportunity to treat the

tumor with antimetabolites during the S-phase. The effectiveness of the antimetabolite is limited to the fraction of the cell population in the susceptible S-phase. Concurrent use of some other means to reduce the cell population would increase the antimetabolites effectiveness by causing a shift in the relative fraction of cells in each phase. By reducing the cell population, a higher fraction of the remaining cells would be recruited into logarithmic growth, making them susceptible to S-phase-specific antimetabolites. Possible means for reducing the cell population may be surgery or radiotherapy. This type of reasoning would support the argument for combined therapy of chemotherapy plus surgery or radiotherapy. Breast cancer, colon cancer, Wilm's tumor, ovarian cancer and small-cell anaplastic cell carcinoma of the lung are examples of successful combined therapy (Skeel, 1991).

C) CLASSIFICATION OF CHEMOTHERAPEUTIC AGENTS

i) BASED ON CELL GROWTH

Chemotherapeutics can be classified based primarily on the phase in which they exert their greatest activity, secondarily on their general chemical class (natural product, hormone, antimetabolite, etc) and finally on the type (enzyme, corticosteroid, pyrimidine analogue, etc) of agent. Tables 1 and 2 show the classification of some of the commonly used agents.

Table 1 Cell cycle phase-specific chemotherapeutic agents (adapted from table 1.1, p.7, Skeel, 1991)

Phase of greatest activity	Class	Type	Agent
G1	Natural Product	Enzyme	Asparaginase
	Hormone	Corticosteroid	Prednisone
S Phase DNA Synthesis	Antimetabolite	Pyrimidine Analog	Cytarabine,
	Antimetabolite	Folic Acid Analog	5-fluorouracil
	Antimetabolite	Purine analog	Methotrexate
	Miscellaneous	Substituted urea	Thioguanine Hydroxyurea
G2	Natural product	Antibiotic	Bleomycin
	Natural product	Topoisomerase inhibitor	Etoposide
	Natural product	Microtubule polymerization & stabilization	Taxol
M Phase Mitosis	Natural product	Mitotic Inhibitor	Vinblastine, vincristine, vindesine

Table 2 Cell cycle-specific and cell cycle non-specific chemotherapeutic agents (adapted from table 1.2, p.8 Skeel, 1991)

Class	Type	Agent
Cell cycle-specific		
Alkylating agent	Nitrogen mustard	Chlorambucil, cyclophosphamide, melphalan
	Alkyl sulfonate	Busulfan
	Triazine	Dacarbazine
	Metal salt	Cisplatin, carboplatin
Natural product	Antibiotic	Dactinomycin, daunorubicin, doxorubicin, idarubicin
Cell cycle-non-specific		
Alkylating agent	Nitrogen mustard	Mechlorethamine
	Nitrosoureas	Carmustine, lomustine, semustine

The initial major drug classification groupings are:

- Cell Cycle Phase specific drugs are most active against cells that are in a specific phase of the cell cycle. These include pyrimidine, purine and folic acid analogues, corticosteroids, mitotic inhibitors (see table 1).

This phase specificity has important implications as related to single exposure cell kill and the effect of prolonged exposure on cell kill. With phase specific drugs the proportion of cells killed with a single exposure is limited to only those cells in the sensitive phase. Prolonging exposure will increase the cell kill over the initial kill, as the cells that were not in the sensitive phase initially, will enter the sensitive phase and now be susceptible. This may be either a prolonged exposure (Harris, 1990) or a repeated dose at a time when initially insensitive cells are known to be in the sensitive phase (Hrushesky, 1990). This is recruitment, which is defined by the following. *Recruitment* takes place when the proportion of cells in the sensitive phase is increased by some means.

- Cell cycle-specific drugs (phase non-specific) are effective while cells are actively in cycle but not dependant on the cell being in a particular phase. These agents (listed in table 2), include drugs such as alkylating agents and some antitumor antibiotics.
- Cell cycle-nonspecific drugs include agents which are effective whether the cancer cells are in cycle or not. They include methchloroethamine (nitrogen mustard) and the nitrosoureas.

ii) CLINICAL CHEMOTHERAPEUTIC AGENTS

Since there are no known specific biochemical pathways essential for tumor cells that are not also essential for normal cells (McKenna, 1991), therapy relies on subtle differences between tumor and normal cells. The following is a brief outline of the classes of chemotherapeutic agents based on their mode of action taken from McKenna et al. 1991.

- Alkylating agents were the original antitumor agents introduced into modern cancer chemotherapy. They may be cycle specific or cycle non-specific. These agents act

by attacking the structure of DNA, causing cross linking and strand breaks. This impairs the ability of DNA to act as a template for replication and transcription. Guanine residues of DNA and biological nucleophiles with nitrogen, sulfur, or oxygen groups are susceptible to attack by alkylating agents. Included in this group are agents such as mechlorethamine, chlorambucil, melphalan, cyclophosphamide, carmustine, lomustine and semustine.

- Intercalating agents are chemical compounds with planar groups in their molecules that can slide between or intercalate the base pairs of the DNA helix, distorting it. This interferes with the DNA's ability to act as a template for RNA synthesis. Some intercalating agents, such as anthracyclines, may also produce breaks in the DNA strands. Some examples of intercalating agents are daunorubicin, doxorubicin, dacinomycin and mithramycin.
- Mitotic inhibitors, rather than interacting with DNA, prevent the assembly of the mitotic spindle. This prevents the cell from undergoing cell division. Mitotic inhibitors include vinca alkaloids such as vinblastine, vincristine and vindesine.
- Miscellaneous compounds. Among important compounds not included in the antitumor classification is bleomycin. This is a mixture of antibiotics with little myelosuppressive toxicity which interacts with DNA to produce single and double strand breaks.

Hydroxyurea inhibits the reductive step in the synthesis of deoxyribonucleotides. L-Asparaginase is an enzyme that reduces the levels of circulating asparagine. Unlike other anticancer drugs, l-asparaginase does not need to gain access to the target cell to be active and its use is confined to the lymphatic leukemias. The semisynthetic plant products, epipodophyllotoxins, (etoposide and teniposide) interact with DNA but their mode of cytotoxic action is not known precisely.

- **Antimetabolites**

These are compounds that resemble natural cellular constituents closely enough to become involved in the biochemistry of the cell. Antimetabolites function by preventing synthesis of DNA or are incorporated into DNA and act as base analogues causing errors in transcription of the DNA code. They may also affect the synthesis of RNA or are incorporated into the RNA. Their activity depends on the activity of enzymes involved in the pathways they are analogues for.

A chemotherapeutic agent of particular importance to this research is fluorouracil (5-fluorouracil, 5FU). 5FU is a pyrimidine analog antimetabolite, falling into the cell cycle phase-specific group of chemotherapeutic agents. The mechanism of action of 5FU (Skeel, 1991), use, toxicity and metabolism are discussed in detail in a separate section. Following initial work with 5FU (Heidelberger, 1957), it has been used against human malignancy since 1957 (Livingston, 1970). Through various administration regimens, 5FU has been used to treat carcinoma of the breast, carcinoma of the colon and rectum (Livingston, 1970), carcinoma of the pancreas, cervical and uterine cancer, gastric carcinomas, ovarian tumors, carcinoma of the prostate, bladder, and hepatoma (Livingston, 1970). 5FU is still in common use in the treatment of a variety of solid tumors, including gastrointestinal (colorectal, stomach), head/neck, mammary and cervical malignancies, pancreas, esophagus, liver and bladder carcinomas. Topical application indicated are for basal and squamous cell carcinomas of skin (Skeel, 1991; Davies, 1982; Grem, 1987).

D) BIOCHEMISTRY OF PYRIMIDINE NUCLEOSIDES

i) INTRODUCTION

Pyrimidine nucleosides play a vital role in the survival, reproduction and function of all living things and, in conjunction with purine nucleosides, comprise the

basic units of the nucleic acids RNA and DNA. Genetic information is carried from one cell generation to another by the nucleic acid making exact copies of itself. The biological function of nucleosides is not restricted to the biosynthesis of DNA and RNA as they perform a variety of other functions, including being intermediates for the formation of glycoproteins, phosphoglycerides, glycogen, constituents of enzymes and metabolic regulators.

This review focuses on the biological systems involving base and sugar metabolism and function, focusing, more specifically on base-sugar combinations to form nucleic acids (NA). The NA's are composed of a sugar phosphate ester backbone to which the bases are attached.

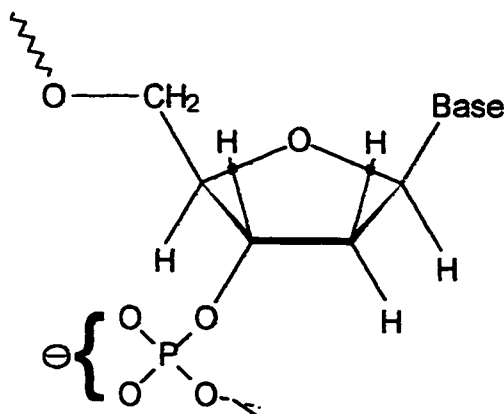
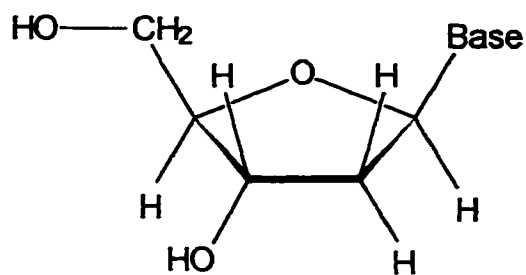
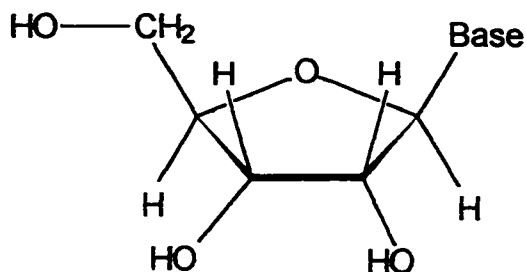


Figure 3 General NA acid structure showing the phosphate-ester linkage with the base attached to the sugar back bone(adapted from fig.6-7, p. 77, Frobisher, 1974).

The principal nucleic acids are RNA and DNA, the difference between the two being the sugar contained in the linkage. A nucleic acid containing D-ribose as the sugar portion is a ribonucleic acid (RNA), while those containing deoxyribose are deoxyribonucleic acids (DNA).

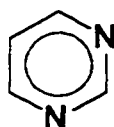


β -D-2-deoxyribofuranose

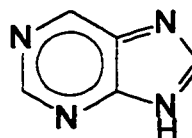


β -D-ribofuranose

Figure 4 Chemical structure of the nucleic acid sugars β -D-ribose and β -D-2-deoxyribose (adapted from p.74, Frobisher, 1974).



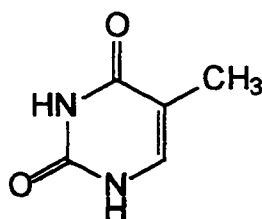
PYRIMIDINE



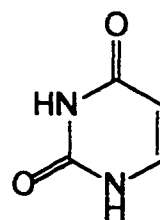
PURINE

Figure 5 The general structures for the two bases found in nature (Frobisher, fig.6-6, 1974)

The base portion are derivatives of pyrimidine and purine. The pyrimidine bases are, cytosine (both RNA & DNA), uracil (RNA), thymine (DNA) and 5-methylcytosine (DNA).



THYMINE



URACIL

Figure 6 Pyrimidine bases thymine and uracil (Frobisher, fig. 6-6, 1974)

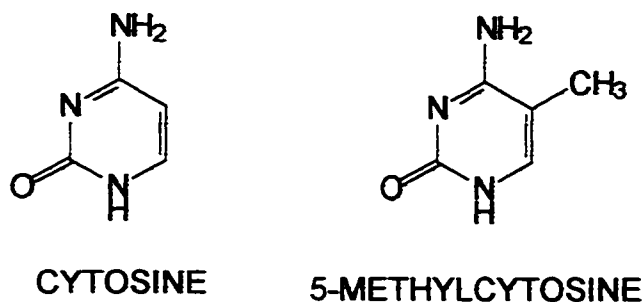


Figure 7 Cytosine and 5-methylcytosine pyrimidine bases (Frobisher, fig. 6-6, 1974)

The other class of bases are the purines, adenine and guanine.

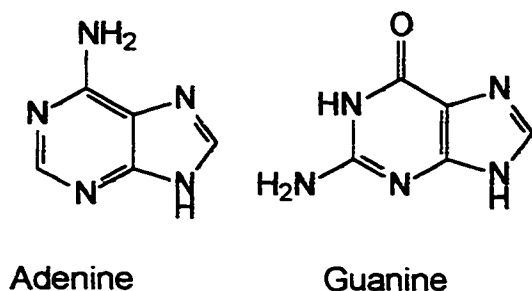


Figure 8 Purine bases adenine and guanine (Frobisher, fig.6-6, 1974)

Criteria for developing effective antitumor agents rely on the differences in transport, enzyme activity or specificity, and chemical environment, between tumor cells and healthy cells and an understanding of the structure and chemical behavior of the analog. The cytotoxic behavior of a nucleoside analog may be due to competition with natural nucleosides for enzymes, feedback inhibition of nucleoside synthesis or incorporation of the nucleoside analog into RNA or DNA molecules causing a point mutation. Since their effect is based on interference with constituents required for high metabolic activity in proliferating neoplasms, there is also risk of toxicity to normal rapidly reproducing cells such as bone marrow or intestinal mucosa.

ii) NATURALLY OCCURRING PYRIMIDINE NUCLEOSIDES

Naturally occurring nucleosides, their interconversion and incorporation into

DNA and RNA have been studied extensively, and their biochemistry is well defined (Henderson, 1973). Figure 7 represents an overview of the anabolic pathways of nucleoside and nucleotide interconversion.

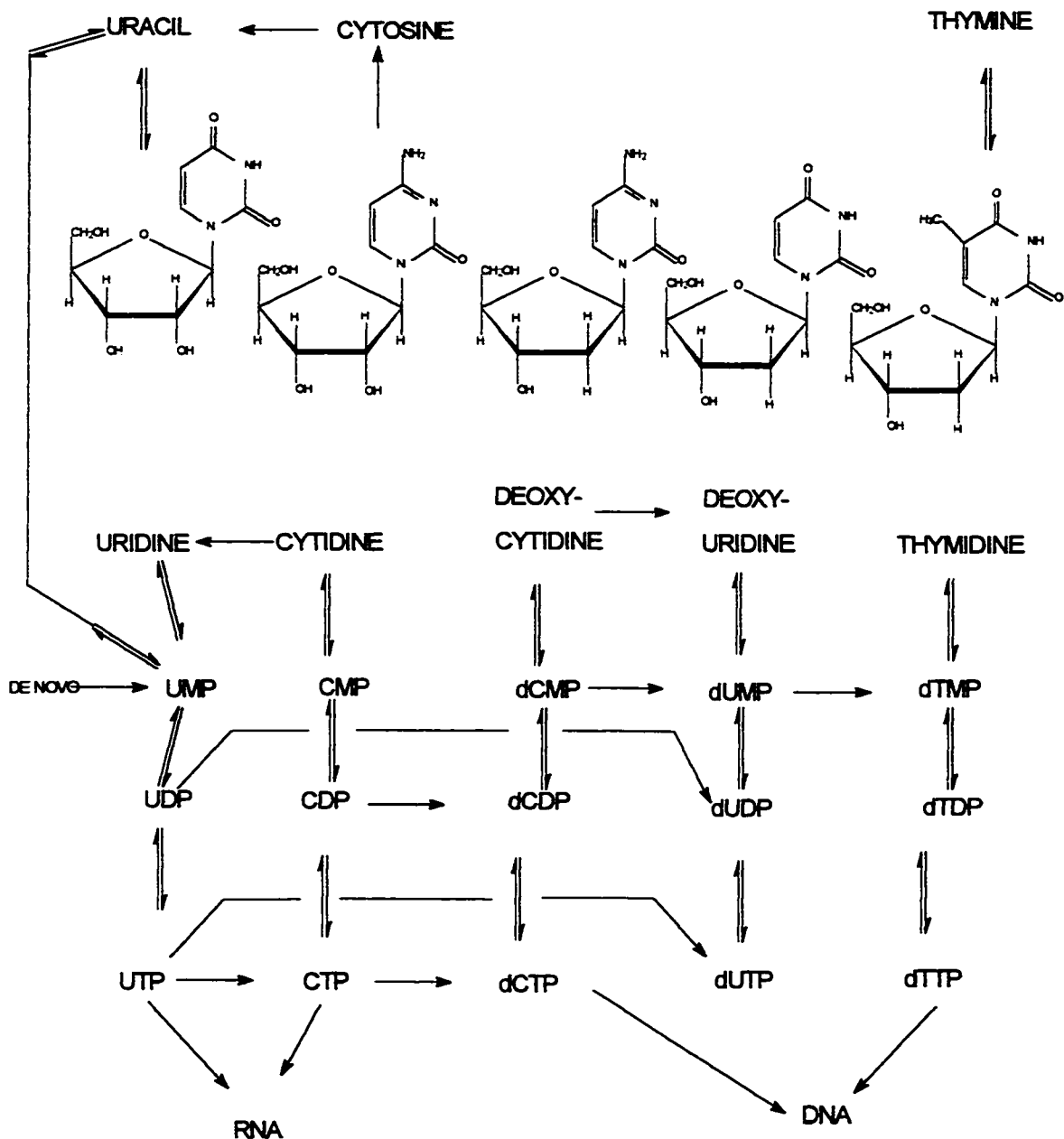


Figure 9 Anabolic interconversions of naturally occurring pyrimidine nucleosides and nucleotides (adapted from Weckbecker, 1991 and Mercer, 1985)

Important items of note include:

- Uracil(Ur) is the precursor of uridine monophosphate (UMP).
- UMP is the progenitor of all the other pyrimidine nucleosides (other than via salvage routes). From the scheme it can be seen that:
 - i) Uridine gives rise to cytidine at the triphosphate level
 - ii) The reverse occurs at either the free base level or via the deoxy nucleotide monophosphate conversion of deoxycytidine monophosphate (dCMP) to deoxyuridine monophosphate (dUMP), then dephosphorylation to deoxyuridine (dUrd).
 - iii) The deoxynucleotides are formed from a uridine nucleotide at the triphosphate level. Uridine triphosphate (UTP) is converted to deoxyuridine triphosphate(dUTP).
 - iv) Formation of thymidine nucleotides is ultimately through conversion of dUMP to dTMP with subsequent kinase interconversion.
- The nucleotide triphosphates are the direct precursors of RNA & DNA
- Once converted to the di or tri phosphates, the uridine deoxynucleotides are not directly incorporated into DNA. The deoxyuridine must first be converted to the thymidine at the monophosphate (TMP) level via methylation of dUMP by thymidylase (TS). The dUMP to TMP conversion is the only source for replenishing thymidine pools. Once TMP is formed it can be reversibly converted to thymidine or undergo phosphorylations, to eventually form thymidine triphosphate (TTP). Unlike dUTP, TTP is incorporated into DNA. The critical points of these interconversions which might be exploited in some way are:
 - 1) UMP is the progenitor of the other pyrimidine nucleosides

- 2) The only source for the thymidine pool is dUMP conversion to TMP
- 3) Thymidine is eventually incorporated into DNA from the triphosphate

iii) NUCLEOSIDE ANALOGUES AS ANTIMETABOLITES

The cytotoxic effect of nucleoside analogues is related to their ability to mimic the naturally occurring nucleosides closely enough to be mistaken for them, yet different enough to malfunction at some point. Pyrimidine nucleoside analogues elicit cytotoxicity related to one or a combination of the following effects.

- 1) The analog may compete with the natural pyrimidine as a substrate for an enzyme in the system, resulting in competitive inhibition of the enzyme. The analog having more affinity for the enzyme than the natural substrate, causes the enzyme to be unavailable for normal function.

Example -Agents which bind to TS

- i) fluorodeoxyuridine monophosphate (FdUMP)

- 2) The analog takes the place of the natural substrate resulting in a certain proportion analog containing product.

Example -Agents which compete with thymidine for incorporation

Idoxuridine (IUdR) competes for incorporation with thymidine (analog of the natural substrate) resulting in less thymidine incorporated.

- 3) Feedback inhibition caused by analog product. The metabolic analog product may be similar enough to the natural product to cause an inhibition of the production of the natural product resulting in sub-normal levels of the natural metabolic product of the pathway.

- 4) Point mutation. The pyrimidine analog incorporation could cause a point mutation or misreading of genetic material, resulting in the production of defective enzymes that don't function optimally or are totally nonfunctional.

Example IUDR after competitive inhibition with thymidine, IUDR can then be incorporated into the DNA resulting in a defective sequence in the DNA (point mutation), resulting in a misread and ultimately, defective enzymes.

Damage or destruction of the biological system incorporating the pyrimidine analog could occur if the analog-containing product has little or no biological activity. In the case of pyrimidine nucleosides, this could result in an underproduction of genetic material (DNA or RNA) or a reduction other vital biological products where nucleosides are biosynthetic intermediates.

iv) 5-FLUOROURACIL

- Initial Development

The era of the 5-fluoropyrimidine antimetabolites started in the late 1950's (Heidelberger, 1957; Heidelberger, 1965). The concept of 5FU was based on the observation that the incorporation of Ur into nucleic acids was increased in hepatomas and other tumors as compared to normal tissues (Rutman, 1954; Heidelberger, 1975). With this, Ur metabolism a potential target for cancer chemotherapy, the fluorine substituted (at the 5 position) analog of Ur was synthesized (Duschinski, 1957). This analog was chosen since this substitution leaves the size of the base almost unchanged and was expected to undergo the same metabolic conversions as Ur.

The uracil conversion of dUMP to TMP (figure 7) is the target of the 5FU analog since it involves a methylation at the 5 position of the base, catalyzed by thymidylase (TS). It was reasoned that the 5 substituted (FdUMP) substrate interference with the conversion (figure 7) of dUMP to TMP is significant, since this conversion is the only

source for thymidine pools, essential for normal DNA synthesis. It was confirmed that 5FU exhibited antitumor activity by binding to TS, blocking TMP formation and DNA synthesis (Danneberg, 1958), explaining the antitumor effects seen with 5FU in preclinical (Rich, 1958) and clinical investigations (Curren, 1958).

The anabolic conversions of 5FU in mammalian systems are shown in figure 8. In addition to the interference with TS as a mechanism for 5FU's antitumor activity, studies have since indicated, interference with RNA synthesis (Wilkinson and Pitot, 1973) and the interference with DNA functions (Kufe, 1981) are also important mechanisms of action. The elucidation and understanding of these metabolic pathways involves a study of fluoropyrimidine metabolism, including; transport across the cell membrane, anabolism and catabolism.

- **Transport Across The Cell Membrane**

Transport is defined as carrier-mediated substance transfer across the cell membrane (Weckbecker, 1991). Ur and 5FU were shown to be transported by facilitated diffusion into Novikoff hepatoma cells (Wohlhueter, 1980; Plagemann and Wohlhueter, 1980), Ehrlich ascites cells (Yamamoto and Kawasaki, 1981) and human erythrocytes (Domin and Mahony, 1990).

A competition between 5FU, adenine and hypoxanthine was demonstrated, pointing to a common carrier for purine and pyrimidine bases (Domin and Mahony, 1990). In human erythrocytes, non-facilitated, as well as facilitated, diffusion of 5FU was observed (Domin and Mahony, 1990).

Comparative studies to determine which carrier systems are involved in transporting nucleobase and nucleoside forms of pyrimidines have been undertaken (Uchida, 1989).

- Anabolism

To summarize mechanisms pointed out for pyrimidine analog antimetabolites, as applied to 5FU, The thymidylase mediated conversion of dUMP to dTMP (figure 4) is a strategically important pathway. The interference by FdUMP with TS, see figure 8 for anabolic interconversions of 5FU, results in a disruption of DNA synthesis for the cell.

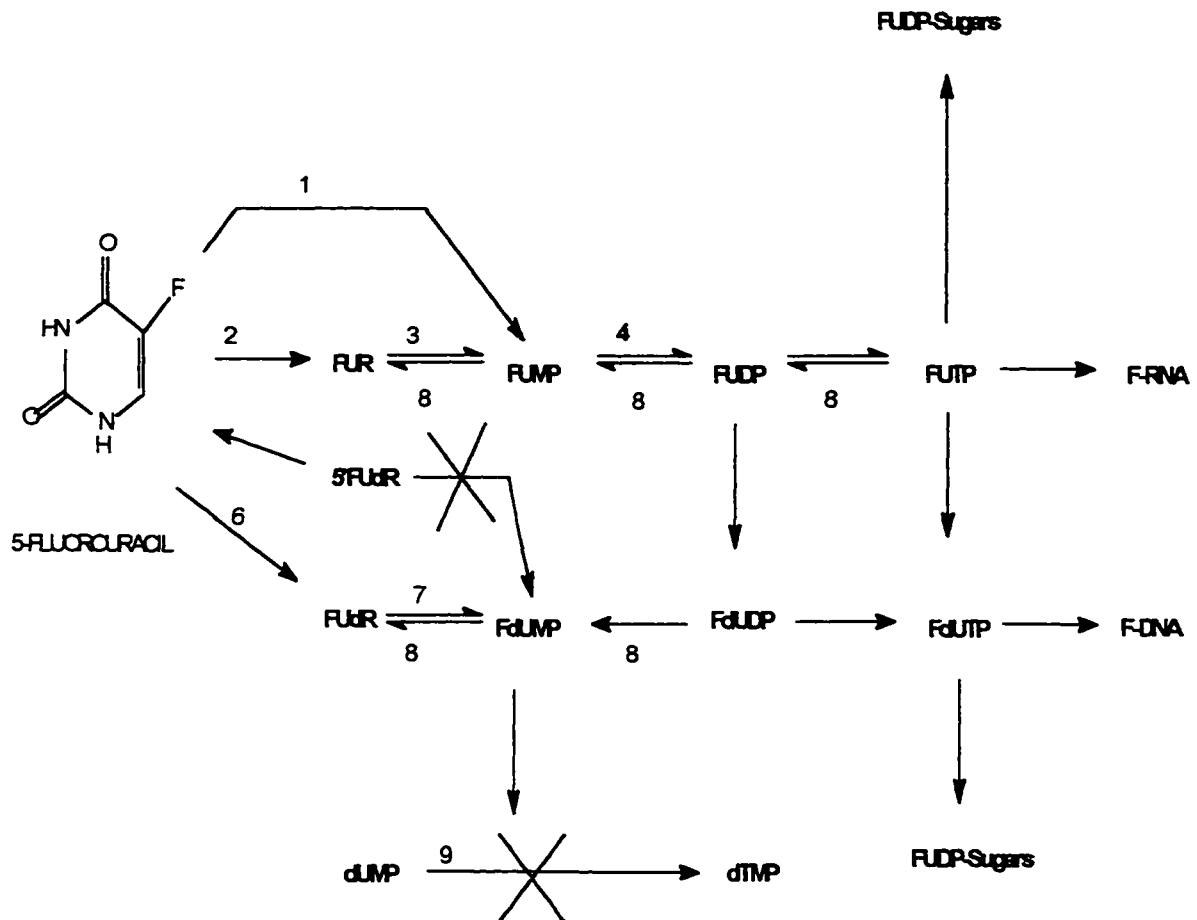


Figure 10 Anabolic conversions of 5FU (Adapted from Weckbecker, 1991, Fig.2, p.370 and Mercer, 1985)

ENZYMES COORESPONDING TO METABOLISM IN FIGURE 9

1. Pyrimidine phosphoribosyl transferase (PRPP)
2. Uridine phosphorylase
3. Uridine kinase (UK)
4. Uridylate kinase
5. Ribonucleotide reductase (RR)

6. Thymidine phosphorylase (TP)
7. Thymidine kinase (TK)
8. Phosphatase
9. Thymidylate synthetase (thymidylase) (TS)
10. Uracil reductase
11. Dihydropyrimidinase (DHPS)
12. β -ureidopropionase

Important metabolites from anabolism of 5FU are FdUMP, FUTP and FdUTP.

FdUMP inhibits TS. FUTP is a direct precursor of F-RNA, while FdUTP is a direct precursor of F-DNA (Weckbecker, 1991).

5FU ACTIVATION

- **5FU conversion to FUMP.** Since 5FU toxicity is due to the formation of toxic metabolites, a correlation would be expected between 5FU toxicity and the activity of the enzyme involved in the prevalent activation step. It was found that the phosphoribosylation of 5FU to FUMP by pyrimidine phosphoribosyltransferase requiring 5-phosphoribosyl 1-pyrophosphate or 5-phosphoribose 1-diphosphate (PRPP) as a co-substrate (Reyes, 1969, Heidelberger, 1983) are crucial for 5FU activation. Their levels enable predictions for tissue sensitivity to 5FU (Reyes and Hall, 1969; Laskin, 1979).
- **5FU conversion to FUR.** Attachment of ribose 1-phosphate to 5FU to yield FUR is another important activation reaction (Skold, 1958), catalyzed by uridine phosphorylase (UrP). Proliferating tissues have been shown to have elevated activity of UrP (Koklitis, 1985; Peters, 1991). A contributing factor to the selectivity of 5FU to tumor tissue may be the absence of this activation route in normal mucosal tissue (Peters, 1991).

The analogous reaction for activating 5FU, forming FdUR from 5FU, is a minor route of 5FU activation. The cellular levels of deoxyribose 1-phosphate were found to be very low in certain types of cancer such as colorectal tumors (Peters, 1987). This

deoxyribosylation reaction is catalyzed by thymidine phosphorylase (TP). The relationship between 5FU sensitivity and TP activity were evaluated to find greater 5FU sensitivity in tissues with higher levels of TP (El-Assouli, 1985).

In the presence of adenosine triphosphate (ATP), FUR is phosphorylated to toxic metabolites (via conversion to FUMP) by uridine kinase (UK) (Cihak and Rada, 1976). In the corresponding deoxy reaction, involving the nucleoside FdR, the subsequent phosphorylations (via conversion to FdUMP) are catalyzed by thymidine kinase (TK) (Harbers, 1959). The first reaction is controlled by feedback inhibitors uridine triphosphate (UTP) and cytidine triphosphate (CTP) (Anderson and Brockman, 1964). The activity of thymidine kinase, in the second reaction, is increased in proliferating tissues (Weber, 1978) and is regulated by the feedback inhibitor TTP (Maley and Maley, 1962).

The next anabolic step is the further phosphorylation of these 5'-monophosphates, FUMP and FdUMP, to FUDP and FdUDP, respectively. This conversion of the monophosphate to the diphosphate takes place in the presence of pyrimidine nucleoside monophosphate kinase (PNMK) (Hande and Chabner, 1978). The respective 5'-triphosphates are generated in the nucleoside diphosphate kinase reaction (Agarwal and Parks, 1971). ATP acts as a cosubstrate in these reactions which lack specificity for the pyrimidine substrates.

Of the 5FU metabolites, FUTP constitutes the major fraction, with FdUTP generally very low (Weckbecker and Keppler, 1984). The low FdUTP levels are due to catabolic cleavage by deoxyuridine triphosphate diphosphohydrolase (DTD) to FdUMP (Weckbecker, 1991).

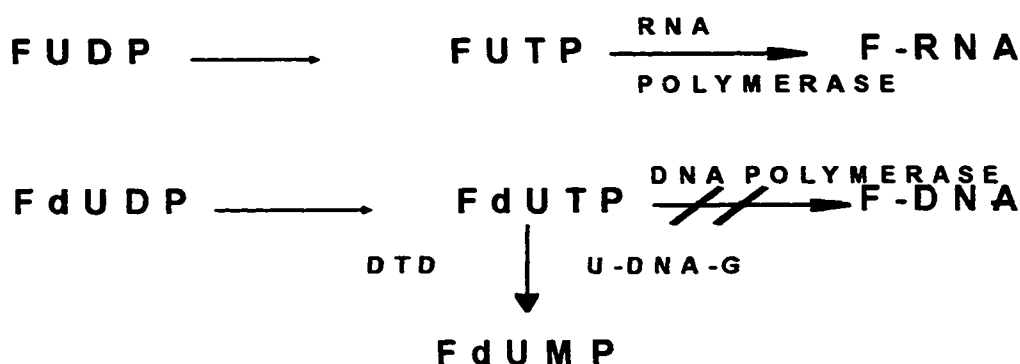


Figure 11 Fate of F-nucleotide triphosphates

Deoxyuridine triphosphate diphosphohydrolase (DTD) along with uracil-DNA-glycosylase (U-DNA-G), physiologically serve to prevent Ur incorporation into DNA, as well as to remove Ur and 5FU residues accidentally incorporated into DNA (Ingram, 1981). F-DNA would not appear to be a significant contributor to 5FU activity since these enzymes are so efficient that it was not possible to detect any F-DNA without the use of extremely sensitive methodologies (Kufe, 1981).

In contrast to the catabolic fate of FdUTP, FUTP is readily accepted as an alternative substrate by RNA polymerase and incorporated into RNA (Chaudhuri, 1958; Kahan and Hurwitz, 1962; Wilkinson and Pitot, 1973). Since it was found that FdUTP is also a substrate for DNA-polymerase, with affinity similar to that of TTP (Tanaka, 1981), it was concluded that the actions of DTD and U-DNA-G are of importance in the prevention of F-DNA formation.

Considering figures 8 and 9, the FdUMP formation should be significant. In addition, there is an alternative pathway for the formation of FdUMP, in which FUDP is reduced by ribonucleotide reductase (RR) to form FdUDP, a precursor of FdUMP (Kent and Heidelberger, 1972). The cellular levels of RR are drastically increased in proliferating normal and neoplastic tissue (Weber, 1980). The combination of these factors would further point to the importance of the actions of DTD and U-DNA-G.

- **FUDP-SUGARS**

In addition to its interconversion in nucleic acid synthesis, 5FU may become involved in related metabolic pathways. A class of fluoropyrimidine metabolites, FUDP-sugars serve as alternative substrates for enzymes of UDP-sugar metabolism (Weckbecker, 1991). Conversion of 5FU to an FUDP-sugar could be viewed as conversion to an intracellular pro-drug. The contribution to pyrimidine cytotoxicity may result from an increased intracellular half-life of fluorinated nucleotides due to the transient trapping of FUTP and its sustained release as FUDP or FUMP in the course of further FUDP-sugar conversions (Weckbecker, 1991).

- **5FU Catabolism**

Studies of 5FU catabolism were carried out by Chaudhuri, Mukherjee and Heidelberger in the late 1950s-early 1960s (Weckbecker, 1991), with clarification not achieved until more sensitive methodologies were available. In the 1980s, HPLC, ¹⁹F-NMR, and combined gas chromatography/mass spectroscopy became available and contributed to elucidation of the reactions that lead to the cleavage of the 5FU ring and subsequent formation of CO₂, NH₄⁺, F⁻, and propionic acid (Malet-Martino, 1988; Sommadossi, 1982, 1985a, b; Hull, 1988) as shown in figure 10.

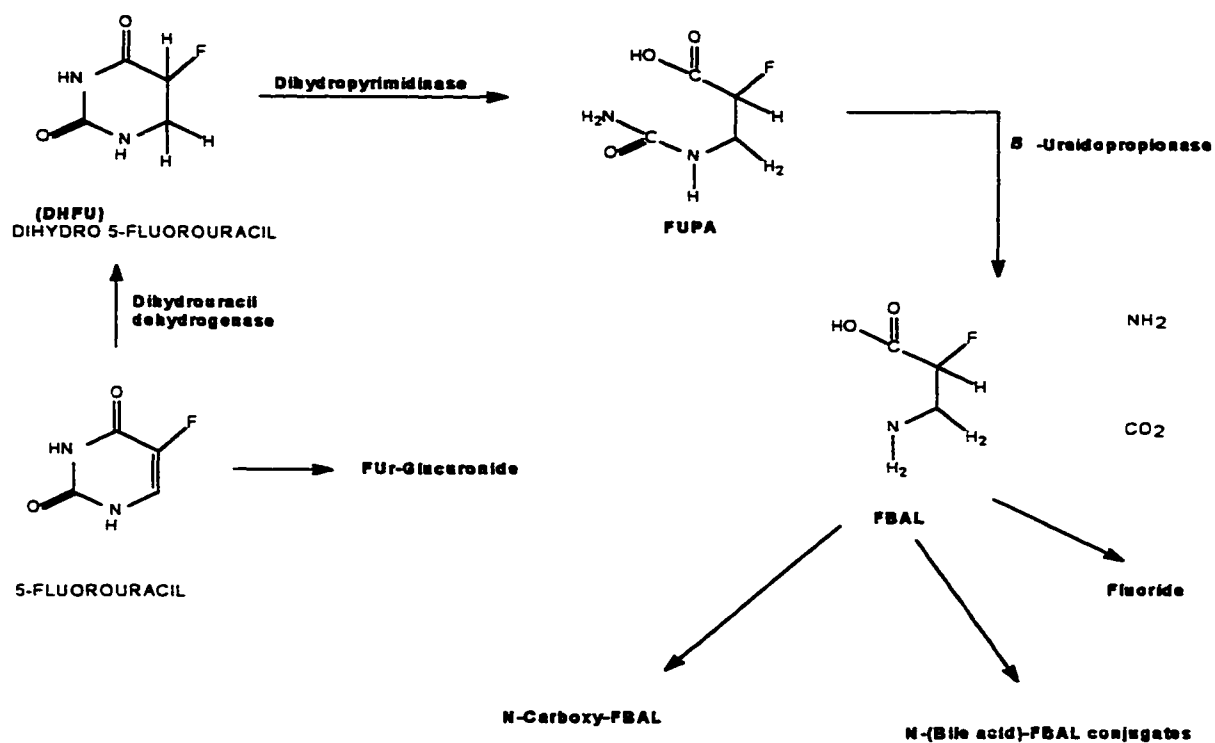


Figure 12 Catabolic pathways of 5FU (adapted from Malet-Martino, 1988; Malet-Martino, 1986; Weckbecker, 1991 and Mercer, 1985)

5FU is a substrate for the same catabolic pathway as Ur and thymine, with initial reduction taking place to form dihydro-5-fluorouracil (DHFU) in the presence of NAD(P)H, catalyzed by dihydrouracil dehydrogenase (DD) (Malet-Martino, 1989; Shiotani and Weber, 1981; Sommadossi, 1982). Theoretically, this step could be more significant if an inhibition of DD would result in potentiation of the antitumor effects of 5FU due to slowed degradation. In fact, 2,4 and 2,6-dihydroxy-pyrimidine derivatives were demonstrated to exhibit affinity for DD (Tatsumi, 1987), with (E)-5-(2-bromovinyl)uracil showing irreversible inhibition of the reductive degradation of 5FU (Desgranges, 1986).

The next step is hydrolytic cleavage of the pyrimidine ring. The reaction is catalyzed by dihydropyrimidinase (DHPS) to form α-fluoro-β-ureidopropanoic acid (FUPA) (Malet-Martino, 1988). Dihydropyrimidinase seems to be the rate limiting

enzyme of 5FU catabolism in the liver since DHFU was accumulated in 5FU treated hepatocytes (Sommadossi, 1982). Further catabolism involves the loss of CO_2 and NH_4^+ from the ureido group of FUPA. The reaction is catalyzed by β -ureidopropionase (BUPS) to form α -fluoro- β -alanine (FBAL) which has been detected by ^{19}F -NMR (Prior, 1990; Malet-Martino, 1988).

FBAL has been found to be further metabolized by at least 3 different reactions. N-Carboxylation to form N-carboxy- α -fluoro- β -alanine (Malet-Martino, 1986; Hull, 1988), C-F bond cleavage (Hull, 1986), or conjugation with bile acids (Sweeny, 1988). As with the degradation of physiological pyrimidines (Keppler and Holstege, 1982), the main site of elimination of fluoropyrimidines appears to be the liver (Sweeny, 1988).

v) MECHANISM OF ACTION AS A FUNCTION OF TOXIC METABOLITES

The toxicity of 5FU, is a function of its metabolism to toxic intermediates that interfere at various key steps with cell replication and viability. The three key intermediates responsible for 5FU's toxic effects are FdUMP, FUTP and FdUTP.

a) 5-Fluoro-2'-deoxyuridine-5'-monophosphate (FdUMP)

The action of FdUMP is related to the inhibition of TS, reaction mechanism and formation of the ternary complex.

- **Thymidylase Inhibition**

FdUMP is involved in the conversion illustrated in figure 11.



Figure 13 Conversion of deoxypyrimidine nucleotide monophosphate (FdUMP)

dUMP is the direct precursor in the TS catalyzed synthesis of thymidylate, with the C and H contributed by 5,10-CH₂-tetrahydrofolate (Friedkin, 1973). With FdUMP competing with the dUMP substrate, TS inhibition triggers the depletion of thymine nucleosides, leading to a shortage of TTP DNA precursor and subsequent cessation of DNA synthesis. Combined with ongoing RNA and protein synthesis this causes unbalanced growth to form the basis for cell kill (thymineless death) (Cohen, 1958; Rueckert and Mueller, 1960; Heidelberger, 1975). The significance is relative to TS activity, which is dependant on cell proliferation, as reflected when TS activity surges in cells entering the S-phase of the cell cycle. Correspondingly, tumor cells have TS activity much above the level found in normal cells (Keppler and Holstege, 1982; Weber, 1983).

- **Reaction Mechanism**

For the binding of FdUMP (or dUMP) to occur via the donation of the carbon by 5,10-tetrahydrofolate to occur, the acceptor must first be activated at the C-5 position. A model was formulated involving the "Friedkin intermediate" (Friedkin, 1973), which suggested a binary complex with a methylene bridge between dUMP and 5,10-CH₂-tetrahydrofolate and activation of C-5 via keto-enol tautomerism (Heidelberger, 1983). The modified Friedkin model is a covalent ternary complex that consists of TS, dUMP and 5,10-CH₂-tetrahydrofolate (Santi, 1974), with bridges between the three parts of the complex. A thioether bridge between a cysteine in the active site of the enzyme

and the C-6 position of the dUMP and a methylene bridge between dUMP and 5,10-CH₂-tetrahydrofolate. Activation of the C-5 is achieved by adding the nucleophile SH-group of thymidylase to the C-6 position of the uracil ring leading to an increased electron density at C-5 and weakening of the C-H bond (Santi and Brewer, 1968; Santi and McHenry, 1972). The one-carbon unit transfer from 5,10-CH₂-tetrahydrofolate to dUMP is concluded by reduction of the methylene group to methyl. This involves elimination of the folate cofactor, hydrogen transfer to the nucleotide and finally cleavage of the thioether bridge so that the complex disintegrates into thymidylate and free enzyme (Pogolotti and Santi, 1974). With the FdUMP as the substrate (F at the C-5 position), the tendency of the ternary complex to disintegrate is strongly diminished (Santi and McHenry, 1972) and consequently, active TS is lost due to the generation of a stable ternary complex (Dannenberg, 1986). Free TS combines with FdUMP first, before 5,10-CH₂-THF binds to form the ternary complex and correspondingly, dihydrofolate is very slowly released before FdUMP is set free (Lockshin and Dannenberg, 1981; Heidelberger, 1983).

- Ternary Complex Determinants

The formation of the ternary complex is dependant on a number of parameters such as the cellular content of FdUMP, dUMP, 5,10-CH₂-tetrahydrofolate and TS.

Increased cellular levels of FdUMP favor TS inhibition (Washtey, 1984), while high levels of dUMP, both basal and induced, have been shown to counteract 5FU cytotoxicity in relation to TS (Heidelberger, 1983). FdUMP competes with dUMP for free enzyme to form the initial binary complex, with many examples of the antagonistic effect of dUMP on the inhibition of DNA synthesis by 5FU (Lockshin and Dannenberg, 1981; Bosch, 1958; Myers, 1975; Mabuchi, 1986). The FdUMP/dUMP ratio is an

important factor regarding favorable responsiveness of human tumors treated with 5FU (Spears, 1988).

The other factor involved the ternary complex, 5,10-CH₂-tetrahydrofolate, if absent, results in very weak binding of FdUMP and TS (Lockshin and Dannenberg, 1981; Dannenberg and Lockshin, 1981). Increasing amounts of the cofactor induced a sharp rise in FdUMP-TS binding (Danneberg, 1986). Conditions to maximize FdUMP activity, would favor high levels of TS, FdUMP, and cofactor, with negligible levels of dUMP and have been found to prolong TS inhibition (Cadman, 1984; Dannenberg, 1986). An influence of the availability of TS for ternary complex formation has been found. Cells with higher TS levels required higher intracellular FdUMP levels to achieve maximal inhibition of TS (Washtein, 1984), while cells with low levels of TS are highly sensitive to 5FU (Peters, 1986a). In summary, to achieve complete inhibition of TS, formation of the *ternary-FdUMP-complex* is essential. This complex involves TS, FdUMP and the cofactor 5,10-CH₂-tetrahydrofolate.

b) 5-Fluorouridine 5'-Triphosphate (FUTP)

- **FUTP Effects On RNA Synthesis**

The significance of 5FU incorporation into RNA, due to the low levels, was difficult to assess (Gleason and Fraenkel-Conrat, 1976). The mechanisms of fluoropyrimidine-mediated cytotoxicity are that FU-RNA serve as an intracellular depot for release of toxic FU-nucleotides, corresponding to the role of FUDP-SUGARS as a storage form of fluorinated nucleotides (Weckbecker and Keppler, 1984). Interference with mammalian ribosomal RNA maturation has also been demonstrated (Wilkinson and Pitot, 1973). The antitumor activity of 5FU was also correlated with the incorporation of 5FU into tumor RNA (Spiegelman, 1980). FUTP is the metabolite

responsible for these mechanisms and can serve as a substrate for the synthesis of all classes of RNA (Carrico and Glazer, 1979a; Heidelberger, 1983).

- **5FU Ribosomal RNA**

Following treatment with 5FU, inhibition of ribosomal RNA synthesis was detected (Hahn and Mandel, 1971; Willen and Stenram, 1970; Wilkinson and Pitot, 1973), indicating FUTP-induced base pair transformations as a mechanism of cytotoxicity (Glazer and Legraverend, 1980).

- **5-FU Messenger RNA**

The effects of 5FU on messenger RNA may impact on RNA synthesis (transcription), RNA processing (splicing), or protein synthesis (translation). The impact is variable and is also difficult to differentiate. In agreement with Heidelberger speculating that splicing was impaired (Heidelberger, 1983), results of studies where cells have been treated with 5FU suggest that splicing is impaired and that various mechanisms may be involved (Doong and Dolnick, 1988).

- **5-FU Transfer RNA**

The effects of 5FU are difficult to assess because of different extents of 5FU substitution. A 5FU induced decrease in the content of minor bases of transfer RNA appears to be restricted to Ur derived base moieties and is the consequence of both their perturbed post transcriptional synthesis and their replacement by 5FU residues (Le, 1976; Frendewey and Kaiser, 1979).

- c) 5-Fluorodeoxyuridine-5'-triphosphate (FdUTP)**

DNA is protected from the incorporation of Ur (or 5FU) by the actions of dUTP diphosphohydrolase and uracil-DNA glycolase. Knowledge of these protection mechanisms and lack of sensitive assays contributed to the assumption that DNA was unaffected by and not a factor in the mechanism of action of 5FU. Eventually 5FU containing DNA was detected in tissue cells (Kufe, 1981; Major, 1982), with its

formation dependent on the concentration of 5FU (Schuetz, 1984) and TTP. The antitumor activity and side effects of 5FU have been shown to involve (at least in part) FU-DNA (Kufe, 1983; Schuetz, 1984; Sawyer, 1984a).

Misincorporation of 5FU into DNA causes the strand to become fragmented by leading to DNA lesions or strand breaks or gaps (Collins, 1978; Lonn and Lonn, 1988a). Since DNA lesions are repairable, the importance of 5FU-DNA induced lesions are a function of the efficiency of repair processes.

E) APPROACHES TO INCREASE THERAPEUTIC EFFECTIVENESS OF 5FU

i) TOXICITY AND EFFECTIVENESS

Factors contributing to the toxic side effects of 5FU include, the metabolism and pharmacokinetics of 5FU and the metabolic activity of the cells involved. Since 5FU exerts its cytotoxic effects via its metabolites, toxic side effects are expected and related to a healthy cell's ability to metabolize 5FU. The degree of toxicity is relative to the rate of cell metabolism, with rapidly reproducing cells being the most susceptible. Those tissues most affected by 5FU cytotoxicity are gastrointestinal, bone marrow and mucous membrane (Robben, 1992).

Cases of unexpected, relative to this model, toxicity to mature cells have occurred. A syndrome of cardiotoxicity (Robben, 1992) during 5FU therapy have occurred where cardiac cells are more susceptible to 5FU toxicity than less mature, reproducing tissues. This is contrary to a cell metabolism mechanism of toxicity due to cardiac muscle tissue, being mature cells, would be expected to be unaffected by 5FU toxicity.

Even with its toxicity to healthy cells, since its introduction, 5FU has been used extensively. Anticancer therapies include solid tumors of the head and neck, skin or basal cell carcinomas and advanced colorectal and gastrointestinal malignancies.

Despite being considered a mainstay of cancer therapy by many because of this extensive list of treatments, 5FU also suffers from poor response rates. Response rates when used as a single agent are as low as 10 to 20% (Sotos, 1994), with little improvement by the addition of other cytotoxic agents for combination use (Sotos, 1994).

The limitations associated with 5FU, such as low response rates and significant toxic side effects, are due, in part to its widespread distribution and lack of specificity. Investigations to improve the efficacy of 5FU employ strategies that improve 5FU delivery and response rate. Strategies in use or showing promise include; adjunctive radiation therapy, infusional 5FU administration, and biomodulation of 5FU.

ii) ADJUNCTIVE RADIATION THERAPY

Adjunctive chemotherapy plus radiation therapy is standard treatment in high risk rectal cancer. However, the use of radiation in colon cancer remains investigational (Minsky, 1995). The standard adjunctive therapy for node positive or high risk colon cancer is post operative 5FU and levamisole (Moertel, 1990). The use of adjunctive radiation therapy, based on the patterns of failure, would be a "last resort" option for high risk patients where conventional methods have failed rather than a progressive method for improving 5FU efficacy. Significant toxicity varied from 5 to 38% (Minsky, 1995), with a case where unacceptable toxicity necessitated a modification of the protocol (Fabien; Minsky, 1995). Current literature indicates the combination of chemotherapy and radiation as a failure recovery treatment used in advanced GI carcinomas where other treatments have failed. The toxic effects with little targeting of malignant tissue renders this method a poor solution to achieve the stated strategy.

iii) INFUSIONAL 5FU ADMINISTRATION

The distribution, effects and toxicity of 5FU may be influenced by the method of administration such as controlled infusion of 5FU for breast cancer (Ng, 1994) and GI malignancies (Leichman, 1994), rather than a simple bolus injection. The rationale to determine the use of infusional therapy considers several factors.

- The short half-life of 5FU, approximately 11 minutes *in vivo*.
- Tumor cell utilization of 5FU is maximized when in the S-phase.

Over a short time (11 minutes) only a small number of tumor cells will be susceptible. By increasing the exposure time to 5FU, potential tumor cell kill may be enhanced. Continuous infusion of 5FU increases antitumor activity and lowers toxicity (Ng, 1994) for treatment of relapse breast cancer.

iv) BIOMODULATION OF 5FU

Knowledge of the metabolic pathways of 5FU that have been elucidated presents a tool to allow the manipulation of biochemical processes to find new ways to improve 5FU. Biomodulation is a manipulation of the metabolism of 5FU and its interaction with target end-points to increase its effectiveness and/or reduce toxic side effects (Allegra, 1991; Rustum and Campbell, 1988).

Some of the agents used to biomodulate 5FU include; interferon, leucovorin, dihydropyrimidine dehydrogenase (DPD), folinic acid, thymidine, N-(phosphonacetyl)-L-aspartate, and dipyridamole.

- Leucovorin and Interferon

The most extensively studied biomodulator is *leucovorin* (Sotos, 1994). 5-Formyltetrahydrofolate (citrovorum factor; leucovorin) is a reduced folate which is metabolized in the cell to various forms of tetrahydrofolate including 5,10-methylenetetrahydrofolate (Sotos, 1994). Investigators found that inhibition of TS by

FdUMP could be enhanced by high intracellular folate levels (Santi, 1974; Dannenberg, 1978). In studying leucovorin's effects, relative to elevated folate levels, one group found they could enhance the growth inhibition of 5FU by five-fold (Ullman, 1978).

Combining chemotherapy with interferons has been of interest in the treatment of various malignancies (Hoffman and Wadler, 1993). Interferons consist of three different classes of glycoprotein molecules: alpha (α), beta (β) and gamma (δ) . α Interferon production is induced in leukocytes by virus-infected cells, tumor cells and bacterial products. β Interferon production is stimulated in fibroblasts, epithelial cells and macrophages by viral and other foreign nuclear acids. δ Interferons are synthesized by sensitized T cells exposed to foreign antigens (Baron, 1991). Interferons exhibit antiviral effects and inhibit the proliferation of both normal and transformed cells (Hoffman and Wadler, 1993) by a mechanism of interference with cell cycle by interferons blocking the traverse of cells from G_0/G_1 to S phase (Lin, 1986; Einat, 1985). Interferon induced structural alterations in the plasma membrane and cytoskeleton also play a role in the antiproliferative effect (Tamm, 1987). Interferons may augment immunity against tumors via modulation of specific effector cells (Neefe, 1985). The mechanism for the potentiation of 5FU by interferons include (Hoffman and Wadler, 1993) two alternative methods of interaction:

- 1) Directly modulating the activity of a given chemotherapy drug by affecting drug disposition within the tumor cell, or
- 2) Act via perturbation of host drug metabolizing systems, immunoaugmentative antitumor effects, or through protection of normal host tissues, to increase cytotoxicity (Wadler and Schwartz, 1990).

Utilization of all three agents (leucovorin, interferon and 5FU) was investigated with the intention of increasing the toxic effects of 5FU to tumor cells while minimizing toxic side effects. Studies suggest that leucovorin and interferon represent two complementary biochemical modulators of 5FU that enhance inhibition of thymidylase (Grem, 1992).

- Dihydropyrimidine Dehydrogenase (DPD)

DPD is an enzyme involved in the catabolic pathway of 5FU conversion from the dihydro 5-fluorouracil metabolite to α -fluoro- β -ureidopropanoic acid and eventual elimination of 5-FU (Milano, 1994). DPD is also present in various other normal, as well as in tumor tissues (Milano, 1994). DPDs presence and activity is variable in the population. This is a factor in explaining the pharmacokinetics of anticancer drugs that are characterized by interpatient variability (Evans, 1989). The significance of DPD variability undergoing 5FU therapy are apparent in patients with DPD deficiency, who exhibit severe 5FU-related toxicities (Milano, 1994). Also, DPD activity in tumor cells (*in vitro* and clinical studies) is related to 5FU sensitivity (Milano, 1994), the lower the DPD activity, the greater the FU efficacy (Newell, 1989).

- Thymidine

Thymidine is a naturally occurring nucleoside directly involved in the metabolic pathways affected by 5FU. Thymidine lacks antitumor activity in its own right (O'Dwyer, 1987), although, has been used to synchronize cells growing *in vitro* in S-phase (Xeros, 1962). Thymidine's potential lies in modulation of the activity of active cytotoxic drugs in a synergistic fashion *in vitro* and *in vivo* (Martin, 1980; Ellims, 1982). For the thymidine-5FU combination, synergistic antitumor activity in animal models was found

to be critically dependent upon the dose and schedule of the two agents (O'Dwyer, 1987).

- **N-(Phosphonacetyl)-L-Asparate (PALA)**

PALA is a potent inhibitor of *de novo* pyrimidine synthesis and demonstrated to enhance the therapeutic activity of 5FU (Martin, 1992). PALA was added to the therapy to enhance 5FU effectiveness by biochemically forcing metabolism to maximize the known mechanism of reaction and to be effective against that portion of the cancer cell population that is less sensitive to 5FU. The use of biochemical modulation is employed in the quasi-drug-resistant (but actually drug sensitive) cells to permit the cell's destruction by doses of the effector agent tolerated *in vivo* (Martin and Kemeny, 1992).

v) PRODRUG DELIVERY TO TARGET 5FU

a) Considerations For 5FU Prodrug Development

The development of a method to target and concentrate the delivery of 5FU directly to tumor cells would overcome the limitations of toxicity to healthy cells and lack of specificity. Prodrugs are derivatives that deliver 5FU to the site of action where metabolic activation of 5FU then takes place (Weckbecker, 1991). The ideal 5FU-prodrug exhibits the following properties:

- non-toxic after administration, while being transported to the site of action
- delivered to the target site of action by some means
- biologically transformed to cytotoxic 5FU at the site of action
- cytotoxic to 100% of the tumor cell population
- biologically transformed to nontoxic metabolite
- excreted without harm to host

Researchers have investigated various 5FU prodrugs for possible antitumor and antiviral use as illustrated by the following;

b) 5-Fluorouracil Prodrugs

- Tegafur (ftorafur: 5-fluoro-1-(tetrahydro-2-furyl)uracil))

Tegafur was developed as an orally active 5FU prodrug with an extended half-life from 0.5 hours (5FU) to a median of 18.6 hours (tegafur) (Myers, 1976).

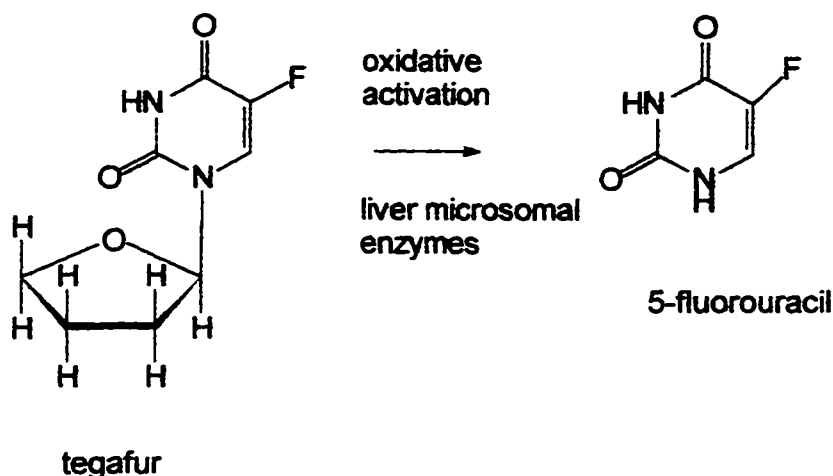


Figure 14 Activation of tegafur to 5-fluorouracil via liver microsomes

Once administered, tegafur undergoes oxidative activation in the liver to 5FU, resulting in a longer duration of action than (Benvenuto, 1978) direct 5FU administration. Two important disadvantages of tegafur are that the activation takes place in the liver rather than being tumor mediated (Benvenuto, 1978) and the doses of tegafur required to achieve antineoplastic effects comparable to those of 5FU are 3 to 7 fold higher. Although neurotoxic side effects can be severe, tegafur appears to be better tolerated than 5FU (Hadfield and Sartorelli, 1984).

- Doxifluridine (5'-deoxy-5-fluorouridine)

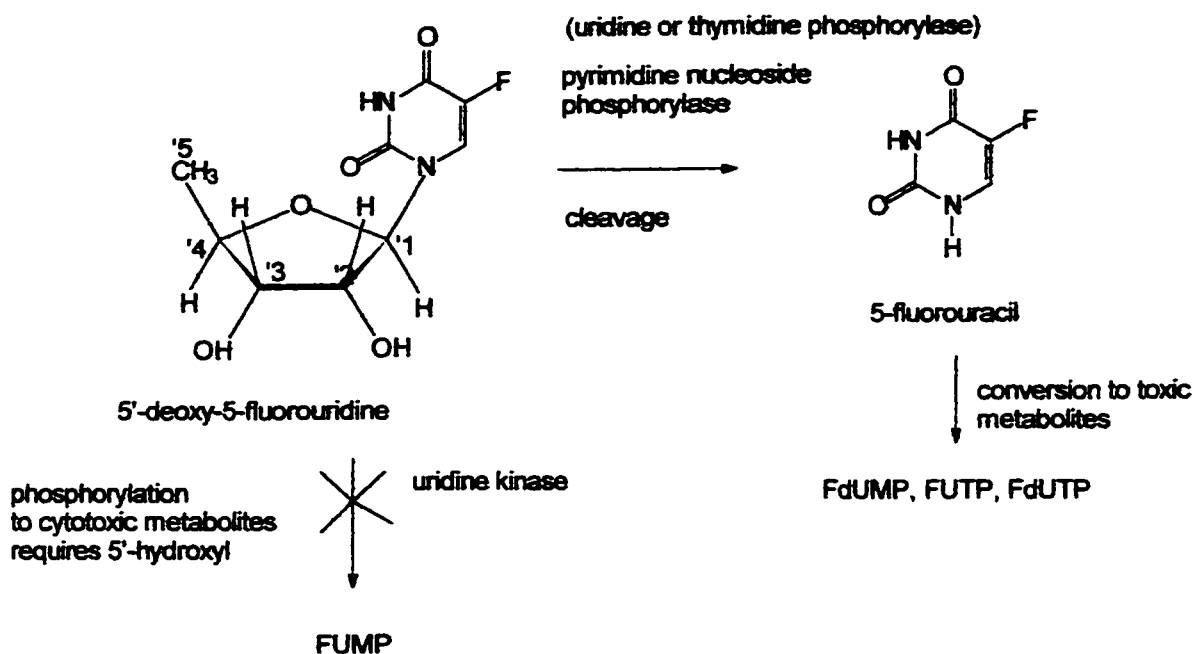


Figure 15 Possible activation routes for doxifluridine

Doxifluridine (dFUR) was synthesized by Cook et al. in 1979 as an antineoplastic agent and appears to have advantages over 5FU (Weckbecker, 1991). dFUR exerts its antimetabolic effect, either by direct cleavage to 5FU, thereby acting as a 5FU prodrug, or by becoming directly involved as a substrate in the nucleoside / nucleotide interconversions. The toxicity of 5FU is related to its interconversions to its nucleoside or deoxynucleoside with subsequent phosphorylations to nucleotides. The kinases that carry out these conversions require the presence of an hydroxyl group at the 5' position of the ribose (or deoxyribose) moiety of its substrates. Doxifluridine (dFUR) differs from the 5FU toxic metabolites by lacking the hydroxyl group at the 5' position. Due to this subtle difference, dFUR is not a substrate to become phosphorylated by kinases and needs to be activated via cleavage to 5FU by pyrimidine nucleoside phosphorylases (Weckbecker, 1991). The predominant activating enzymes are uridine phosphorylase and thymidine phosphorylase (Armstrong and Cadman, 1983; Kono, 1983).

F) RATIONALE FOR THE DEVELOPMENT OF FUF

Many of the prodrug agents developed are nucleosides of 5FU employing metabolically strategic variations on the 5FU structure. Another possible approach could be a targeting, carrier molecule of 5FU. In this 5FU-carrier form, the inactive carrier molecule, would function to target a specific tissue by some mechanism. Once at the site of action the 5FU would be cleaved, releasing it to exert its cytotoxic activity to the target tissue. Various 5FU-sugar combinations have been investigated as possible antimetabolic agents, as illustrated by the two previous examples, tegafur and doxifluridine. It is through this prodrug approach that the rationale for the development of fucosyl-5-fluorouracil (FUF) lies.

The fucosyl nucleoside of 5FU was selected as a potential antimetabolite warranting investigation for reasons pertaining to the pharmacokinetic properties of the fucose moiety, as follows:

- Intact FUF would not be toxic to normal healthy cells prior to conversion, thereby act to decrease toxic 5FU side effects.
- The fucosyl sugar portion of the nucleoside will act to target FUF to the liver.
- Once at the site of action the fucose would be cleaved, releasing 5FU to exert its toxic effects on the target cells.

The rationale for these expected properties lies in the characteristics of the fucose sugar. Specifically, fucose is known to concentrate in the liver via immunorecognition sites. How this fact relates to the expected results is the focus of the rationale for FUF and the subject of this investigation.

FUF is investigated as a prodrug specifically for use in hepatic carcinomas. Since fucose concentrates in the liver, it is postulated that FUF would retain that property. In addition, once in the liver, FUF would then be cleaved to release 5FU. 5FU

would then be available to exert its antimetabolic effect on hepatic tumor cells. As the focus of this investigation, the significant factors to determine are:

- 1) Does fucose retain its ability to concentrate in the liver when coupled with 5FU?
- 2) Upon administration, to what degree does FUF remain intact?
- 3) Once in the liver is FUF cleaved to release 5FU?

G) DETECTION AND ANALYSIS OF FLUOROPYRIMIDINES

Fluorides are widely distributed in nature. In regard to natural sources, man obtains the fluorides from the ingestion of water, with plant or food sources being a rare occurrence. It is commonly known that most major centers in the developed world add fluoride to drinking water supplies as a measure to prevent dental caries.

Establishing fluorine's natural occurrence and distribution is of importance, in relation to this study, because the study involves compounds containing fluorine. Two important considerations in this study of fluorine substituted compounds are:

- 1) The natural absorption, distribution, excretion and occurrence(or lack) of fluorine as a possible source of interference, contamination or background.
- 2) The method, efficiency, accuracy, precision and specificity of fluorine analysis.

By considering these two factors, the degree of confidence can be established for the method of fluorine analysis of the compound under investigation. Fluorine is not a natural constituent of living plant or animal tissue, with absorption by living organisms usually in its ionic form as a constituent of water. After absorption fluorine is not incorporated into soft tissue, but in its anionic form localizes in bones and teeth. Here fluorine substitutes for hydroxyl and bicarbonate at the surface of the apatite crystals (Nusynowitzl, 1965; Blau, 1962). Therefore, when investigating a fluorine containing compound, a method of fluorine analysis is useful to distinguish the compound of

interest. Since the investigation concerns cytotoxic effects on soft tissue systems such as tumors, gastrointestinal tract, basal cells, etc., fluorine incorporation into tooth and bone structure is not of concern.

Detection and analysis of new intracellular metabolites and elucidation of drug mechanisms, pertaining to fluoropyrimidine pharmacology, has been dependant on the sensitivity and specificity of the analytical methods used (Weckbecker, 1991). Various methods have been employed for the detection and analysis of fluoropyrimidines. These include; column chromatography, paper chromatography, thin layer chromatography, electrophoresis, high-performance liquid chromatography (HPLC), spectrophotometry, nuclear magnetic resonance (NMR) spectroscopy and ligand binding and enzymatic techniques (Weckbecker, 1991).

The focus of analysis for this study is the detection, isolation and quantification of 5FU and FUF. A combination of methods traditionally used for analysis of fluoropyrimidine in general, with methods specific to the characterization of fluorine were employed. The results of the methods of analysis of the biological samples were correlated in attempts to determine the metabolic fate of FUF. The traditional methods were, HPLC, NMR (proton), and radiolabelled tracers ^{14}C and ^3H . Methods more specific to fluorine detection, characterization and quantification were NMR (fluorine nuclear magnetic resonance) and NAA. Each method contributed information to identify, detect and quantify the test pharmaceuticals.

III) EXPERIMENTAL

A) SYNTHESIS OF FUCOSYL 5-FLUOROURACIL

Both the cold and radiolabelled FUF, L-[1'-¹⁴C]fucose-5-fluorouracil and L-(+)-fucose-[6-³H]-5-fluorouracil, molecules used in the biodistribution studies were synthesized by V.J. Somayaji via coupling peracetylated fucose with 2,4-bis(trimethylsilyloxy)-5-fluorouracil in the presence of stannic chloride, followed by deblocking. All reagents used were reagent grade chemicals. Solvents were distilled before use. Where anhydrous solvents were required, they were dried by standard methods. The 5FU and L-(+)-fucose were purchased from Aldrich Chemical Co. Inc. For the dual label studies the [6-³H]-5fluorouracil and L-[1-¹⁴C]-fucose were purchased from Aldrich Chemical Co. Inc.

For synthesis procedures of FUF, including labelled products, see appendix 2. The ¹⁴C labelled product was characterized and radiochemical purity of the sample determined by TLC analysis and LSC. After developing the TLC plate, it was divided into 14 equal parts and the silica gel sections scraped directly into individual scintillation vials for radioactivity measurements.

The activity of the tritium labelled product was determined to be 425 mCi. The product was characterized and radiochemical purity determined by TLC analysis and LSC in the same manner as for the ¹⁴C samples. After developing, the TLC plate showed a single spot with TLC RF=0.22.

B) ANIMAL STUDIES

i) ANIMAL AND TUMOR MODEL

The test subjects, B₆D₂F₁ mice, were obtained from the Health Sciences Small Animal Program, University of Alberta. Lewis Lung Tumor cell suspensions were obtained from Mr. Bert Meeker, Cross Cancer Institute, Edmonton, as a suspension in

a frozen state in waymouth's + 10% DMSO with a labelled cell count of 4×10^7 cells/ml. Other supplies required to carry out the experimental animal procedures were obtained from commercial supply houses.

Approximately 2 million cells in 0.1 mL were injected subcutaneously (SC) into the left flank of the recipient mouse (weighing 20 to 25 g). These mice were left for 10 to 14 days to allow the subcutaneous tumors to develop to the appropriate size. The initial group acted as donor mice with a harvest of tumor cells was used to propagate and continue the tumor cell line. The candidates for tumor harvesting were selected and processed as follows.

Mice possessing subcutaneous lumps on their left flank (tumor size 1 to 2 cm diameter) were selected and sacrificed by asphyxiation with carbon dioxide. The asphyxiation was carried out by placing the mice in a large beaker, prepared by placing dry ice in the bottom as a CO₂ source and covering the top, after placing the mouse in, to prevent oxygen from entering the beaker. The CO₂ was allowed to accumulate, asphyxiating the mouse. The mice were removed from the beaker and the tumors were surgically removed and placed in a petri dish containing invert sugar solution and sliced into fragments of approximately 2-3 mm. The fragments were drawn into a trochar (14 gauge, Custom Spinal, Popper and Sons Inc.) and inserted SC into the host mouse which was under light metofane anesthesia.

The recipient mice were left to allow the tumors to mature to 1 to 2 cm in diameter. At 10 to 14 days the tumor growth, according to the raw data, ranged from 700 mg to 1.2 g. The mice were maintained in standard plastic cages with 4 to 6 mice per cage. Nourishment was *ad lib* with food pellets and tap water.

ii) ADMINISTRATION OF 5FU & FUF

The mature tumor bearing mice were selected for injection with either FUF or 5FU. The compounds, reconstituted just prior to use, in a multidose vial with sterile saline for injection, to a concentration to allow dosing of 0.05 to 0.25 mL per injection for each animal.

The dose administered was determined by considering the actual therapeutic dose of 5FU (12 mg/kg)(for the NAA study) and the required concentration of radioactivity needed for detection(for the dual labelled study). The FUF dose was equimolar to the 5FU dose used. The radiolabelled compounds, quantified by LSC, were reconstituted to appropriate dilutions to give the required activity to volume. To determine activity of ^3H and ^{14}C labelled compounds a partial dilution in saline was made. From this, an aliquot was counted by LSC and further dilution was made to give the required concentration of radioactivity. As with the cold compound for NAA, the activity was adjusted to allow a dose volume for injection of 0.05 to 0.25 mL per animal.

Once reconstituted and adjusted for proper dose and activity, the test compounds were injected to the restrained test animal via tail vein injection with a preloaded 1/3cc (30 unit) insulin syringe.

iii) BIOLOGICAL SAMPLE COLLECTION

Following injection, the subjects were sacrificed at predetermined time intervals, by the same method as was used with the tumor donor mice. In this case, the mouse was placed in the beaker on a mesh covered watch glass, to allow for collection of urine excreted during asphyxiation. To ensure collection of all samples, including blood, the mice were removed from the beaker as soon as breathing had ceased. The chest cavity was immediately opened and blood sample removed from the heart by

cardiac puncture. The remaining urine sample was then taken by bladder puncture via syringe and combined with urine collected in the watch glass. The mice were then dissected for recovery of the remaining tissue samples. These were liver, kidney, tumor, gastro-intestinal tract (GIT) and tail. From this point the treatment of the tissue samples differed, depending on the method of analysis being employed.

C) NAA

The biodistribution studies of FUF were carried out in B₆ D₂ F₁ mice, bearing implanted Lewis lung carcinomas. The concentrations of FUF in hepatic tissue were determined by measuring fluorine using nuclear activation analysis (INAA). This approach allows for the measurement of FUF and all of its fluorine containing metabolites. It does not provide information on the chemical nature of the metabolites being detected.

Materials required to prepare samples for NAA were provided through the courtesy and generosity of Gordon Haverland and Peter Ford. The samples were activated in the University of Alberta's SLOWPOKE nuclear reactor and analyzed by γ ray-spectrometry.

The samples intended for neutron activation analysis (NAA) were placed in specially prepared plastic sample containers that were cleaned prior to use to ensure contaminant free samples. The washing procedure is as follows.

Latex sterile gloves were worn at all times to prevent Na contamination from body fluids or skin. All lab bench surfaces were washed down with an ethanol solution. The sample vials were cleaned thoroughly with a Na free soap solution, twice, to ensure contaminant free samples. They were then rinsed with ethanol and left to dry.

The dissected mouse samples were placed in the prepared sample vials under the same conditions as for vial preparation. Attention was paid to the volume occupied by the sample in the vial. Samples occupying the full volume of the vial were considered "Full Geometry Samples". Smaller samples, occupying one-half or less of the sample vial volume were considered "Half Geometry Samples".

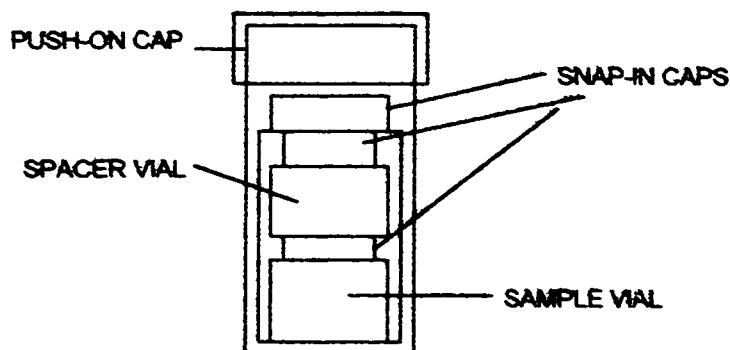


Figure 16 Method of sample vial arrangement for immobilizing samples for NAA

The smaller samples were immobilized within larger sample containers as shown in figure 16. This ensures consistent geometry for bombardment of large and small samples. Each mouse's weight was recorded before dissection, with the organ samples weighed directly into the small NAA sample vials. The excess plastic was trimmed off the vials, then they were sealed by pushing and turning the vials in the heat sealer for approximately 7 to 10 seconds. Once sealed, the small vials were placed inside medium sample vials. A second small empty sample vial was also placed in the medium vial to act as a spacer, then the medium vial capped and heat sealed. Any vials not immediately undergoing NAA were frozen until it was convenient for analysis.

Each sample was then checked in a "GO JIG" to ensure ease of passage into the reactor sample chamber. The samples then underwent neutron irradiation using the SLOWPOKE facility in the Faculty of Pharmacy at the University of Alberta.

Following the irradiation, a gamma spectrum was obtained for each sample to permit identification and quantification of radionuclides produced. The first set of samples analyzed were for establishing detection limits. Prior to analysis, these mice were administered a variable dosage range (12 to 100 mg/kg) of 5FU.

Standard curves were prepared for fluorine and sodium. The data obtained for the construction of standard curves allowed for correlation of the of the decay data with fluorine present and sodium contamination. Standard curves were prepared for both full and half geometry samples.

The final set of samples analyzed by NAA were the biological samples from mice dosed with 5FU or FUF at various predetermined times.

D) DUAL LABEL STUDY USING ^3H AND ^{14}C LABELLED FUF

In this study, the injected material was dual labelled FUF, with ^{14}C in the fucose portion and ^3H in the pyrimidine base. Since both radionuclides decay 100% via beta emissions, the samples were analyzed by LSC. This required combustion of the samples with quantitative recovery of $^{14}\text{C-CO}_2$ and $^3\text{H-H}_2\text{O}$. The sample size upper limit of approximately 200 mg is necessary in order to achieve reproducible, efficient trapping of the labelled combustion products. Therefore, in the case of larger tissue samples, aliquots of the tissues were combusted. The wet tissue samples were weighed into paper combustion cups (Packard Instrument Company Inc.) and dried under a heat lamp prior to combustion.

The samples were combusted at 900°C in an oxygen atmosphere in an H. J. Harvey Instrument Corporation Biological Oxidizer. In this instrument the $[^{14}\text{C}]\text{-CO}_2$ produced by combustion is bubbled through and trapped in Harvey ^{14}C Cocktail. The

^3H is separated by condensing the $[^3\text{H}]\text{-H}_2\text{O}$ from combustion and flushing it into Harvey Tritium Cocktail. These combustion products are collected in separate standard liquid scintillation vials. A Beckman LS 9000 or Searle Mark III liquid scintillation counter was used for radiometric counting of these vials.

The combustion and collection efficiency for of the Harvey Instrument Corporation Biological Oxidizer for ^{14}C and ^3H was determined by combusting and counting ^{14}C and ^3H standards. The LSC efficiency alone for ^{14}C was determined by adding standard $[^{14}\text{C}]\text{-n-hexadecane}$ to the compound samples and recounting them. This was also done for ^3H counting, using a $[^3\text{H}]\text{-n-hexadecane}$ standard. In this way, the combustion, recovery and counting efficiencies, including quenching effects, are accounted for.

IV) RESULTS AND DISCUSSION

A) SYNTHESIS OF 1-(β -L-FUCOSYL)-5-FLUOROURACIL (FUF)

Synthesis of FUF carried out by V.J. Somayaji afforded FUF in an overall yield of 78% (m.p. = 239-241⁰ C, TLC RF=0.22, HRMS = 276.0754 for C₁₀H₁₃N₂O₆F, calculated 276.0757) (appendix 2).

I) RADIOLABELLED FUF (¹⁴ C LABELLED) FUCOSYL-5-FLUOROURACIL

TLC analysis showed a single spot with TLC RF=0.22, the same as for the authentic FUF with the same solvent system. The starting materials for L-[1-¹⁴C]fucosyl-5-fluorouracil included a ¹⁴C at the 1' position, L-[¹⁴C]fucose (0.149mg, 50 mCi, 55 mCi/mmol), obtained from Amersham Canada Limited, Oakville, Ontario. This was mixed with 0.6 mg of cold L-fucose as part of the regular starting materials. The specific activity was decreased to 10.94 mCi/mmol.

The radioactive purity was determined by LSC of the TLC sections, (see table 3) with sections 4 through 10 corresponding to compound (3) in figure 55 (see appendix 2). These sections account for 99.9% of the activity of the TLC plate. Therefore, compound (3) in figure 43 represents radiolabelled 1(β -L-[1-¹⁴C]fucosyl)-5-fluorouracil with a radiochemical purity of 99.9%.

Table 3 LSC of TLC analysis of ^{14}C labelled FUF showing the counts obtained from the scrapings of each section of the TLC plate

SECTION	# OF COUNTS	% OF TOTAL ACTIVITY
1	7	0
2	0	0
3	36	0.1
4	5846	4.5
5	10325	7.9
6	23135	17.7
7	25390	19.5
8	56384	43.3
9	25286	19.4
10	7035	5.4
11	2021	1.5
12	19	0
13	0	0
14	0	0

ii) SYNTHESIS OF $[6-^3\text{H}]$ LABELLED FUF

TLC analysis showed a single spot (RF=0.22) using the same solvent system.

The compound (4) (2.45 mg), figure 56, had an activity of 425 μCi . The radiochemical purity of the was determined by the same method as with the final ^{14}C product. The results are given in table 3.

Table 4 LSC of plate scrapings from TLC analysis of ^3H labelled FUF used to determine the radiochemical purity.

SECTION	# OF COUNTS	% OF TOTAL ACTIVITY
1	5	0
2	26	0.1
3	172	0.2
4	184	66.9
5	50006	29.3
6	21843	1.9
7	1425	0.6
8	419	0.4
9	319	0.3
10	246	0
11	3	0
12	6	0
13	16	0
14	11	0

The area of the plate corresponding to 1-(β -L-fucosyl-5-fluoro-[6- ^3H]-uracil (RF=0.22) are fractions 5 through 7. These fractions represent 73,274 counts out of the total 74,681 counts for the total plate. The radiochemical purity of compound (4) represented by these fractions is 98.1%.

B) NEUTRON ACTIVATION ANALYSIS (NAA) STUDY

i) STANDARD CURVES

The NAA study involved neutron activation of F using the $^{19}\text{F}(\text{n},\gamma)^{20}\text{F}$ reaction. The ^{20}F decays emitting a quantifiable γ photon (1634 keV) with a half-life ($T_{1/2}$) of 11 seconds. Standards, containing incremental amounts of F, were irradiated and counted at 1634 keV to construct a calibration curve (figure 17).

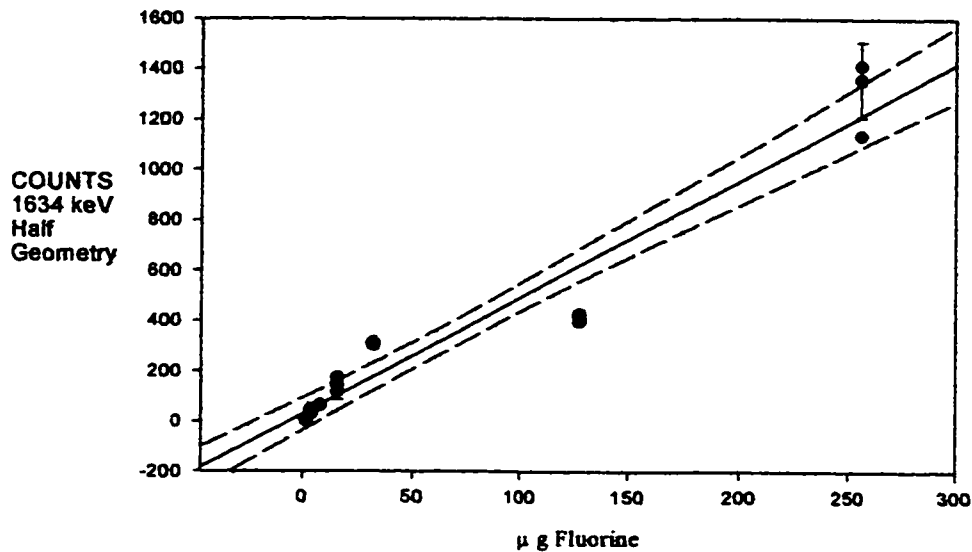


Figure 17 F standard curve, a linear regression plot of mean counts at 1634 keV with error bars representing standard deviation from the mean vs $\mu\text{g F}$ for Half Geometry samples (———represents the 95% confidence limits). Derived from this plot; Coefficients are: $b[0] = 28.23$, $b[1] = 4.64$ and $r^2 = 0.93$.

It was also possible that the target size (volume occupied) in the sample vial might affect the results. Therefore, two sets of calibration curves were constructed representing each of two sample geometries, one set for full sample vials (full geometry, figure 18) and the second set for samples occupying 50% or less of the vial volume (half geometry, figure 17). From these calibration curves, the μg of F in a sample is correlated with activity at 1634 keV.

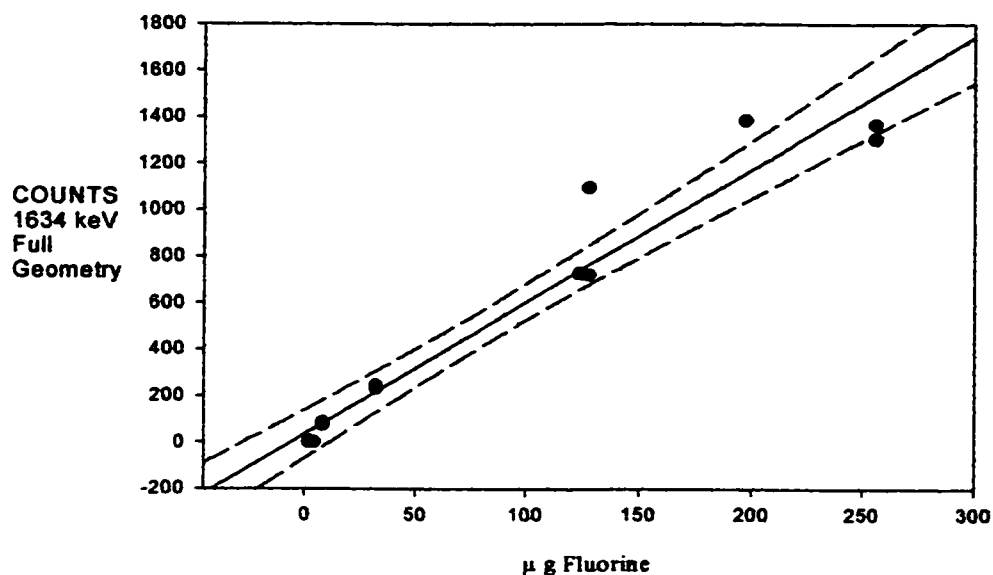


Figure 18 F standard curve, a linear regression plot of counts at 1634 keV vs $\mu\text{g F}$ for Full Geometry samples ($r^2 = 0.94$ — represents the 95% confidence limits). Derived from this plot; Coefficients: $b[0]=36.20$, $b[1]=5.68$ and $r^2 = 0.94$.

The most significant interference in this method is not from contamination by extraneous F, but from a nuclear side reaction. NA of Na also produces ^{20}F via the $^{23}\text{Na} (\eta, \alpha) ^{20}\text{F}$ reaction. Calibration curves were constructed relating activity at 1634 keV with incremental mass standards of Na. for full (figure 21) and half geometry (figure 19) samples.

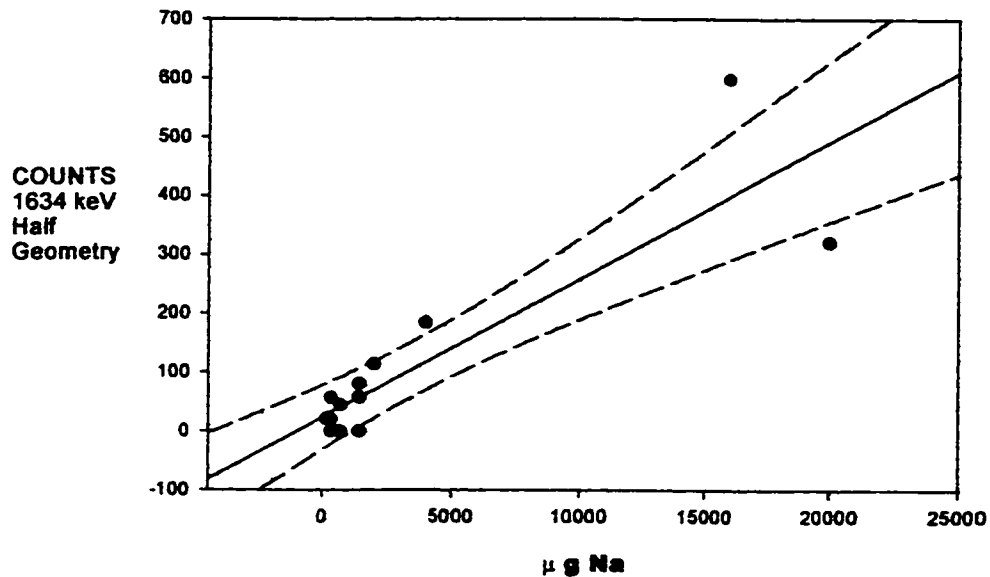


Figure 19 Na standard curve, a linear regression plot of counts at 1634 keV vs $\mu\text{g Na}$ for Half Geometry (— represents 95% confidence limits). Derived from this plot; Coefficients: $b[0]=23.83$, $b[1]=0.02$, $r^2=0.77$.

This competing activation (η, α) reaction occurs in a fixed ratio, as a function of the irradiating neutron spectrum, to a parallel $^{23}\text{Na}(\eta, \gamma)^{24}\text{Na}$ reaction. Fortunately, as well, the ^{24}Na decays emitting a quantifiable γ photon at 1368 keV. Calibration curves were constructed relating the activity at 1368 keV to the incremental mass Na standards for half (figure 20) and full (figure 22) geometry samples.

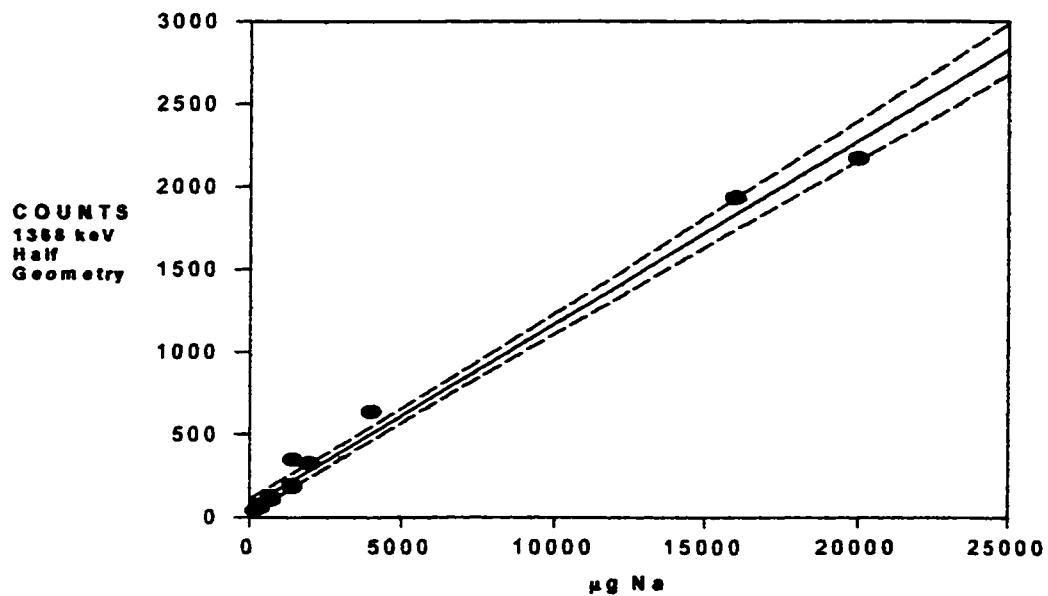


Figure 20 Na standard curve, a linear regression plot of counts at 1368 keV vs $\mu\text{g Na}$ for Half Geometry (— represents 95% confidence limits). Derived from this plot; Coefficients: $b[0] = 60.15$, $b[1] = 0.111$, $r^2 = 0.989$.

The occurrence of these reactions in a fixed ratio provides a tool for determining Na produced ^{20}F in a given sample. The calibration curves were used to establish the ratio of the competing Na activation reactions.

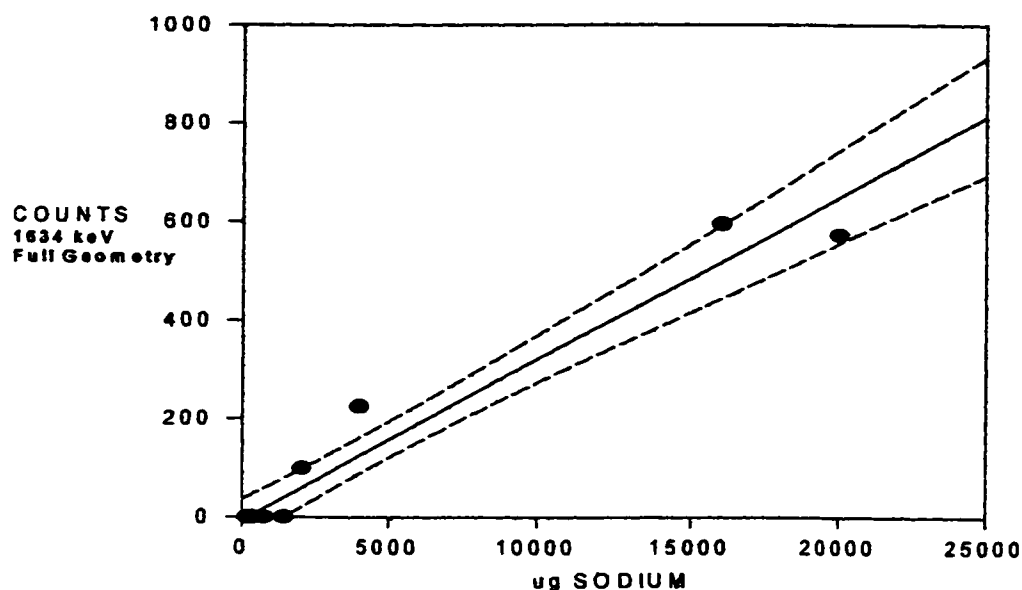


Figure 21 Na standard curve, a linear regression plot of counts at 1634 keV vs $\mu\text{g Na}$ for Full Geometry (— represents 95% confidence limits). Derived from this plot; Coefficients: $b[0] = 6.384$, $b[1] = 0.033$, $r^2 = 0.95$.

First, the mass of Na present in a sample is determined using the calibration curves for half (figure 20) and full (figure 22) geometry samples. Then the contamination to be expected from the Na is determined using the calibration curves in figures 17 (half geometry) and 19 (full geometry).

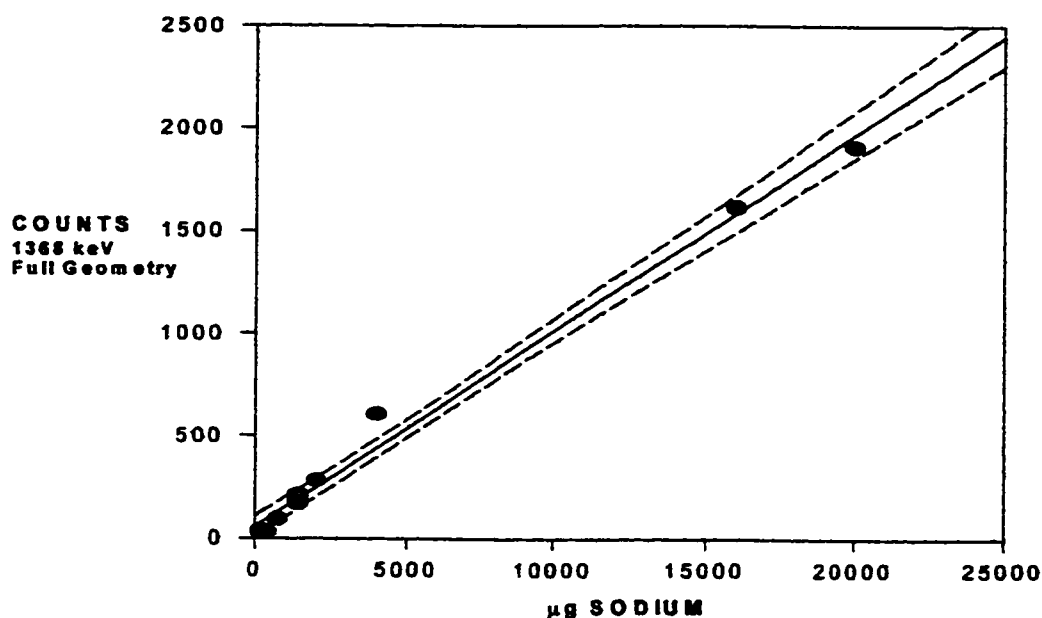


Figure 22 Na standard curve, a linear regression plot of counts at 1368 keV vs $\mu\text{g Na}$ for Full Geometry (— represents 95% confidence limits). Derived from this plot; Coefficients: $b[0] = 58.26$, $b[1] = 0.096$, $r^2 = 0.9904$.

The calibration curves in figures 20 (half) and 22 (full geometry) are used to correlate the counts, due to the $^{23}\text{Na}(\eta,\gamma)^{24}\text{Na}$ reaction, at 1368 keV with the μg of Na. For a given sample, a method of correlation of the Na calibration curve information, allows for the determination of activity at 1634 keV due to Na interference (see Appendix 3). The specific calculations are outlined in the appendix as determined by the following procedure. After neutron activation of a sample, the activity at 1634 and 1368 keV are measured. The mass of Na was determined by using the calibration curve. The activity at 1368 keV was used to determine interference via the figure 20 (full geometry-figure 22) calibration curve (with the corresponding derived equation, Appendix 3). This Na mass represents activity at 1634 keV as correlated with the figure 19 (full geometry-figure 21) calibration curve (via equation Appendix 3). The equations

derived from all of the standard curves are summarized in Appendix 1. Preceding the equations, are the mathematical details correlating the standard curves with the sample results to determine Na interference. As a double check of the data interpretation, the fixed ratio relationship of the 1634 and 1368 keV reaction activities were plotted directly (figures 23 and 24).

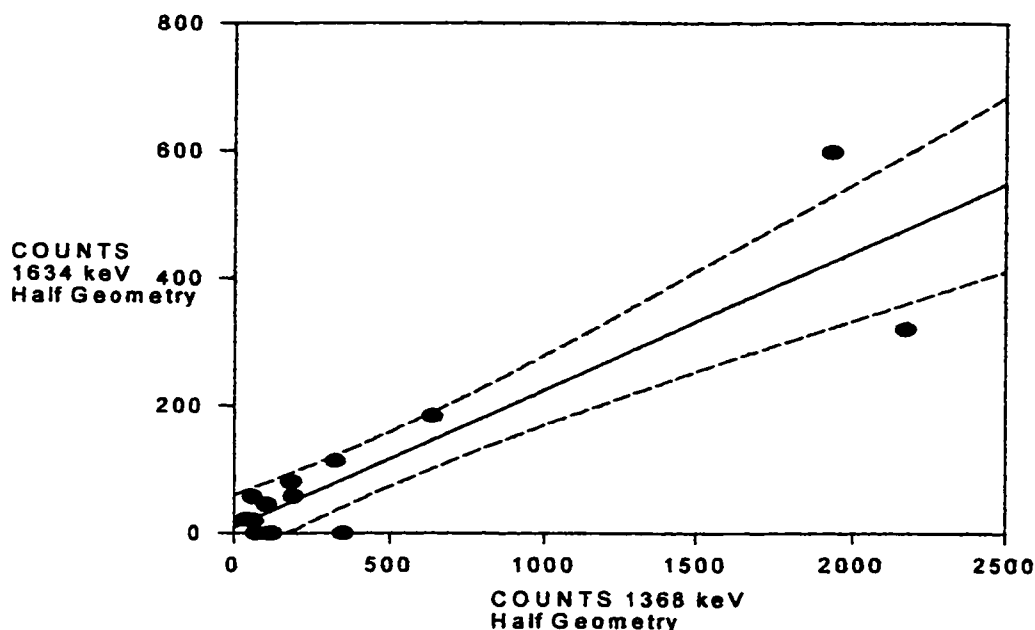


Figure 23 Na standard curve half geometry linear regression plot relating the activity detected at the two γ energies for incremental standards of Na via counts 1634 keV vs 1368keV. (— represents 95% confidence limits). Derived from this plot; Coefficients: $b[0] = 9.065$, $b[1] = 0.2157$, $r^2 = 0.80918$.

For a given sample, the activities at 1368 keV and 1634 keV were measured and their correlation determined. Figure 23 and figure 24 represent this correlation for "Half" and "Full" geometries, respectively.

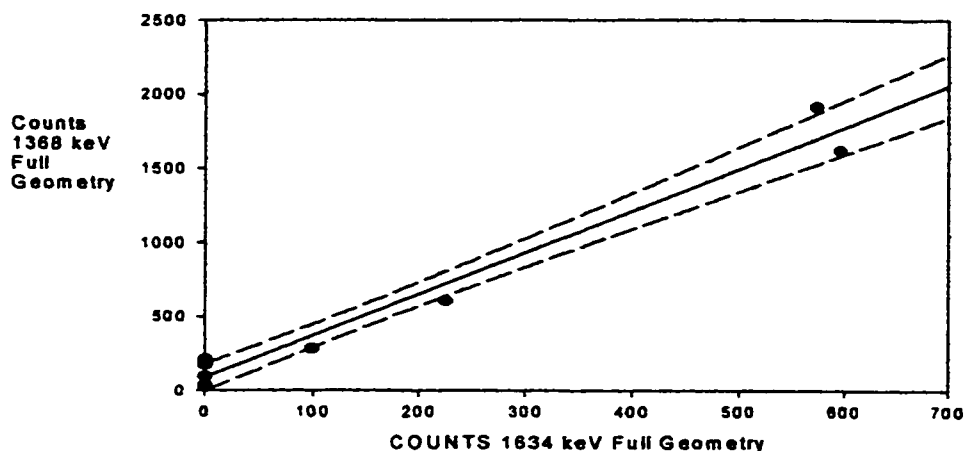


Figure 24 Na standard curve full geometry linear regression plot relating the activity detected at the two γ energies for incremental standards of Na via counts 1634 keV vs 1368keV. (— represents 95% confidence limits). Derived from this plot; Coefficients:

The measured activity at 1368 keV represents Na, with the mass determined from figures 22 & 24 for half & full geometries respectively. The measured activity at 1634 keV represents the total ^{20}F decay, produced from conversion of both ^{18}F and ^{23}Na . From this total 1634 keV activity, the Na source activity, as determined from figure 21 & 23 was subtracted, leaving the remaining activity of F source. To determine the mass of F represented by this activity, the fluorine standard curves were used. Activity was attributed to μg F as correlated with the F calibration curves in figure 17 (half geometry) & 18 (full geometry)

ii) FLUORINE ANALYSIS AFTER DOSING WITH 5FU OR FUF

After determining the amount of F in each sample as described, following correlation with corresponding data (the recorded mouse and tissue sample mass), the concentration or amount of fluorine in each sample was mathematically derived as the percent injected dose per organ sample. The results were obtained for both 5FU and

FUF for predetermined intervals after administration. The data for 5FU and its interpretation to % injected dose for each organ are shown in tables 8 to 12. Final summary of the 5FU data is shown in table 13 and represented graphically expressed as % injected dose per organ Vs time (minutes).

The initial discussion pertains to examining the data and results from the calibration curves relative to the mass of F within detection limits. This initial discussion is intended as a general overview of the results with attention to the optimum detection range expected, the normal drug dosage range and the expected drug distribution. Of particular interest is the interrelationship of these factors to one another and how the optimum detection range compares with the normal dosage range and subsequent distribution. The discussion will then focus on the data obtained from 5FU and FUF distribution studies in animals.

a) Dosage & Detection of 5FU & FUF by NAA Relative to Calibration Results

The preliminary detection limit dosages of 5FU was high (100 mg/kg), relative to the recommended dose of 12 mg/kg, to achieve detectable levels in test tissues. The method would not be suitable for human studies. In addition, the results of the calibration curves data can be used as a consideration for detection limits relative to dose administered. The F calibration data (figure 17 & 18) show the least variation (most accurate data) from 150 to 250 μg F per sample. The translation represented by this mass of F; assuming uniform distribution in all tissues, the liver as the representative organ, a mass of 2 g in a 20 g mouse, calculates back to an initial dose of more than 600 mg/kg (see Appendix 1, item 2). With an initial dose of 100 mg/kg ($684/100 = 6.84$), the drug would need to be concentrated in the target tissue 6 to 7 fold to be in the optimum detectable range. These considerations lead to the following conclusions concerning NAA as a method of analysis for F in a 5FU biodistribution study;

1) The NAA is not a sufficiently sensitive method of analysis for FUF & 5FU due to the high doses of 5FU and FUF required to achieve results within the detectable limits.

2) The delivery system of the 5FU prodrug would need to be effective enough to deliver a 7 fold enhancement of 5FU in the target tissue.

In conclusion, since the detection limits of NAA for 5FU at a 100 mg/kg dose, would be satisfactory only in the case of a 7 fold enhancement of delivery to the test tissue, this is not a satisfactory method of analysis.

b) NAA Results for 5FU Animal Studies

The results for 5FU are shown in Appendix 3 with the only discernable feature being the tail. Despite the variability of the results for the distribution of 5FU over time, the study does provide some information about 5FU's biodistribution and, at the very least, further insight into the methodology and technique employed.

The 5FU concentration in the tail is significantly higher than in other organs, ranging from 18% to 55%. This indicates poor tail vein injection technique rather than some distribution mechanism. This results in concentrations in the tail with an ultimate reduction of the administered dose by 18 to 55%. Nonetheless, of interest is the distribution of 5FU after entering the circulation. The following discussion focuses on the results of the data of the remaining test tissues, liver, kidney, tumor and GIT, recalculated after adjusting the administered dose(for loss in tail). The data are corrected for loss of dose in the tail to provide a clearer representation of 5FU distribution.

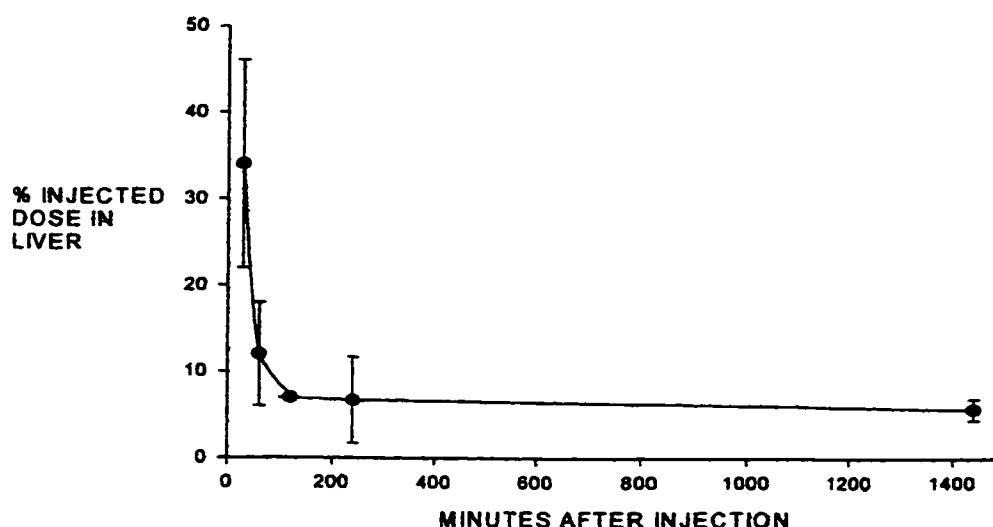


Figure 25 5FU distribution to the liver expressed as mean of % injected dose(solid line, vertical bars representing the standard deviation from the mean) vs time (minutes).

The liver results (figure 25), are consistent with results for drugs that undergo metabolic conversion in the liver. During the first 30 to 60 minutes the levels of 5FU are a little higher than in the other tissues tested, reflecting initial distribution and liver uptake of 5FU. Metabolic conversion of 5FU is reflected by continuing higher levels in the liver relative to the other tissues, with subsequent redistribution of the metabolite (figure 26).

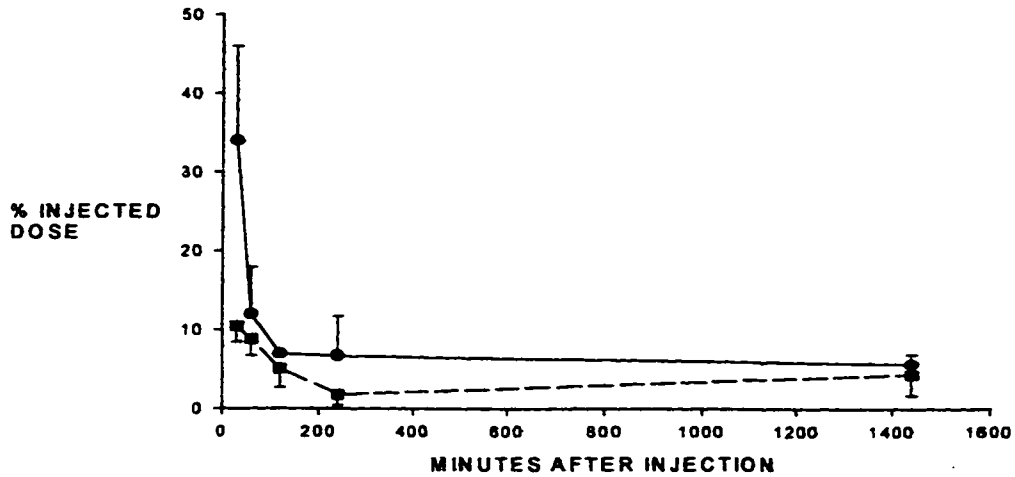


Figure 26 5FU distribution to the liver (black line with standard deviation (stdv) positive) and kidney (dashed line with stdv negative) tissue expressed as the mean of % injected dose vs time

After two to four hours, the 5FU levels in the liver drop off rapidly to levels of a similar range to that of the other test organs. This decrease of distribution to the liver to levels relatively lower than to other tissues continues from 4 hours on. The profile of the detected F levels in the remaining test organs relative to the liver reflect the subsequent redistribution of this metabolite. The last results show a drop of 5FU detected in the liver to nearly below levels detected in the kidney for the 1440 minute time interval.

Overall high levels of 5FU reflect the initial distribution of the administered dose. Confirmation of the subsequent metabolism, redistribution and elimination of 5FU is revealed by examination of the small differences in 5FU distribution between tissues. 5FU is involved in metabolism in many tissues as part of the anabolic pyrimidine pathways. Ultimately, a proportion undergoes catabolism in the liver, with eliminated via excretion in the urine and/or feces.

Examination of the result for kidney and liver analysis over time are consistent with this pattern of metabolism. The kidney shows some initial distribution with gradual decline over the first few hours, reflecting the initial distribution of the drug and some excretion of 5FU. The distribution of 5FU to the kidney, relative to the liver, from 2 to 24 hours (120 minutes on), the kidney levels are initially lower, after 2 hours the levels increase relative to the liver. After the initial liver uptake and metabolism, 5FU shows steadily increasing levels in the kidney as the metabolic products are redistributed to the kidney and excreted in the urine.

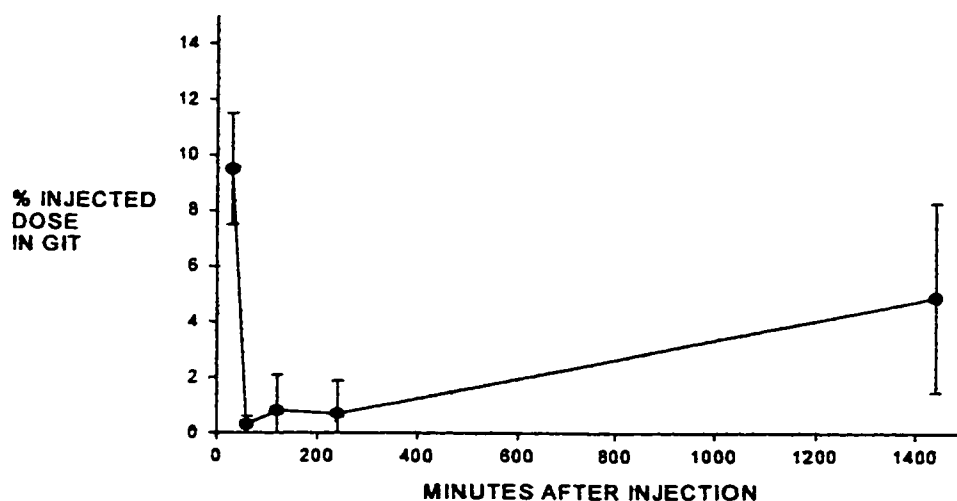


Figure 27 Distribution of 5FU to GIT over time expressed as mean (solid line) of % injected dose (vertical bars representing stdv) vs. time.

The 5FU distribution to the GIT are shown in figure 27. The pattern of distribution, relative to the other tissues, reflect some initial GIT distribution with high levels to start, then dropping from 30 to 240 minutes. However, from 240 to 1440 minutes a very gradual rise in 5FU detected reflects a small proportion of GIT excretion.

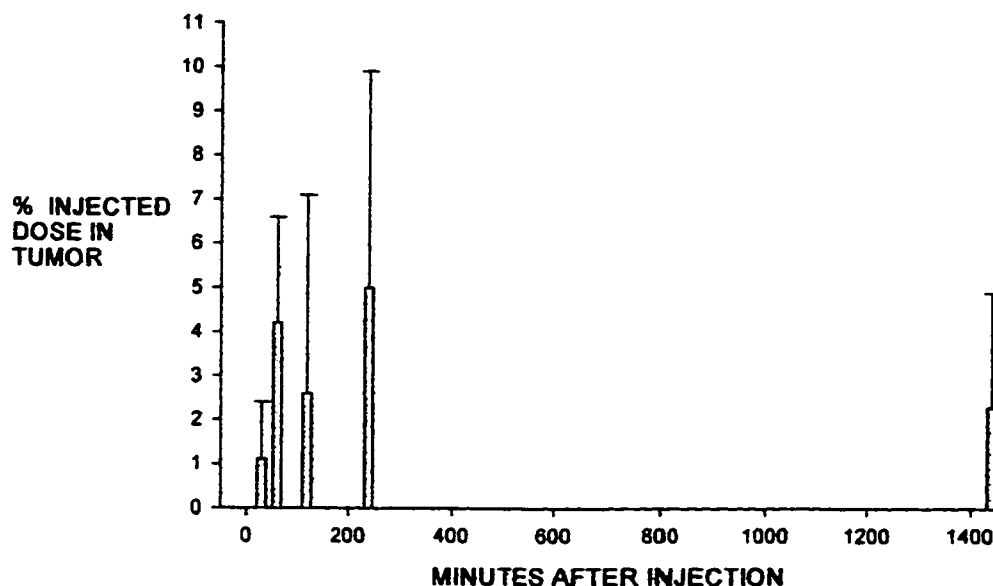


Figure 28 Tumor distribution for 5FU expressed as mean (vertical bar) of % injected dose (with vertical lines representing stdv) vs time.

The tumor tissue results, like other tissues, show some initial 5FU distribution that slightly increases over the first two hours (see figure 28). After the initial detectable levels, 5FU tumor levels show a steady decrease in concentration over time. Overall, the removal of 5FU from the subject is supported by initial concentration in the liver while undergoing metabolic conversion, then excretion via the urine with a small proportion of GIT excretion.

c) Biodistribution of FUF in Mice

Graphic interpretation of the data, expressed as % injected dose Vs time, like the 5FU complete plot, was difficult to interpret, but did reveal a feature also common to the 5FU animal data. The high tail activity which was also attributed to poor FUF administration technique resulting in extravasation at the site of injection. Therefore, the dose administered was corrected for FUF in the tail.

The following is a summary of FUF distribution results followed by a comparison of this data with the results for the 5FU data. The liver FUF (figure 29) data show initially high levels with a steady decrease over time.

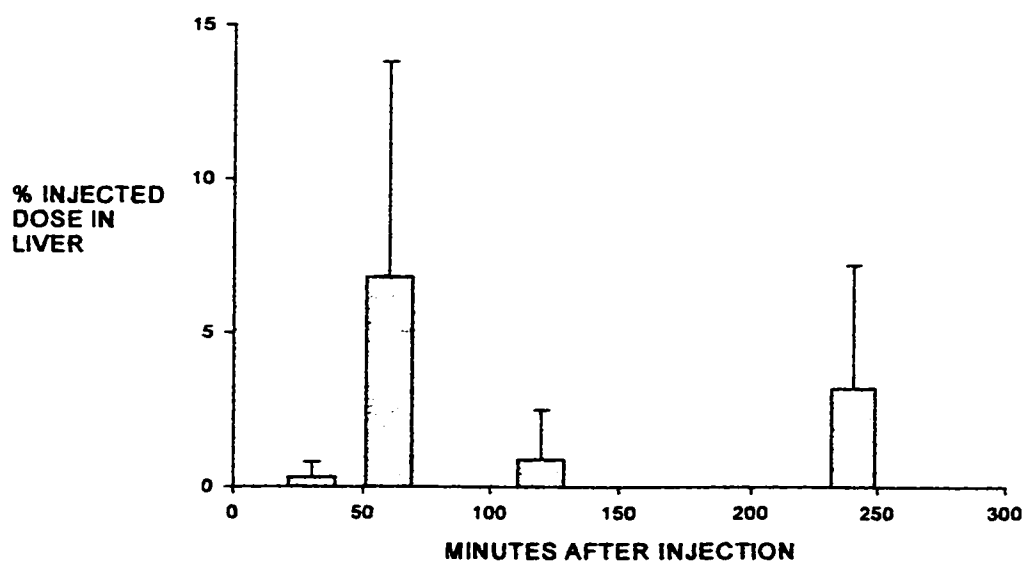


Figure 29 Distribution of FUF to liver expressed as mean of % injected dose (vertical bar with vertical line representing stdv) vs time.

FUF distribution in the GIT (figure 30) shows some initial uptake followed by a small decrease and then gradually increasing overtime.

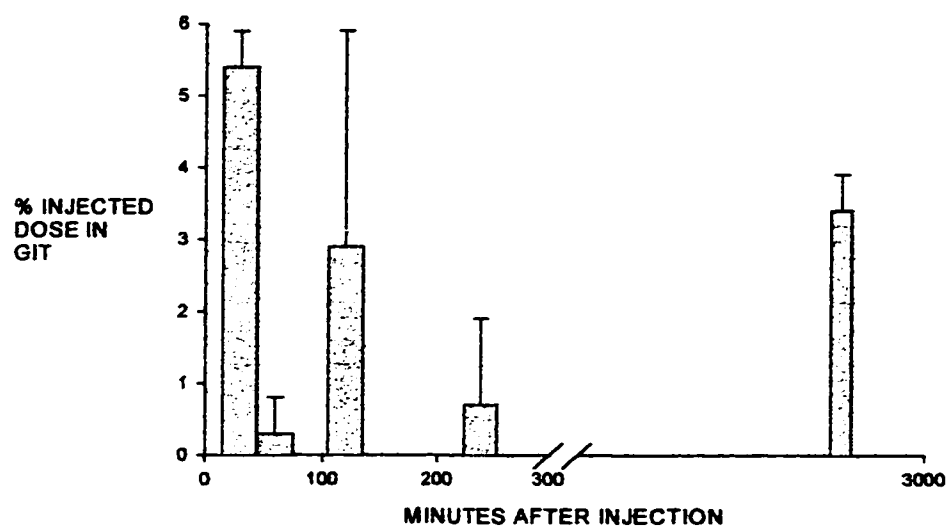


Figure 30 Distribution of FUF to GIT expressed as mean of % injected dose (vertical bars with vertical lines representing stdv) vs. time.

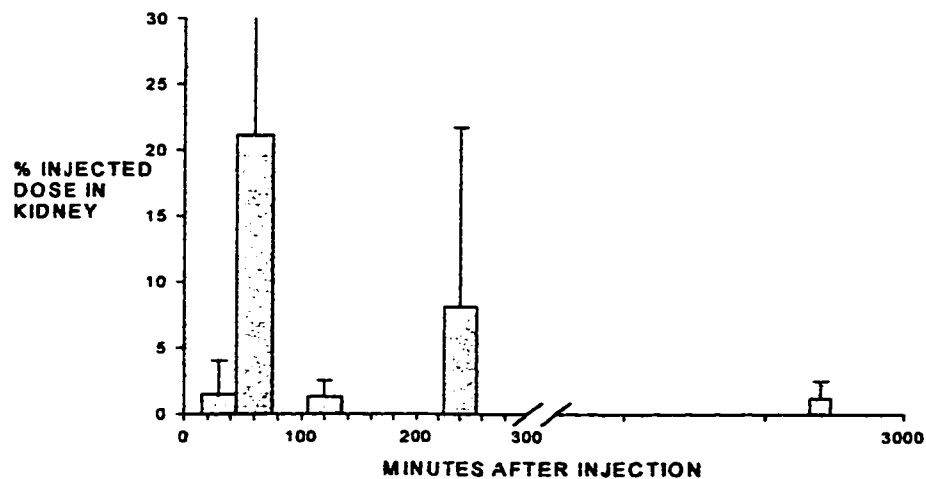


Figure 31 FUF distribution to kidney expressed as mean of % injected dose (vertical bars with vertical lines representing stdv) vs time.

The kidney levels show the highest initial results relative to the other test tissues. After the initially high levels there is a steady decrease in kidney levels over time.

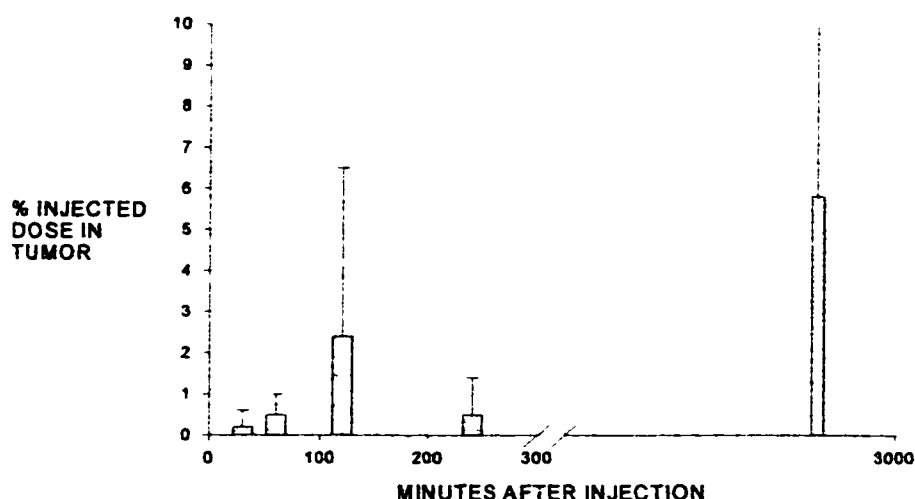


Figure 32 FUF distribution to the tumor expressed as mean % injected dose (vertical bars with vertical lines representing stdv) vs time.

Initially the concentration of FUF in tumor are relatively low. From 2 hours to 24 hours the tumor levels gradually increase, especially in comparison to the pattern in other tissues. Due to the loss of a proportion of the dose in the tail and for purpose of consistent results for comparison, a correction factor was also applied to the FUF data. The % injected dose of each organ is recalculated after first subtracting the portion of the dose deposited in the tail from the initial dose. This reduced dose was then taken as the initial dose and the % injected dose in each organ recalculated.

d) Relative Comparison of 5FU and FUF Animal Data

The following is a table presented to allow a rough comparison of the distribution data of 5FU and FUF over time to organs tested (see table 5).

Table 5 Comparison of 5FU and FUF animal data corrected for tail loss, expressed as mean of % injected dose per organ, + /- standard deviation

MIN	LIVER	LIVER	KIDNEY	KIDNEY	TUMOR	TUMOR	GIT	GIT
	5FU	FUF	5FU	FUF	5FU	FUF	5FU	FUF
30	34.40	0.30	10.53	1.47	1.07	0.20	9.53	5.43
	12.59	0.52	4.04	2.54	1.29	0.35	2.01	0.47
60	11.80	6.83	8.77	2.95	4.17	0.47	0.27	0.33
	6.05	6.95	1.97	1.71	2.42	0.57	0.25	0.57
120	7.37	0.90	5.07	1.27	2.60	2.37	0.77	2.93
	0.32	1.56	2.40	1.21	4.50	4.10	1.32	3.00
240	6.67	3.17	1.77	7.90	4.97	0.53	0.70	0.70
	5.13	4.03	1.42	13.52	4.91	0.92	1.21	1.21
1440	5.70		4.40		2.33		4.87	
	1.25		2.66		2.35		3.40	
2880		0.0		1.23		5.77		3.70
		0		1.43		6.13		0.50

If FUF liver levels were initially high with steady decrease over time, as with 5FU, this would be consistent with drugs which undergo metabolic conversion in the liver.

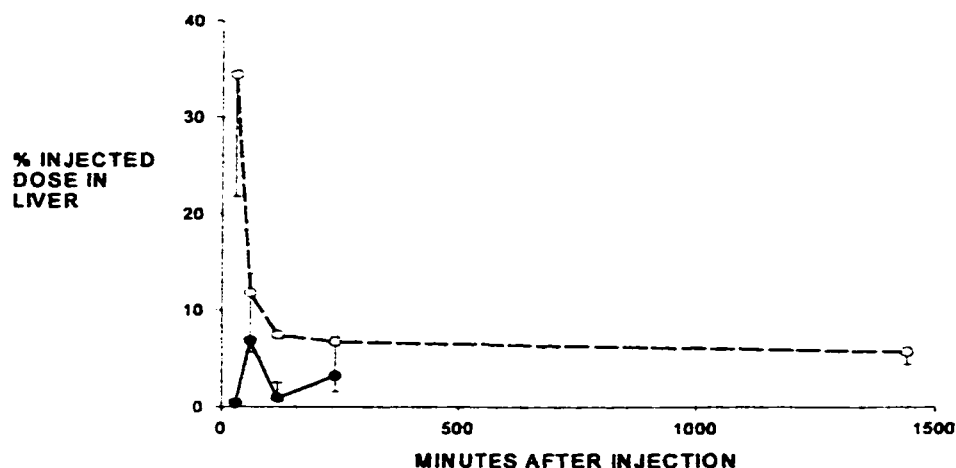


Figure 33 Comparison of 5FU (dashed line with open circle and negative vertical line representing stdv) and FUF (solid line with filled circle and positive vertical line representing stdv) distribution to the liver using the mean of the % injected dose vs time.

For 5FU, even with very large variability, there is an initial distribution to the liver (34%) with steady decrease over time(to 5%). FUF distribution to the liver, however, is negligible to start but actually increases over time (table 5, figure 33, almost 10 fold). On the surface, this would indicate the FUF molecule is initially distributed elsewhere, gradually finding its way to the liver as a secondary distribution

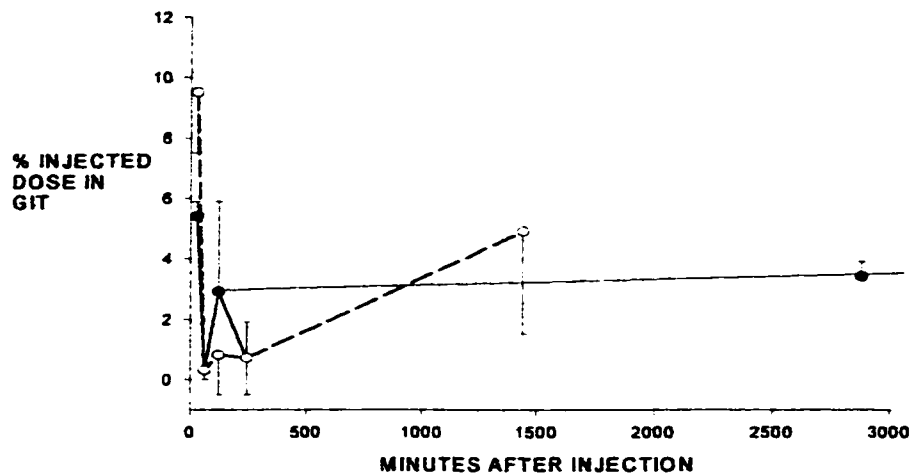


Figure 34 Comparison of 5FU (dashed line with open circle and negative vertical line representing stdv) and FUF (solid line with filled circle and positive vertical line representing stdv) distribution to the GIT using the mean of the % injected dose vs time.

The GIT FUF results start off similarly to 5FU. There is some initial distribution to the GIT with, some increase from 2 to 24 hours. This would be consistent with a proportion of fecal excretion, reflecting distribution to GIT tissues then excretion into GIT contents followed by slow movement of the contents out of the system from there. The slow GIT process may result in some accumulation which would explain the slight increase from 2 to 24 hours.

Although the precision of the analysis was unsatisfactory, it can be considered that the data profile for FUF distribution in mice differs from 5FU distribution. Especially in the kidney and liver. Distribution of both 5FU and FUF to tumor tissue doesn't seem to follow a discernable pattern (see table 5).

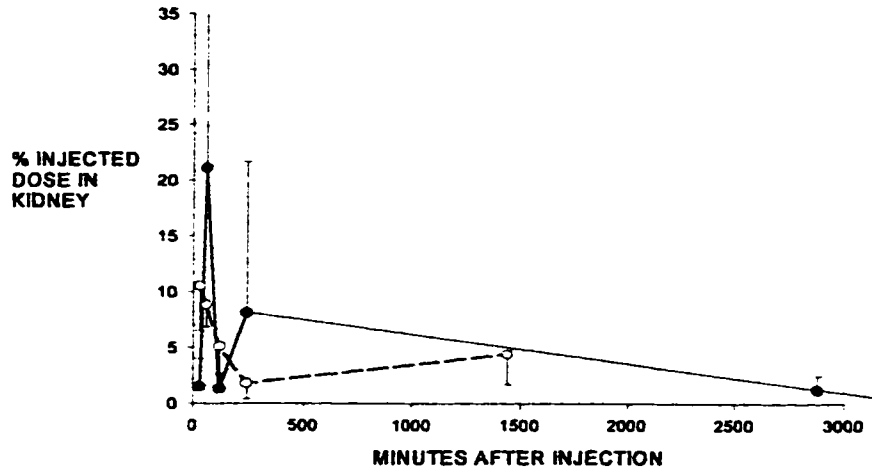


Figure 35 Comparison of 5FU (dashed line with open circle and negative vertical line representing stdv) and FUF (solid line with filled circle and positive vertical line representing stdv) distribution to the kidney using the mean of the % injected dose vs time.

Distribution to the kidney differs from 5FU & FUF over time. Similar to the liver distribution, 5FU to the kidney is, initially, relatively high, with a steady decrease over time. The FUF kidney distribution is initially low, steadily rising over time. FUF may be trapped elsewhere initially, with subsequent cleavage, resulting, ultimately in excretion in the urine,

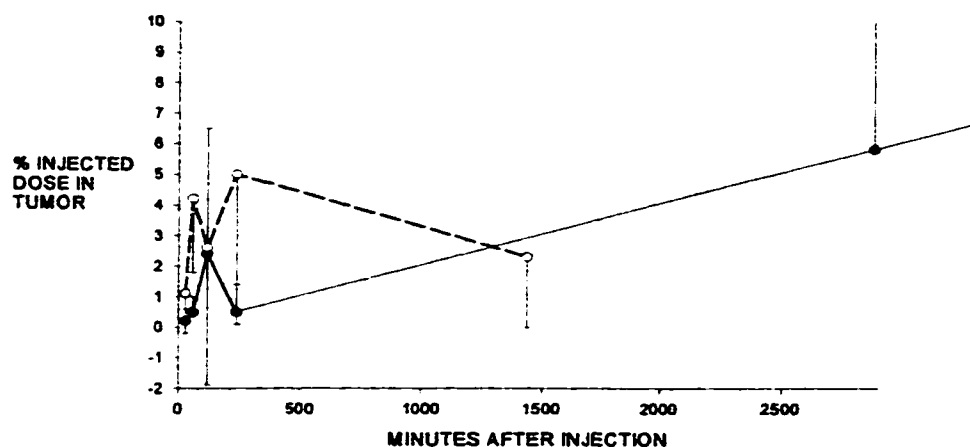


Figure 36 Comparison of 5FU (dashed line with open circle and negative vertical line representing stdv) and FUF (solid line with filled circle and positive vertical line representing stdv) distribution to the tumor using the mean of the % injected dose vs time.

After initially low levels, FUF tumor levels show steady increase from 2 to 24 hours. This may reflect a slow trapping and accumulation of FUF by immunorecognition sites, with subsequent redistribution to the kidney.

Due to the variability of results and the discussed inherent problems with using neutron activation analysis as the detection tool in this particular study, more information was needed. Subsequent work was done using a dual label technique.

C) DUAL LABELLED FUF BIODISTRIBUTION STUDY

A biodistribution study using dual labelled, ^3H and ^{14}C , FUF has also been undertaken to determine the distribution of FUF and to determine the extent of base / sugar cleavage. This is important to determine if FUF is acting as a prodrug to deliver 5FU to the liver. This study will provide evidence as to where and when the FUF is cleaved to release 5FU.

The radionuclides used for this study were ^{14}C and ^3H labelled compounds. The test pharmaceuticals studied were ^3H labelled fucosyl-5-fluorouracil, labelled with ^3H at the "6" position of the 5FU portion of FUF, fucosyl-5-fluoro-[6- ^3H]-uracil ($^3\text{HFUF}$) and the ^{14}C labelled compound with a ^{14}C label at the "1" position of the sugar (fucose) moiety, [1'- ^{14}C]fucosyl-5-fluorouracil ($^{14}\text{CFUF}$). ^{14}C and ^3H are both radionuclides that decay exclusively via β emission of different but overlapping characteristic energies.

The mice were administered labelled FUF material containing predetermined amounts of fucosyl-5-fluoro-[6- ^3H]-uracil and [^{14}C -1']-fucosyl-5-fluoro-uracil in order to provide the appropriate overall dosage (mg/kg) while maintaining each radionuclide within optimum detection limits. The ^{14}C activity was taken to represent the distribution of the fucose portion of the FUF molecule, while the ^3H activity was taken to represent the 5FU portion of the FUF molecule. With their overlapping β spectra, it was necessary to separate and determine the activity of each β emitting radionuclide. Two significant resolution problems occur when attempting the direct analysis of biological samples containing both of these radionuclides:

- 1) Overlap of the pulse height spectra of ^{14}C and ^3H necessitate resolving one from the other. Any such resolution would be at the expense of counting efficiency.
- 2) Variable quench due to the physical and chemical properties of the biological samples themselves has a further negative impact on the separation and counting efficiencies of the radionuclides.

Both of these problems are usually accounted, but not compensated for, by the use of a method of "Dual Label" counting in a liquid scintillation (DLLSC) system. The

"Dual Label" method of resolving the radionuclides is a complicated, time consuming method involving several procedures subject to loss of efficiency and therefore increasingly inaccurate.

To overcome the primary concerns of energy spectrum overlap and interference from quench, a different method of sample treatment was selected. The biological samples were first processed in a biological oxidizer. This combustion method allows for the separation of the radionuclides and results in samples in which quench correction is not a concern. Consequently, this technique allows for the separation of the two β emitters without complicated window setting and efficiency calculations.

Figure 37 shows the distribution of ^3H and ^{14}C to the liver as the mean of the % injected dose per organ.

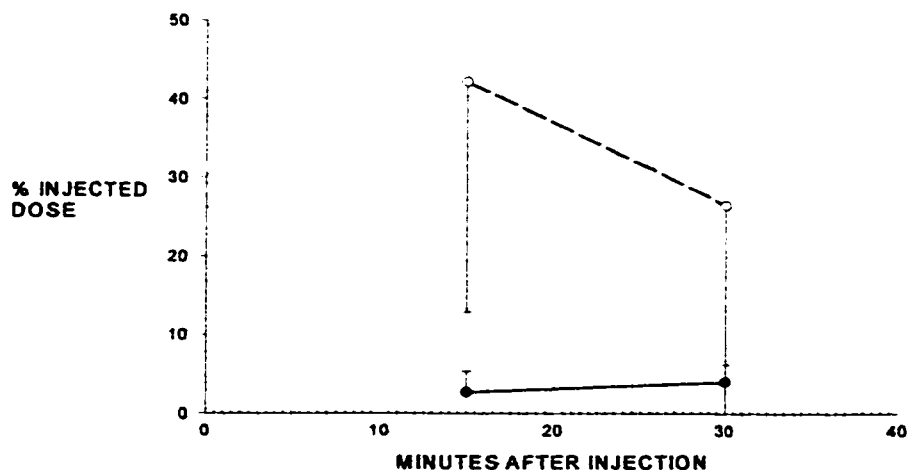


Figure 37 Distribution of labelled FUF to the liver (dashed line with open circle represents 5FU with negative vertical line representing stdv and solid line with filled circles representing fucose with positive vertical line representing stdv) expressed as the mean and stdv of the % injected dose vs time.

It is possible to discern a pattern of distribution to the liver, from 15 to 30 minutes, in figure 35, of the ^3H and ^{14}C labelled components of FUF. These data indicate that at least a proportion of the FUF dose, has been cleaved and that the base portion of the molecule accumulates in the liver. The cleavage appears to represent a significant proportion of the FUF dose within 15 to 30 minutes, even when considering the large deviation of the data.

The 5FU component in the liver declines more rapidly between 15 and 30 minutes than in any other tissue. In sharp contrast, the fucose liver distribution is the only tissue result showing an increase from 15 to 30 minutes. This definitely supports a conclusion of FUF cleavage prior to, or at least during the 15 to 30 minute period.

Figure 38 shows the ^3H and ^{14}C distribution data for the tumor.

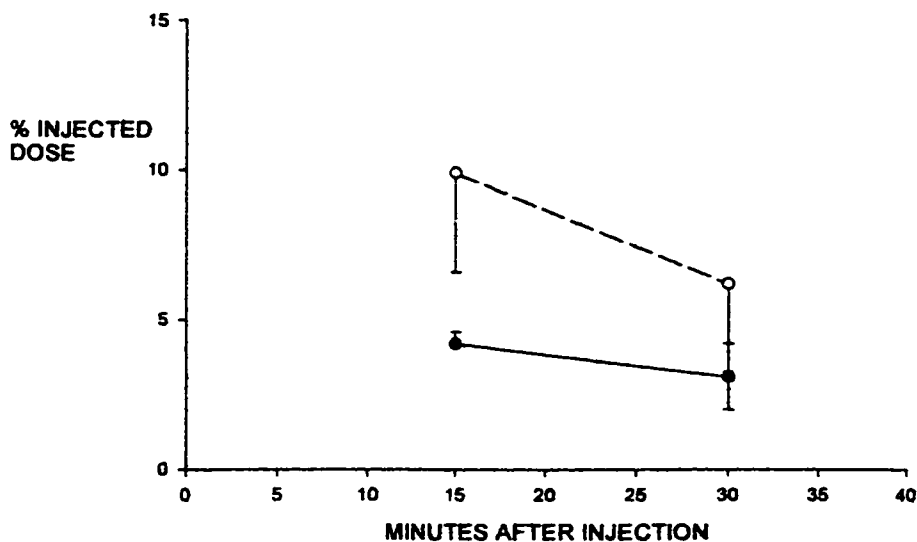


Figure 38 Distribution of labelled FUF to the tumor (dashed line with open circle represents 5FU with negative vertical line representing stdv and solid line with filled circles representing fucose with positive vertical line representing stdv) expressed as the mean and stdv of the % injected dose vs time.

In tumor tissue there are initially higher levels of both the base (^3H) and the sugar (^{14}C), with tritium levels being comparatively higher. The base levels follow a downward trend from 9 to 13 % after 15 minutes to 2 to 10 % after 30 minutes. The fucose levels do not follow the same pattern. Initial levels don't change much from 15 to 30 minutes at about 3 to 4 %. A model which may represent this type of outcome would be the following.

During initial distribution FUF is metabolized to its component base and sugar. This initial cleavage of the base-sugar complex is followed by metabolism and elimination of the base that is more rapid than the sugar elimination. A tissue of interest which is involved in the elimination of most foreign substances is the kidney. Figure 39 shows the kidney results with a comparison of the ^{14}C and ^3H vs time.

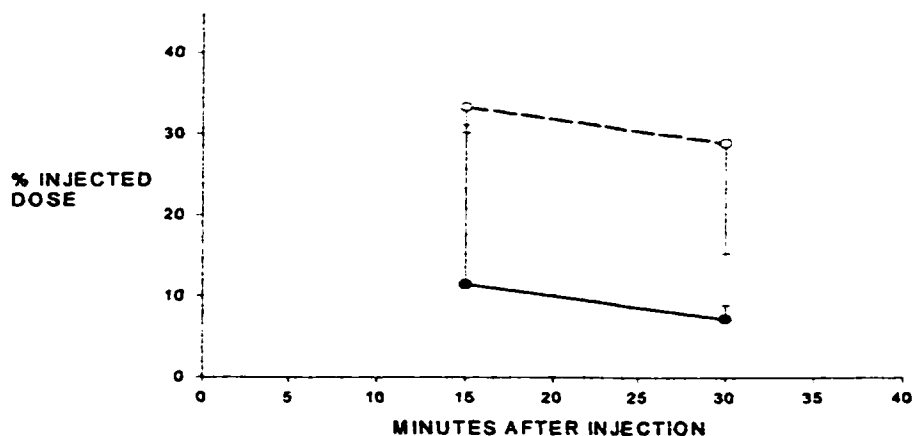


Figure 39 Distribution of labelled FUF to the kidney (dashed line with open circle represents 5FU with negative vertical line representing stdv and solid line with filled circles representing fucose with positive vertical line representing stdv) expressed as the mean and stdv of the % injected dose vs time.

There were relatively high levels of both ^{14}C and ^3H (30 to 34%) at 15 minutes. The tritium levels, representing the labelled base, remain fairly high after 30 minutes (15 to 40%). The ^{14}C levels, representing the labelled fucose, are low to start, with a slight increase after 30 minutes.

The differential pattern of distribution between the base and the sugar would tend to support the idea that the FUF molecule is broken down to its components rapidly after its administration. The remaining biological sample tested was the blood, with the results shown in figure 38 as a comparison of the % injected dose of ^3H and ^{14}C Vs time.

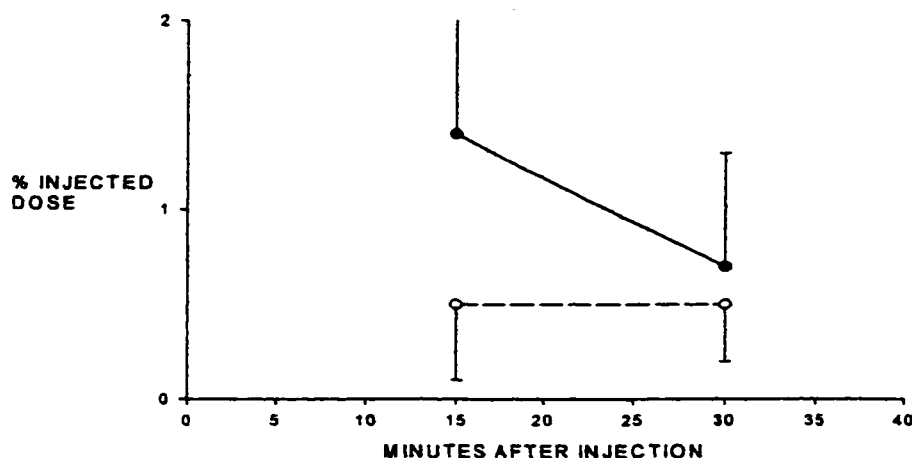


Figure 40 Distribution of labelled FUF to the blood (dashed line with open circle represents 5FU (^3H) with negative vertical line representing stdv and solid line with filled circles representing fucose (^{14}C) with positive vertical line representing stdv) expressed as the mean and stdv of the % injected dose vs time.

Relative to the other test tissues, the blood levels are low for both ^3H and ^{14}C , with levels at anytime below 3% of injected dose. The fucose portion of the molecule shows slight steady decline in blood levels from 15 to 30 to 60 minutes of 2% to 1% to .5%. The 5FU (^3H) levels show a fairly constant concentration from 15 minutes (0.4-0.8%) to 30 minutes (0.4 to 0.8%) to 60 minutes (0.5%).

Based on analysis of the pattern of radionuclide distribution, FUF is cleaved to its component base and sugar rapidly upon entering the system. This conclusion is based on the pattern of results obtained for tumor, kidney, and blood samples. In each of these tissues, the pattern of distribution of ^3H differed from that of ^{14}C . The only tissue samples analyzed that resulted in a similar pattern was for the liver.

V) SUMMARY & CONCLUSIONS

A) ANALYSIS OF FUF BY INAA

The detection limits for neutron activation analysis of samples for fluorine content are too high to be useful for this study. The results in IV. B. ii. a.) (p. 62) illustrate a comparison of the optimum detection limits for analysis of fluorine containing samples by this method with optimum detection limits. The sensitivity of this method would require a 70 fold concentration of the test drug to acquire the optimum detectable range.

In addition, the fluorine content of the samples is outside detection limits enough to be reflect by the variability of the results. The variability of the results in the detectable range, indicate they are not reliable.

B) DUAL LABEL FUF RESULTS RELATIVE TO METABOLISM

Analysis of the $^3\text{H}/^{14}\text{C}$ ratio would tend to support evidence of cleavage of the FUF molecule soon after administration. If the FUF molecule were intact until reaching the liver, where it is released as 5FU to exert its cytotoxicity, a certain pattern would be expected. That is, each component should show identical initial distribution, with concentration in the liver. Here cleavage would occur, releasing the components for redistribution. At this point the relative concentrations of the components would become disparate. The results indicate a diversity of distribution right from the beginning. This would be consistent only with initial cleavage of the FUF molecule.

VI) BIBLIOGRAPHY

- Abe, Y., Fukuda, H., Ishiwata, K., Yoshioka, S., Yamada, K., Endo, S., Kubota, K., Sato, T., Matsuzawa, T., Takahashi, T., Ido, T., "Studies on ^{18}F -Labelled Pyrimidines, Tumor Uptakes of ^{18}F -5-fluorouracil, ^{18}F -5-fluorouridine and ^{18}F -5-fluorodeoxyuridine in Animals", *Eur. J. Nucl. Med.*, **8**, 258 (1983)
- Abrams, D., Knaus, E., and Wiebe, L., "Tumor Uptake of Radiolabelled pyrimidine Bases and Pyrimidine Nucleosides in Animal Models I. [^3H]-5-fluorouracil.", *Int. J. Nucl. Med. Biol.*, **6** 97 (1979)
- Abrams, D., Knaus, E., Lentle, B. and Wiebe, L., "Tumor Uptake of Radiolabelled Pyrimidine Bases and Pyrimidine Nucleosides in Animal Models-II. [^3H]-5-fluoro-2'-deoxyuridine.", *Int. J. Nucl. Med. Biol.*, **6** 103 (1979)
- al-Arafaj, A. Ryan, C., Hutchinson, K. Mannan, R., Mercer, J., Wiebe, L. and McEwan, A., "An evaluation of [^{123}I] Iodoazomycin-araboside as a Marker of Localized Tissue Hypoxia in Patients with Diabetes Mellitus.", *Eur. J. Nucl. Med.*, **21**(2) 1338 (1994)
- Allen, P., "In Vivo Applications of NMR to Medicine", *Radiat. Phys. Chem.*, **24**(3/4) 419 (1984)
- Allen-Mersch, T., Earlam, S., Ford, C., Abrams, K. and Houghton, J., "Quality of Life and Survival With Continuous Hepatic Artery Floxuridine Infusion for Colorectal Liver Metastasis", *Lancet*, **344** 1255 (1994)
- Anderson, E. and Brockman, R., "Feedback inhibition of Uridine Kinase by Cytidine Triphosphate and Uridine Triphosphate.", *Biochim. biophys. Acta*, **91** 380 (1964)
- Appleman, E and Thompson, R., "Studies on the Aqueous Chemistry of Fluorine and Hypofluorous Acid", *J. Amer. Chem. Soc.*, **106** 4167 (1984)
- Ardalan, B., Buscaglia, M. and Schein, P., "Tumor 5-Fluorodeoxyuridylate Concentrations as a Determinant of 5-Fluorouracil Response.", *Biochem. Pharmacol.*, **27** 2009 (1978)
- Armstrong, R. and Diasio, R., "Metabolism and Biological Activity of 5'-Deoxy-5-fluorouridine a Novel Fluoropyrimidine.", *Can. Res.*, **40** 3333 (1980)
- Awumey, E., Somayaji, V., Wiebe, L., Tyrrell, D. and Paterson, A., "Synthesis, Hepatocyte Uptake and *in-vivo* Biodistribution of Lactosyl-9-b-D-arabinofuranosyl adenine (lactosyl-araA), a Proposed Pro-drug for Targeting the Delivery of 9-b-D-Arabinofuranosyl Adenine (araA) to Liver.", *Pharmaceutical Science Communications*, **4**(1) 59 (1993)
- Bading, J., Sigurdson, E., Finn, R., Yeh, S., Ginos, J., Kemeny, N. and Larson, S., "Transport Limits Cellular Entry of Hepatic Arterially Injected 5-Fluoro-2'-deoxyuridine in Human Intrahepatic Tumors.", *Drug Metab. Disposition*, **22**(4) 643 (1994)
- Baltarini, J., Morin, K., Knaus, E., Wiebe, L. and DeClercq, E., "Novel (E)-5-(2-iodovinyl)-2'-deoxyuridine Derivatives as Potential Cytostatic Agents Against Herpes Simplex Virus Thymidine Kinase Gene Transfected Tumors.", *Gene Therapy*, **2**(5) 317 (1995)

- Bernadou, J. Martino, R., Malet-Martino, M. and Armand, J., "Fluorine -19 NMR: A Technique for Metabolism and Disposition Studies of Fluorinated Drugs.", *Trends Pharmacol. Sci.*, 6(3) 103 (1985)
- Bernadou, J., Armand, J., Lopez, A., Malet-Martino, M. and Martino, R., "Complete Urinary Excretion Profile of 5-Fluorouracil During a Six Day Chemotherapeutic Schedule, As Resolved by ^{19}F NMR.", *Clin. Chem.*, 31 846 (1985)
- Bertalanffy, F. and Lau, C., "Rates of Cell Division of Transplantable Malignant Rat Tumors.", *Can. Res.*, 22 627 (1962)
- Beteille, J., Lopez, A., Bon, M., Malet-Martino, M. and Martino, R., "Simultaneous Assay of Organic Fluorine Compounds in Biological Fluids by ^{19}F NMR Resonance Spectrometry Over a Large Spectral Width.", *Anal. Chem. Acta.*, 171 225 (1985)
- Bhat, C. and Munson, H., "The Diethyl and Dimethyl ethers of 2,4-pyrimidinediol and of 5-Methyl-2,4-pyrimidinediol Pyrimidine Intermediates in the Hilbert-Johnson Synthesis.", *Synth. Proc. in Nucl. Acid Chem.*, 30 82 (1968)
- Bishop, J., "The Molecular Genetics of Cancer.", *Science*, 235 303 (1987)
- Bitonti, A., Bush, T., Lewis, M. and Sunkars, P., "Response of Human Colon and Prostate Tumor Xenographs to (E)-2'-Deoxy-2'-(fluoromethylene) cytidine, An Inhibitor of Ribonucleotide Reductase.", *Anticancer Research*, 15 1179 (1995)
- Bobek, M. and Kawai, I., "Synthesis of 5-(2,2-difluorovinyl)-2'-deoxyuridine.", *Nucleic Acid Research Symposium Series*, 14 239 (1984)
- Bobek, M., Kawai, I. and DeClercq, E., "Synthesis and Biological Activity of 5-(2,2-difluorovinyl)-2'-deoxyuridine.", *J. Med. Chem.*, 30 (1987)
- Bransome, E., "The Current Status of Liquid Scintillation Counting", Grune and Stratton, USA, (1970)
- Brinkman, G. and Visser, J., "Production of $\text{Tc}^{99\text{m}}$.", *Int. J. Appl. Radiat. Isotopes*, 30 515 (1979)
- Burman, P., "Analogues of Nucleic Acid Components, Recent Results in Cancer Research.", *Springer-Verlag*, Berlin Germany, (1970)
- Burt, C., Koutcher, J., "Multinuclear NMR Studies of Naturally Occurring Nuclei.", *J. Nucl. Med.*, 25 237 (1984)
- Cheraghali, A., Kumar, R., Knaus, E. and Wiebe, L., "Pharmacokinetics and Bioavailability of 5-Ethyl-2'-deoxyuridine and its Novel (5R,6R)-5-bromo-6-ethoxy-5,6-dihydro pro-drugs in mice.", *Drug Metab. Disposition*, 23(2) 223 (1994)
- Cheraghali, A., Kumar, R., Knaus, E., Wang, L. and Wiebe, L., "Synthesis, Biotransformation, Pharmacokinetics and Antiviral Properties of 5-Ethyl-5-halo-6-methoxy-5,6-dihydro-2'-deoxyuridine Diastereomers.", *Biochem. Pharmacol.*, 47(9) 1615 (1994)
- Chew, W., Moseley, M., Mills, P., Sessler, D., Gonzalez-Mendez, R., James, T. and Litt, L., "Spin-echo Fluorine Magnetic Resonance Imaging at 2 T: *In-vivo* spatial distribution of halothane in the rabbit head.", *Magnetic Resonance Imaging*, 5 51 (1987)

- Cihak, A. and Rada, B., "Uridine Kinase: Properties, Biological Significance and Chemotherapeutic Aspects (a review).", *Neoplasia*, 23 233 (1976)
- Cohen, S., "Annals of the New York Academy of Sciences.", New York Academy of Sciences, New York, USA, p.195-199, (1987)
- Curreri, A., Ansfield, F., McIvor, F., Waisman, H. and Heidelberger, C., "Clinical studies with 5-Fluorouracil.", *Can. Res.* 18 478 (1958)
- Cushley, R., Wempen, I and Fox, J., "Nucleosides XLIV. Long-range Proton-fluorine Spin-spin Coupling in 5-Fluoropyrimidine Nucleosides." *J. Am. Chem. Soc.*, 90 709 (1968)
- Danenberg, P. and Lockshin, A., "Fluorinated Pyrimidines as Tight-binding Inhibitors of Thymidylate Synthetase.", *Pharmacol. Therap.*, 13 69 (1981)
- Danenberg, P., Montag, P. and Heidelberger, C., "Studies on Fluorinated Pyrimidines. IV. Effects on Nucleic Acid Metabolism *in vivo*.", *Can. Res.*, 18 239 (1958)
- Davies, H., "Chemotherapy of Large Bowel Cancer.", *Cancer*, 50 2638 (1982)
- Decesare, M., Pratesi, G., DeBraud, F. Zunino, F. and Stampina, C., "Remarkable Antitumor Activity of 5'-Deoxy-5-fluorouridine in Human Colorectal Tumor Xenographs.", *Anticancer Research*, 14 549 (1994)
- Desgranges, C., Razaka, G., DeClercq, E., Heredewun, P., Balzarini, J., Drouiller, F. and Bricaud, H., "Effect of (E)-5-(2-bromovinyl)uracil on the Catabolism and Antitumor Activity of 5-Fluorouracil in Rats and Leukemic Mice.", *Can. Res.*, 46 1094 (1986)
- Domin, B. and Mahoney, W., "5-Fluorouracil Transport into Human Erythrocytes.", *Proc. Am. Ass. Can. Res.* , 31 10 (1990)
- Drewinko, B. and Humphrey, R., "Growth Kinetics and Biochemical Regulation of Normal and Malignant cells.", Williams and Wilkins, Baltimore, USA, (1977)
- Druckenbrod, R., Williams, C. and Gelfand, M., "Iofetamine Hydrochloride ¹²³I : a New Radiopharmaceutical for Cerebral Perfusion Imaging.", *DICP, The Annals of Pharmacotherapy*, 23 19 (1989)
- Duesberg, P., "Cancer Genes: Rare Recombinants Instead of Activated Oncogenes (a review).", *Proc. Natl. Acad. Sci.*, 84 2117 (1987)
- Duschinsky, R., Plevan, E. and Heidelberger, C., "The Synthesis of 5-Fluoropyrimidines.", *J. Am. Chem. Soc.*, 79 4559 (1957)
- El-Assouli, S., "The Molecular Basis for the Differential Sensitivity of B and T Lymphocytes to Growth Inhibition by Thymidine and 5-Fluorouracil.", *Leuk. Res.* , 9 391 (1985)
- Elkerbout, F., Thomas, P. and Zwaveling, A., "Cancer Chemotherapy", The Williams and Wilkins Company, Baltimore, USA, p.1-3 (1971)
- Falcons, A., Pfanner, E., Ricci, S., Bertuccelli, M., Ciani, C., Carrai, M., Demarco, S., Ceribelli, A., Barduagni, M. and Calabresi, F., "Oral Doxifluridine in Elderly Patients With Metastatic Colorectal Cancer: A Multicenter Phase II Study.", *Annals of Onc.*, 5 760 (1994)

- Feldman, M. and Eisenbach, L., "What Makes a Tumor Cell Metastatic?", *Scientific America*, 11 61 (1988)
- Filler, R., "Reactions of Organic Compounds With Xenon Fluorides.", *Israel J. Chem.*, 17 71 (1978)
- Fox, B., "Techniques of Sample Preparation for Liquid Scintillation Counting.", North-Holland Pub. Co., Amsterdam, Holland (1976)
- Freeman, C., Kimes, B., Martin, M. and Marks, C., "An Overview of Tumor Biology.", *Cancer Invest.*, 7 247 (1989)
- Friedkin, M., "Thymidylate Synthetase.", *Adv. Enzym.*, 38 (1973)
- Frobisher, M., Hinsdill, R., Crabtree, K. and Goodheart, C., "Fundamentals of Microbiology", W. B. Sanders Company, Philadelphia, USA, p.77, (1974)
- Fuqua, S. Duncan, W. and Silverstein, R., "A One Step Synthesis of 1,1-Difluoroolefins From Aldehydes By a Modified Wittig Synthesis.", *Tetrahedron Letters*, 23 1461 (1964)
- Glazer, R., "Developments In Cancer Chemotherapy", CRC, Boca Raton, USA, p.61-90, (1984)
- Gochin, M. James, T. and Shafter, R., "*In-vivo* ¹⁹F-NMR of 5-Fluorouracil Incorporation into RNA and Metabolites In Esherichia Coli Cells.", *Biochim. biophys. Acta*, 804 118 (1984)
- Grem, J., Hamilton, J., King, S. and Leyland-Jones, B., "Overview of Current Status and Future Direction of Clinical Trials With 5-Fluorouracil In Combination With Folic Acid.", *Cancer Treat. Rep.*, 71 1249 (1987)
- Groshar, D., McEwan, A., Parliament, M., Urtasun, R., Goldberg, L., Hoskinson, M., Mercer, J., Mannan, R., Wiebe, L. and Chapman, J., "Imaging Tumor Hypoxia and Tumor Perfusion.", *J. Nucl. Med.*, 34(6) (1993)
- Gunther, H., "NMR Spectroscopy; An Introduction.", John Wiley & Sons, Toronto, Canada, p. 342-354 (1980)
- Hande, G. and Mandel, H., "Pyrimidine Nucleoside Monophosphate Kinase From Human Leukemic Blast Cells.", *Can. Res.*, 38 579 (1978)
- Harbers, E., Chaudhuri, N. and Heidelberger, C., "Studies On Fluorinated Pyrimidines VIII. Further Biochemical and Metabolic Investigations.", *J. Biol. Chem.*, 234 1255 (1959)
- Haverland, G. and Wiebe, L., "The Determination of Platinum in Biological Tissue by Instrumental Neutron Activation Analysis.", *Internat. J. Rad. Applications & Instrumentation-Part A. Applied Radiation & Isotopes*, 42(8) 775 (1991)
- Heggie, G., Sommadossi, J. Cross, D., Huster, W. and Diasio, R., "Catabolism of 5-Fluorouracil in Man: Evaluation of Dihydrofluorouracil Formation at Different Doses of 5-Fluorouracil With Evidence of a Novel Metabolite in Bile.", *Proceedings of AACR*, 27 174 (1986)

- Heidelberg, C., "Fluorinated Pyrimidines and Their Nucleosides. In: Antineoplastics and Immunosuppressive Agents. Vol.2", Sartorelli, A. and Johns, D., Springer, New York, USA, p. 193, (1975)
- Heidelberg, C., Boohar, J. and Kampachroer, "Fluorinated Pyrimidines XXIV. In Vivo Metabolism of 5-Trifluoromethyluracil-2-¹⁴C and 5-Trifluoromethyl-2'-deoxyuridine-2-¹⁴C", *Cancer Research*, 25 377 (1965)
- Heidelberg, C., Chaudhuri, N., Dannenberg, P., Mooren, D., Griesbach, L., Duschinsky, R., Schnitzer, R., Pelven, E. and Scheiner, J., "Fluorinated Pyrimidines, A New Class of Tumor Inhibitory Compounds", *Nature*, 179 663 (1957)
- Heidelberg, C., Danenberg, P. and Moran, R., "Fluorinated Pyrimidines and Their Nucleosides.", *Adv. Enzym.*, 54 57 (1983)
- Henderson, J. and Paterson, P., "Nucleotide Metabolism; An Introduction" Academy Press, New York, USA, (1973)
- Herkes, F. and Burton, D., "The Synthesis of b-Substituted Perfluoro Olefins.", *Tetrahedron Letters*, 32 1311 (1967)
- Hewitt, H., "The Choice of Animal Tumors For Experimental Studies in Cancer Therapy.", *Adv. Can. Res.*, 27 149 (1978)
- Horowitz, J., Cotton, M., Hardin, C. and Gollnick, P., "Characterization of the Fluorouracil Substituent in the 5-Fluorouracil-containing Escherichia Coli Transfer RNA.", *Biochem. Pharmac.*, 741 70 (1983)
- Horrocks, D., "Applications of Liquid Scintillation Counting", Academic Press, New York, U.S.A. (1974)
- Hull, W., Port, R., Herrmann, R., Britsch, B. and Kunz, W., "Metabolites of 5-Fluorouracil in Plasma and Urine as Monitored by ¹⁹F nuclear Magnetic Resonance Spectroscopy, for Patients Receiving Chemotherapy With or Without Methotrexate Pretreatment.", *Can. Res.*, 48 1680 (1988)
- Hurat, D., "Chemistry and Biochemistry of Pyrimidines, Purines and Pteridines.", John Wiley and Sons, Chichester, England, (1980)
- Inoue, H., Saito, N. and Ueda, T., "Reaction of 5-bromouridine Derivatives With Dimethyl Malonate Carbanion. A Novel Entry to the Synthesis of Uridine-5-acetic acids.", *Chem. Pharm. Bull.*, 11 4585 (1986)
- Ishikawa, T., Ura, M., Yamamoto, T., Tanaka, Y. and Ishizuka, H., "Selective inhibition of Spontaneous Pulmonary Metastasis of Lewis Lung Carcinomas by 5'-Deoxy-5-fluorouridine.", *Int. J. Cancer*, 61 516 (1995)
- James, T., Pogolotti, Jr. A., Ivanetich, K., Wataya, Y. Lam, S. and Santi, D., "Thymidylate synthetase: Fluorine-19 NMR Characterization of the Active Site Peptide Covalently Bound to 5-Fluoro-2'-deoxyuridylate and 5,10-Methylenetetrahydrofolate.", *Biochem. & Biophys. Research Comm.*, 72 404 (1976)
- Jelinski, L., Behling, R., Tubbs, H. and Cockman, M., "NMR Imaging: From Whole Bodies to Single Cells.", *Amer. Biotech. Labor.*, 7 34 (1989)

- Jung, M. and Lyster, M., "Quantitative Dealkylation of Alkyl Ethers Via Treatment With Trimethylsilyl Iodide. A New Method For Ether Hydrolysis.", *J. Org. Chem.*, **42**(23) 3761 (1977)
- Kartner, N. and Ling, V., "Multidrug Resistance In Cancer.", *Scientific America*, **3** 44 (1989)
- Kennedy, G., Galinier, J. and Zikovsky, L., "Measurement of Some Primary Nuclear Interferences in Neutron Activation Analysis With a SLOWPOKE Reactor.", *Can. J. Chem.*, **64** 790 (1986)
- Keppler, D. and Holstege, A., "Pyrimidine Nucleotide Metabolism and Its Compartmentation. In: *Metabolic Compartmentation*", Academic Press, London, UK, p.147-203, (1982)
- Kessel, D., "Cell Surface Alterations Associated With Exposure of Leukemia L1210 Cells to 5-Fluorouracil.", *Can. Res.*, **40** 322 (1980)
- Klubes, P., Connelly, K., Cerna, I. and Mandel, H., "Effects of 5-Fluorouracil on 5-Fluorodeoxyuridine-5'-monophosphate and 2'-deoxyuridine-5'-monophosphate Pools, and DNA Synthesis in Solids Mouse L1210 and Rat Walker 256 Tumors.", *Can. Res.*, **38** 2325 (1978)
- Knoll, G., "Radiation Detection and Measurement.", John Wiley & Sons, Inc., Toronto, Canada, (1979)
- Kobayashi, Y. and Maudsley, D., "Biological Applications of Liquid Scintillation Counting", Academic Press, U.S.A., (1974)
- Koklitis, P., Kelleher, J., King, R. and Giles, G., "Activities of 5-Fluorouracil Metabolizing Enzymes in Human Colorectal Tumors and Normal Colorectal Mucosa.", *Biochem. Soc. Trans.*, **13** 1192 (1985)
- Koutcher, J. and Burt, C., "Principals of Nuclear Magnetic Resonance.", *J. Nucl. Med.*, **25** 101 (1984)
- Koutcher, J., Burt, C., Lauffer, R. and Brady, T., "Contrast Agents and Spectroscopic Probes in NMR.", *J. Nucl. Med.*, **25** 506 (1984)
- Kufe, D. and Major, P., "5-Fluorouracil Incorporation into Human Breast Carcinoma RNA Correlates With Cytotoxicity.", *J. Biol. Chem.*, **256** 9802 (1981)
- Kufe, D., Major, P., Egan, E. and Loh, E., "5-Fluoro-2'-deoxyuridine Incorporation in L1210 DNA.", *J. Biol. Chem.*, **256** 8885 (1981)
- Kumar, R., Wiebe, L., Knaus, E., Allen, P. and Tempest, M., "Synthesis, Antiviral and Cytotoxic Activity of 2'-Deoxyuridines, 2'-Fluoro-2'-deoxyuridines and 2'-Arabinouridines Containing 5-(1-Hydroxy-2-halo-2-ethoxycarbonylethyl)-5-(1-hydroxy-2-iodo-2-carboxyethyl) and 5- α -1-hydroxy (or methoxy)-2-iodoethyl Substituents.", *Drug Design and Discovery*, **8**(3) 179 (1992)
- Kumar, R., Wang, L., Wiebe, L. and Knaus, E., "Synthesis, *in-vitro* Biological Stability and Anti-HIV Activity of 5-Halo-6'-alkoxy(or azido)-5,6-dihydro-3'-azido-3'-deoxythymidine.", *J. Med. Chem.*, **37**(21) 3554 (1994)

- Laskin, J. Evans, R., Slocum, H., Burke, D. and Hakala, M., "Basis For Natural Variation in Sensitivity to 5-Fluorouracil in Mouse and Human Cells in Culture.", *Can. Res.*, **39** 383 (1979)
- Leaback, D., Heath, E. and Roseman, S., "A New Experimental Approach to Fluorometric Enzyme Assays Employing Disposable Micro-reaction Chambers", *Biochemistry*, **8** 135 (1969)
- Lederer, M. and Shirley, V., "Table of the Isotopes, 7th Edition.", Wiley Interscience, New York, USA, (1978)
- Lee, Y., Knaus, E. and Wiebe, L., "Tumor Uptake of Radiolabelled Pyrimidine Bases and Pyrimidine Nucleosides in Animal Models - III. 2'-⁸²Br-Bromo-2'-deoxyuridine.", *Int. J. Nucl. Med. Biol.*, **6** 109 (1979)
- Livingston, R., and Carter, S., "Single Agents in Cancer Chemotherapy", IFI/Plenum, New York, U.S.A., p. 195-199, (1970)
- Malcolm-Lawes, D., "The Production of High Specific Activity ³⁴Cl By Fast Neutron Irradiation of Fluorocarbons.", *Int. J. Appl. Radiat. Isotopes*, **29** 698 (1978)
- Malet-Martino, M., Bernadou, J., Martino, R. and Armand, J., "¹⁹F NMR Spectrometry Evidence For Bile Acid Conjugates of α -Fluoro- β -alanine As The Main Biliary Metabolite of Antineoplastic Fluoropyrimidines in Humans.", *Drug Metab. Disposition*, **16** 78 (1988)
- Malet-Martino, M., Cabanac, S., Martino, R. and Armand, J., "Direct Observation of 5-Fluorouracil Hepatic Metabolism in Isolated Perfused Mouse Liver With ¹⁹F Magnetic Resonance Spectroscopy.", *Proc. Am. Ass. Can. Res.*, **30** 537 (1989)
- Malet-Martino, M., Faure, M., Vialaneix, J., Palevody, C., Hollandre, E. and Martino, R., "Noninvasive ¹⁹F NMR.", *Canc. Chemother. Pharmacol.*, **18** 5 (1986)
- Malet-Martino, M., Lopez, A., Bernadou, J., Martino, R., Beteille, J., Bon, M. and Armand, J., "Evidence for the Importance of 5'-Deoxy-5-fluorouridine Catabolism in Humans From ¹⁹F NMR Spectrometry.", *Can. Res.*, **46** 2105 (1986)
- Malet-Martino, M., Lopez, A., Bernadou, J., Martino, R., Beteille, J., Bon, M. and Armand, J., "New Approach to Metabolism of 5'-Deoxy-5-fluorouridine in Humans With ¹⁹F NMR.", *Canc. Chemother. Pharmacol.*, **13** 31 (1984)
- Maley, F. and Maley, G., "On the Nature of a Sparing Effect by Thymidine on the Utilization of Deoxycytidine.", *Biochemistry*, **1** 847 (1962)
- Mandel, H., Klubes, P. and Fernandes, D., "New Challenges With an Old Drug, From Advances In Cancer Chemotherapy.", Japan Science Society Press, Tokyo, Japan p.255, (1978)
- March, J., "Advanced Organic Chemistry: Reactions, Mechanisms and Structure.", McGraw-Hill Inc., New York, USA, p. 26, (1968)
- Marshall, C., "Meeting Report: Oncogenes and Growth Control.", *Cell*, **49** 723 (1987)

- Martino, R., Lopez, A., Malet-Martino, M., Bernadou, J. and Armand, J., "Release of Fluoride Ion From 5'-Deoxy-5-fluorouridine, an Antineoplastic Fluoropyrimidine, in Humans.", *Amer. Soc. Pharmacol. Exp. Therapeutics*, **8** 116 (1985)
- Martino, R., Malet-Martino, M., Vialaneix, C., Lopez, A. and Bon, M., "F NMR Analysis of the Carbamate Reaction of α -Fluoro- β -alanine (FBAL), the Major Catabolite of Fluoropyrimidines.", *Drug Metab. Disposition*, **15** 897 (1987)
- McCredie, J., Inch, W., Kruuv, J. and Watson, T., "The Rate of Tumor Growth in Animals.", *Growth*, **29** 331 (1965)
- McKenna, R. and Murphy, G., "Fundamentals of Surgical Oncology.", Macmillan Publishing Company, New York, USA, p. 233-245, (1985)
- Mercer, J., "Synthesis and Evaluation of Radiolabelled 5-Halo-1-(2'-fluoro-2'-deoxy- β -D-ribofuranosyl)-uracil Analogues as Non-invasive Tumor Diagnostic Radiopharmaceuticals.", Thesis, (1985)
- Mercer, J., Knaus, E. and Wiebe, L., "Synthesis and Tumor Uptake of 5-Halo-1-(2'-fluoro-2'-deoxy- β -D-ribofuranosyl)[2-¹⁴C]uracils.", *J. Med. Chem.*, **30** 670 (1987)
- Mikanagi, K., "Transport and Intracellular Metabolism of Fluorinated Pyrimidines in Cultured Cell Lines. In: Purine and Pyrimidine Metabolism in Man VI", Plenum Press, New York, USA, p. 321-326, (1989)
- Mooney, E., "An Introduction to ¹⁹F NMR Spectroscopy.", Heyden & Sons Ltd, New York, USA, p. 1-95, (1970)
- Moore, R., Chapman, J., Mercer, J., Mannan, R., Wiebe, L., McEwan, A. and McPhee, M., "Measurement of PDT - Induced Hypoxia in Dunning Prostate Tumors by [¹²³I]-Iodoazomycin Arabinosides.", *J. Nucl. Med.*, **34(3)** 405 (1993)
- Morin, K., Wiebe, L. and Knaus, E., "Synthesis of Brain Targeted 1-(2-deoxy-2-fluoro- β -D-ribofuranosyl)-(E)-5-(2-iodovinyl)uracil Coupled to a Dihydropyrimidine—pyridium Salt Redox Chemical-delivery System.", *Carbohydrate Research*, **249(1)** 109 (1993)
- Murray, A. and Williams, D., "Organic Synthesis With Isotopes, Part I.", Interscience, New York, USA, p. 588, (1958)
- Ng, B., Lenert, J., Weksler, B., Port, J., Ellis, J. and Burt, N., "Isolated Lung Perfusion With FUDR is an Effective Treatment for Colorectal Adenocarcinoma Lung Metastases in Rats.", *Annals Thoracic Surg.*, **59** 205 (1995)
- Noujaim, A., Ediss, C. and Wiebe, L., "Liquid Scintillation Science and Technology.", Academic Press, New York, U.S.A. (1976)
- Olah, G. and Arvanaghi, M., "Aldehydes by Formylation of Grignard or Organolithium Reagents with n-Formylpiperidine.", *Angew. Chem. Int. Ed. Engl.*, **10** 878 (1981)
- Olah, G., Nohma, M. and Kerekes, I., "Synthetic Methods and Reactions II. Hydrofluorination of Alkenes, Cyclopropane and Alkynes With Poly-hydrogen Fluoride/pyrimidine (trialkylamine) Reagents.", *Communications*, **December** 779 (1973)
- Olah, G., Narang, S., Gupta, B. and Malhotra, R., "Hexamethyldisilane/iodine: a Convenient *in situ* Generation of Iodotrimethylsilane." *Angew. Chem. Int. Ed. Engl.*, **8** 612 (1979)

- Olah, G., Narang, S., Gupta, B. and Malhotra, R., "Synthetic Methods and Reactions. 62. Transformations With Chlorotrimethylsilans/sodium Iodide, A Convenient *in situ* Iodotrimethylsilane Reagent.", *J. Org. Chem.*, **44**(8) 1247 (1979)
- Parliament, M., Chapman, J., Urtasun, R., McEwan, A., Goldberg, L., Mercer, J., Mannan, R. and Wiebe, L., "Non-invasive Assessment of Human Tumor Hypoxia With [¹²³I]-Iodoazomycin Arabinoside: Preliminary Report of a Clinical Study.", *Br. J. Can.*, **65**(1) 90 (1992)
- Parliament, M., Wiebe, L. and Franko, A., "Nitroimidazole Adducts as Markers For Tissue Hypoxia: Mechanistic Studies in Aerobic Normal Tissues and Tumor Cells.", *Br. J. Can.*, **66**(6) 1103 (1992)
- Patterson, A., Zhang, H., Moghaddam, A., Bicknell, R., Talbot, D., Stratford, I. and Harris, A., "Increasing Sensitivity in MCF-7 Cells Transfected With Thymidine Phosphorylase.", *Br. J. Can.*, **72** 669 (1995)
- Perry, C., "The Chemotherapy Source Book.", Williams and Wilkins, Baltimore, USA, p.241,. (1992)
- Peters, G., Laurensse, E., Leyva, A., and Pinedo, H., "Purine nucleosides as cell specific modulators of 5-fluorouracil metabolism and cytotoxicity.", *Eur. J. Cancer clin. Oncol.*, **23** 1869 (1987a)
- Peters, G., Laurensse, E., Leyva, A., and Pinedo, H., "Purine Nucleosides as Cell Specific Modulators of 5-Fluorouracil Metabolism and Cytotoxicity.", *Eur. J. Cancer clin. Oncol.*, **23** (1987a)
- Peters, G., Laurensse, E., Leyva, A., Lankelma, J. and Pinedo, H., "Sensitivity of Human, Murine and Rat Cells to 5-Fluorouracil and 5'-Deoxy-5-fluorouridine in Relation to Drug Metabolizing Enzymes.", *Can. Res.*, **46** 21 (1986a)
- Peters, G., van Groeningen, C., Laurensse, E. and Pinedo, H., "A Comparison of 5-Fluorouracil Metabolism in Human Colorectal Cancer and Colon Mucosa.", *Cancer*, **61** 259 (1991)
- Plagemann, P. and Wohlhueter, R., "Permeation of Nucleosides and Nucleic Acid Bases, and Nucleotides in Animal Cells.", *Curr. Top. Membr. Transport*, **14** 225 (1980)
- Pool, M., Cork, J. and Thornton, R., "A Survey of Radioactivity Produced by High Energy Neutron Bombardment.", *Phys. Rev.*, **52** 239 (1937)
- Prihar, H., Tsai, H., Wanamaker, S. and Duber, S., "A Gas Chromatographic Method for the Quantitative Determination of Hexuronic Acids in Alginic Acid", *Carbohydr. Res.*, **56** 315 (1977)
- Prior, M., Maxwell, R. and Griffiths, J., " *In-vivo* fluorine-19 NMR Spectroscopy of the Antimetabolite 5-Fluorouracil and Its Analogs. An Assessment of Drug Metabolism.", *Biochem. Pharmac.*, **39** 857 (1990)
- Prusoff, W. and Fischer, P., "Nucleoside Analogs. Chemistry, Biology and Medical Applications.", Plenum Press, New York, USA, p. 281, (1979)
- Ratain, M., Schilsky, R., Connelly, B. and Egorin, M., "Pharmacodynamics in Cancer Therapy.", *J. Clin. Oncol.*, **8** 1739 (1990)

- Reyes, P. and Hall, T., "Synthesis of 5-Fluorouridine 5'-phosphate by a Pyrimidine Phosphoribosyltransferase of Mammalian Origin II. Correlation Between the Tumor Levels of the Enzyme and the 5-Fluorouracil-promoted Increase in Survival Time of Tumor Bearing Mice.", *Biochem. Pharmac.*, 18 2587 (1969)
- Reyes, P., "The Synthesis of 5-Fluorouridine 5'-Monophosphate by a Pyrimidine Phosphoribosyltransferase of Mammalian Origin. I. Some Properties of the Enzyme From p1534J Mouse Leukemic Cells.", *Biochemistry*, 8 2057 (1969)
- Rich, M., Bolaffi, J., Knoll, J., Cheong, L. and Eidinoff, M., "Growth Inhibition of a Human Cell Strain by 5-Fluorouracil, 5-Fluorouridine and 5-Fluoro-2'-deoxyuridine - Reversal Studies.", *Can. Res.*, 18 730 (1958)
- Riemenschneider, T., Ruf, C., Spath, G., Stuhldreier, G. and Elmouaouy, A., "Continuos or Bolus Chemotherapy With 5-Fluoro-2'-deoxyuridine in Transplanted Experimental Liver Tumors.", *J. Canc. Res. Clin. Oncol.*, 114 482 (1988)
- Robins, M., "Chemical Transformations of Naturally Occurring Nucleosides to Otherwise Difficulty Accessible Structures.", *Ann. N. Y. Acad. Sci.*, 255 105 (1975)
- Robins, M., MacCoss, M. and Naik, S., "(156) 5-Fluorouridine and 5-Fluorocytidine in: Nucleic Acid Chemistry.", Wiley Interscience, New York, USA, p. 895, (1978)
- Roobol, G., Dobbelaer, G. and Bernheim, J., "5-Fluorouracil and 5-Fluoro-2'-Deoxyuridine Follow Different Metabolic Pathways in the Induction of Cell Lethality in L-1210 Leukemia.", *Br. J. Can.*, 49 739 (1984)
- Rueckert, R. and Mueller, G., "Studies on Unbalanced Growth in Tissue Culture. I. Induction and Consequences of Thymidine Deficiency.", *Can. Res.*, 20 1584 (1960)
- Ruiz Van Haperan, V., Veerman, G., Bovin, E., Noordhuis, P., Vermorken, J. and Peters, G., "Schedule Dependence of Sensitivity to 2',2'-Difluorodeoxycytidine (gemcitabine) in Relation to Accumulation and Retention of its Triphosphate in Solid Tumor Cell Lines and Solid Tumors.", *Biochem. Pharmac.*, 48(7) 1327 (1995)
- Rutman, R., Cantarow, A. and Paschkis, K., "Studies in 2-Acetylaminofluorene Carcinogenesis. III. The Utilization of Uracil-2-¹⁴C by Preneoplastic Rat Liver and Rat Hepatoma.", *Can. Res.*, 14 119 (1954)
- Sawyer, R., Stolfi, R., Nayak, R. and Martin, D., "Mechanisms of Cytotoxicity in 5-Fluorouracil Chemotherapy of Two Murine Solid Tumors. in : Nucleosides and Cancer Treatment.", Academic Press, Australia, p. 309 (1981)
- Schwarz, B., Cech, D., Holy, A. and Skoda, J., "Preparation, Antibacterial Effects and Enzymatic Degradation of 5-Fluorouracil Nucleosides.", *Coll. Czech. Chem. Commun.*, 45 3217 (1980)
- Shewach, D., Hahn, T., Chang, E., Hertel, L. and Lawrence, T., "Metabolism of 2',2'-Difluoro-2'-deoxycytidine and Radiation Sensitization of Human Colon Carcinoma Cells.", *Can. Res.*, 54 3218 (1994)
- Shionoya, S., Lu, Y. and Scanlon, K., "Property of Amino Acid Transport Systems in K562 Cells Sensitive and Resistant to *cis*-Diaminedichloroplatinum (II)." *Can. Res.*, 46 3445 (1986)

- Shiotani, Y., and Weber, G., "Purification and Properties of Dihydrothymine Dehydrogenase From Rat Liver.", *J. Biol. Chem.*, 256 219 (1981)
- Simpson-Herren, L., Sanford, A. and Holmquist, J., "Cell Population Kinetics of Transplanted and Metastatic *Lewis lung carcinoma*.", *Cell Tissue Kinet.*, 7 349 (1974)
- Skeel, R., "Handbook of Cancer Chemotherapy Third Edition", Little Brown and Company, Boston, USA, p. 3-16, 110-111. (1991)
- Sket, B. and Zupan, M., "Fluorination With Xenon Difluoride. 23. Fluorination of Ortho Substituted Aromatic Molecules.", *Bull. Chem. Soc. Jap.*, 54 279 (1981)
- Skold, O., "Enzymatic Ribosidation and Ribotidation of 5-Fluorouracil by Extracts of the Ehrlich Ascites Tumor.", *Biochim. biophys. Acta*, 29 651 (1958)
- Slagel, R., "The Effects of the Cation on the Thermolysis of Chlorodifluoroacetate Salts.", *Chemistry and Industry*, 22 848 (1968)
- Sommadossi, J., Aubert, C., Cano, J., Gouvela, J., Ribaud, P. and Mathe, G., "Kinetics and Metabolism of a New Fluoropyrimidine, 5'-Deoxy-5-fluorouridine, in Humans.", *Can. Res.*, 43 930 (1983)
- Sommadossi, J., Cross, D., Gewirtz, D., Goldman, I., Cano, J. and Diasio, R., "Evidence From Rat Hepatocytes of an Unrecognized Pathway of 5-Fluorouracil Metabolism With the Formation of a Glucuronide Derivative.", *Can. Res.*, 45 2454 (1985)
- Sommadossi, J., Gewirtz, D., Diasio, R., Aubert, C., Cano and Goldman, I., "Rapid Catabolism of 5-Fluorouracil in Freshly Isolated Rat Hepatocytes as Analyzed by High Performance Liquid Chromatography (HPLC).", *J. Biol. Chem.*, 257 8171 (1982)
- Steel, G. and Adams, K., "Stem Cell Survival and Tumor Control in the *Lewis lung carcinoma*.", *Can. Res.*, 35 1530 (1975)
- Sweeny, D., Barnes, S. and Diasio, R., "Formation of Conjugates of 2-Fluoro- β -Alanine and Bile Acids During the Metabolism of 5-Fluorouracil and 5-Fluoro-2-deoxyuridine in the Isolated Perfused Rat Liver.", *Can. Res.*, 48 2010 (1988)
- Sweeny, D., Heggie, S., Barnes, S. and Diasio, R., "Characterization of a Unique 5-Fluorouracil Metabolite Isolated From Human Bile.", *Proc. Am. Ass. Can. Res.*, 28 443 (1987)
- Tandon, M., Kumar, P. and Wiebe, L., " α -Trifluoromethyl- β -alanylglycine (f3MBAG): A Novel Mammalian Metabolite of Trifluridine (F_3 TdR).", *Biochem. Pharmacol.*, 48 1033 (1994)
- Tandon, M., Kumar, P. and Wiebe, L., " α -Trifluoromethyl- β -ureidopropionic Acid (F_3 TdR).", *Nucleos. and Nucleot.*, 12 803 (1993)
- Tandon, M., Kumar, P., Wiebe, G. and Wiebe, L., "Detection of New Metabolites of Trifluridine (F_3 TdR) using ^{19}F -NMR Spectroscopy.", *Biochem. Pharmacol.*, 44(11) 2223 (1992)
- Tandon, M., Singh, S., Kumar, P., Wiebe, L., Knaus, E., Gati, W. and Tempest, M., "Synthesis of the Diastereomers of 5-(2,2'-dichlorocyclopropyl) and 5-(2-

chlorocyclopropyl)-2'-Deoxyuridine and the Antiviral and Cytotoxic Activity of These Bromo Analogues.", *Drug Design and Del.*, 7(4) 295 (1991)

Tandon, M., Singh, S., Xu, L., Kumar, P., Wiebe, L., Knaus, E., Gati, W. and Tempest, M., "Synthesis and Biological Activity of 5-(2,2'-difluorocyclopropyl)-2'-Deoxyuridine Diastereomers.", *Drug Design and Discovery*, 9(1) 79 (1992)

Tatsumi, K., Fukushima, M., Shirasaka, T. and Fujii, S., "Inhibitory Effects of Pyrimidine, Barbituric Acid and Pyrimidine Derivatives on 5-Fluorouracil Degradation in Rat Liver Extracts.", *Jap. J. Can. Res. (Gann)*, 78 748 (1987)

Teder, H., Erichsen, C., Christensen, P., Jonsson, P. and Stenram, U., "5-Fluorouracil Incorporation Into RNA of a Rat Liver Adenocarcinoma After Hepatic Artery Injection Together With Degradable Starch Microspheres.", *Cancer Drug Delivery*, 4(3) 748 (1987)

Tokuzen, R., Yamaguchi, T., Saneyoshi, M., Yoshida, M. and Maeda, M., "Augmentation of 5-Fluoro-2'-deoxyuridine Cytotoxicity by 5-Phenethyl-2'-deoxyuridine in Human Gastric Cancer Cells in Culture.", *Anticancer Drugs*, 5 419 (1994)

Tovell, D., Samuel, J., Mercer, J., Misra, H., Xu, L., Wiebe, L., Tyrrell, D. and Knaus, E., "The *In Vitro* Evaluation of Nucleoside Analogues as Probes For Use in the Noninvasive Diagnosis of Herpes Simplex Encephalitis.", *Drug Design and Del.*, 3 213 (1988)

Townsend, L. and Tipson, R., "Nucleic Acid Chemistry, Part I", Wiley, J. and Sons, New York, USA, p. 375, (1978)

van der Wilt, C., van Laar, J., Smid, K., Rustum, Y. and Peters, G., "Comparison of 5-Fluoro-2'-deoxyuridine and 5-Fluorouracil in the Treatment of Murine Colon Cancer: Effects On Thymidylate Synthetase.", *Advan. Exp. Med. Biol.*, 370 109 (1994)

vanBekkum, D., "Tumor Model Test Systems.", *Natl. Cancer Inst. Monogr.*, 40 83 (1974)

Vialaneux, J., Benjamin, A., Malet-Martino, M., Martino, R. and Michel, G., "Reduction of the Antineoplastic Fluoropyrimidine, 5-Fluorouracil to 5,6-Dihydro-5-fluorouracil in *Escherichia coli*.", *Biotech. Lett.*, 9 715 (1987)

Vialaneux, J., Malet-Martino, M., Hoffman, J., Pris, J. and Martino, R., "Direct Detection of New Flucytosine Metabolites in Human Biofluids by ¹⁹F NMR.", *Drug Metab. Disposition*, 15 718 (1987)

vonHerauagegeben, R. and Ernst-Jucker, B., "Progress in Drug Research", Birkhauser Verlag, Cheshire, England, p.127-191 (1984)

Walder, S. and Schwartz, E., "Antineoplastic Activity of the Combination of Interferon and Cytotoxic Agents Against Experimental and Human Malignancies: A Review.", *Can. Res.*, 50 3473 (1990)

Wasternack, C., "Degradation of Pyrimidine Analogues - Pathways and Mutual Influences.", *Pharmacol. Therap.*, 8 629 (1980)

Watanabe, K., Su, T., Klein, R., Chu, C., Matsuda, A., Chun, M., Lopez, C. and Fox, J., "Nucleosides. 123. Synthesis of Antiviral Nucleosides: 5-Substitued 1-(2-deoxy-2-

- halogeno-b-D-arabinofuranosyl)cytosine and -uracils. Some Structure Activity Relations.", *J. Med. Chem.*, 26 152 (1982)
- Weber, G., "Biochemical Strategy of Cancer Cells and the Design of Chemotherapy, G. H. A. Clowes Memorial Lecture.", *Can. Res.*, 43 3466 (1983)
- Weber, G., "Nuclear Magnetic Resonance: A Review of the Literature Published Between June 1983 and May 1984.", Burlington House, London, England, p. 288-339, (1984)
- Weber, G., Shiotani, T., Kizaki, H., Tzeng, D., Williams, J. and Gladstone, N., "Biochemical Strategy of the Genome as Expressed in Regulation of Pyrimidine Metabolism.", *Adv. Enzyme Regul.*, 16 3 (1978)
- Weckbecker, G., "Biochemical Pharmacology and Analysis of Fluoropyrimidines Alone and in Combination With Modulators.", *Pharmacol. Therap.*, 50 367 (1991)
- Wiebe, L. and Knaus, E., "Drug-induced Perturbations in the *in vivo* Distribution of Oncological Radiotracers - I. 5-Fluoro-[³H]-2'-deoxyuridine Influenced by Nitrobenzylthionosine 5'-phosphate (NBMPR-P).", *Nucl. Med. Biol.*, 13 257 (1986)
- Wiebe, L., Flanagan, R., Helus, F., Knapp, W., Knaus, E. and Maier-Borat, W., "Radiolabelled L-Fucose for Diagnostic Oncology: Preliminary Studies in Mice and Rats Using L-[¹⁴C]-fucose.", *Int. J. Nucl. Med. Biol.*, 12(2) 111 (1985)
- Wiebe, L., Shysh, A., Apps, S. and Ediss, C., "Bone Fluoride in Chronically Uremic Rats.", *J. Radioanalytical Chem.*, 79 337 (1983)
- Wilbur, D., Anderson, K., Stone, W. and O'Brien, H., "Radiohalogenation of Non-activated Aromatic Compounds Via Aryltrimethylsilyl Intermediates.", *J. Label. Comp. Radiopharm.*, 14 1171 (1982)
- Wilkinson, D. and Pitot, H., "Inhibition of Ribosomal Ribonucleic Acid Maturation in Novikoff Hepatoma Cells by 5-Fluorouracil and 5-Fluorouridine.", *J. Biol. Chem.*, 248 63 (1973)
- Wilkinson, D., Tlsty, T. and Hanas, R., "The Inhibition of Ribosomal RNA Synthesis and Maturation in Novikoff Hepatoma Cells by 5-Fluorouridine.", *Can. Res.*, 38 3014 (1975)
- Wohlhueter, R., McIvor, R. and Plagemann, P., "Facilitated Transport of Uracil and 5-Fluorouracil and Permeation of Orotic Acid into Cultured Mammalian Cells." *J. Cell Physiol.*, 104 309 (1980)
- Wolf, W., Albright, M., Silver, M., Weber, H., Reichardt, U. and Sauer, R., "Fluorine-19 NMR Spectroscopic Studies of the Metabolism of 5-Fluorouracil in the Liver of Patients Undergoing Chemotherapy.", *Magnetic Resonance Imaging*, 5 165 (1987)
- Wolf, W., Albright, M., Souter, R., Silver, M., Weber, H., Reichardt, U. and Sauer, R., "Non-invasive Studies of Drug Biodistribution and Metabolism: NMR Spectroscopy of 5-Fluorouracil in Patients With Squamous Cell Carcinomas of the Head and Neck.", *Proc. Am. Ass. Can. Res.*, 28 189 (1987)
- Yamamoto, S. and Kawasaki, T., "Active Transport of 5-Fluorouracil and its Energy Coupling in Ehrlich Ascites Tumor Cells.", *J. Biochem.*, 90 635 (1981)

A) APPENDIX 1: DATA INTERPRETATION CALCULATIONS

i) DUAL LABEL COUNTING TECHNIQUE

The following outlines a technique used to determine the activity of two different β emitting radionuclides contained in the same sample by the method of dual label liquid scintillation counting (DLLSC).

The overlapping energy spectra of ^3H and ^{14}C are shown in figure 41.

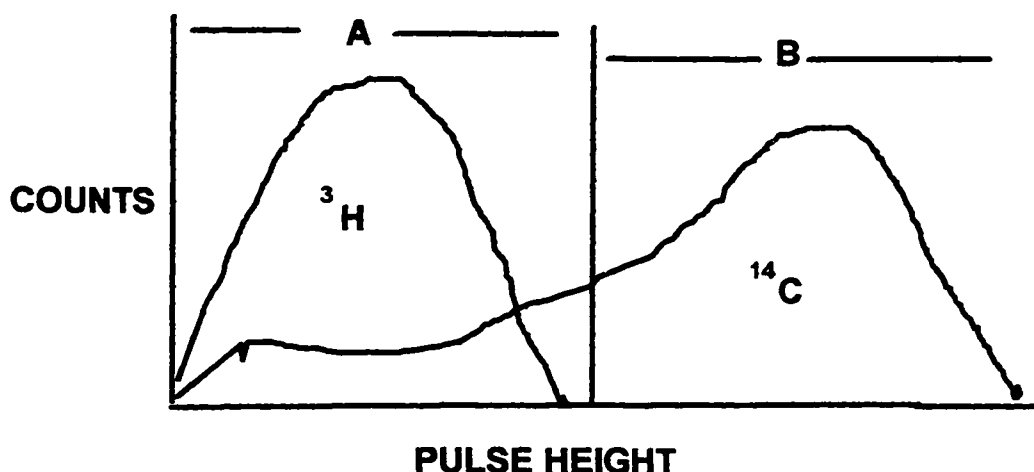


Figure 41 Unquenched pulse height spectra of ^3H and ^{14}C indicating possible window settings for dual label counting

This technique strategically employs window settings of differing energies to discern and quantify these mixtures of β emissions. In figure 41, "A" and "B" represent window settings. Window "B" can be set to record counts due to only ^{14}C . Although this window setting results in a decreased overall counting efficiency for ^{14}C than a window encompassing "A" and "B", it would allow for determination of the activity of ^{14}C alone in a sample containing both ^3H and ^{14}C .

In such a mixture, no window setting can be chosen to count ^3H that would not also include ^{14}C . The dual label technique allows for the activity of ^3H to be determined

by first determining the ^{14}C activity in that window, then subtracting the ^{14}C activity from the total activity with the remaining activity being attributed to ^3H (Horrocks, 1974). This is achieved by the following steps:

- Use window B to count a known ^{14}C standard.
- After determining the counts per minute (cpm) in window B for the ^{14}C standard, the counting efficiency (CE) for ^{14}C in window B can be calculated.

$$\text{i.e.) } \text{CE} = \text{cpm}(-\text{background})/\text{dpm} \times 100$$

- The total counts in window A are then determined
- The CE of ^{14}C in window A is determined by added a standard of ^{14}C (known dpm). The counting efficiency of ^{14}C in window A is calculated after determining the change in cpm after addition of the ^{14}C standard.
- The total cpm in window A are determined
- With the CE of ^{14}C in window A, that was calculated, the portion of activity due to ^{14}C in window A is calculated.
- The activity of ^3H is then determined by subtracting the contribution in window A from ^{14}C (as calculated) followed by a calculation of the dpm for ^3H from the remaining cpm value and the CE of ^3H in window A.

ii) OPTIMUM DOSE FOR DETECTION USING NAA

The following is a calculation of the theoretical detectable dose of 5FU needed when using NAA as the method of sample analysis. Using the results of the calibration curves data, in combination with the relative detection limits, the dose needed to produce samples within the optimum detectable dosage range can be calculated back as follows:

- 200 μg of fluorine detected represents x g of 5FU
- mwt F = 19
- mwt 5FU = 130
- $130/19 = (x) \mu\text{g } 5\text{FU} / 200 \mu\text{g F}$
- $x = 1368 \mu\text{g } 5\text{FU}$ or 1.37 mg of 5FU in a 2 g liver
- $1.37 \text{ mg}/2\text{g} \times 1000 \text{ g/kg} = 1368 \text{ mg of } 5\text{FU}/2\text{kg} = 684 \text{ mg/kg of } 5\text{FU}$ as optimum detectable in the liver

iii) NAA DATA CALCULATIONS

a) Standard Curve Equation For $\mu\text{g F}$

1) Half Geometry

From figure 17;

- Y axis = counts (peak area) @ 1634 keV
- X axis = $\mu\text{g fluorine}$
- using first order regression statistics the resulting equation is
- counts @ 1634 keV = $28.23 + (4.64 \times \mu\text{g F})$
- $b[0]$ 28.229002201
- $b[1]$ 4.6443878578
- r^2 0.9308422535

The first order linear regression equation for the variables involved in this standard curve is:

$$\text{counts} = b[0] + (b[1] \times \mu\text{g F})$$

rearranged:

$$\mu\text{g F} = \frac{\text{counts}(1643) - b[0]}{b[1]}$$

substituting:

$$= \frac{\text{counts} - 28.23}{4.64}$$

$$\text{Equation 1} \quad \mu\text{g F} = 0.22(\text{counts at 1634 keV}) - 6.08$$

2) $\mu\text{g F FULL GEOMETRY}$

From figure 18, the first order regression statistics result in the following equation:

- Y axis = counts (peak area) @ 1634 keV
- X axis = $\mu\text{g fluorine Coefficients}$:
- $b[0]$ 36.2019485135
- $b[1]$ 5.688227152
- r^2 0.7982998791

using first order regression statistics, the resulting equation is

$$\text{counts @ 1634 keV} = 36.2 + (5.69 \times \mu\text{g F})$$

rearranged: $\mu\text{g F} = \frac{\text{counts}(1643) - b[0]}{b[1]}$

$$b[1]$$

substituting:

$$= \text{counts} - 36.2/5.69$$

Equation 2 Full Geometry $\mu\text{g F} = 0.18(\text{counts } 1634 \text{ keV}) - 6.36$

b) STANDARD CURVE EQUATION FOR SODIUM INTERFERENCE

1) Half Geometry

a) Counts at 1634 keV

From figure 19,

- Y axis = counts (peak area) @ 1634 keV
X axis = $\mu\text{g Na}$

• Coefficients:

- $b[0]$ 23.827176436
- $b[1]$ 0.0234302278
- r^2 0.77

The first order linear regression equation for $\mu\text{g Na}$ standard curve

$$\mu\text{g Na} = \frac{\text{counts}(1643) - 23.83}{0.0234}$$

Equation 3 $\mu\text{g Na} = 42.74 (\text{counts}1634) - 1018.38$

b) Counts at 1368 keV

From figure 20,

- Y axis = counts (peak area) @ 1368 keV
- X axis = $\mu\text{g Na}$ Coefficients:

- $b[0]$ 60.1534094674
- $b[1]$ 0.1109137971
- r^2 0.989

The first order linear regression equation for $\mu\text{g Na}$ standard curve:

$$\mu\text{g Na} = \frac{\text{counts}(1368) - 60.15}{0.111}$$

Equation 4 $\mu\text{g Na} = 9.01 (\text{counts}1368) - 541.89$

To solve for the counts at 1634 keV (Equation 3) relative to the counts at 1368 keV (Equation 4), for a given sample with a known μg of Na, the common factor is mass of Na. Therefore, for a given mass of Na;

Equation 3 $\mu\text{g Na} = 42.74 (\text{counts}_{1634}) - 1018.38$

Equation 4 $\mu\text{g Na} = 9.01 (\text{counts}_{1368}) - 541.89$

then

$$42.74 (\text{counts}_{1634}) - 1018.38 = 9.01 (\text{counts}_{1368}) - 541.89$$

$$42.74(\text{counts}_{1634} \text{ keV}) = 9.01 (\text{counts}_{1368} \text{ keV}) + 476.49$$

Equation 5 $\text{counts}_{1634} = 0.21(\text{counts}_{1368} \text{ keV}) + 11.15$

The above equation 5 is calculated by a correlation of the regression lines of figures 21 & 22. To double check, another was employed. Figure 23 is a direct regression plot of half geometry counts at 1368 keV Vs counts at 1634 keV. The equation derived directly from this plot is :

$$\text{counts}_{1634} = 0.216(\text{counts}_{1368} \text{ keV}) + 9.07$$

2) FULL GEOMETRY

The full geometry equations were derived in the same manner as with the half geometry equations using information derived from figures 21, 22 & 24. The resulting equations, for a given mass of Na, are:

Equation 6 $\mu\text{g Na} = 30.30 (\text{counts}_{1634}) + 193.33$ (figure 21)

Equation 7 $\mu\text{g Na} = 10.42 (\text{counts}_{1368}) - 606.88$ (figure 22), then

$$30.30 (\text{counts}_{1634}) + 193.33 = 10.42 (\text{counts}_{1368}) - 606.88, \text{ which simplifies to,}$$

Equation 8 $\text{counts}_{1634} \text{ keV} = 0.34 (\text{counts}_{1368} \text{ keV}) - 26.41$

To verify this calculation, figure 24 is a direct regression plot of full geometry counts at 1368 keV Vs counts at 1634 keV. The equation derived from figure 24 is;

$$\text{counts}_{1634} \text{ keV} = 0.346 (\text{counts}_{1368} \text{ keV}) - 27.6$$

c) NAA SUMMARY OF EQUATIONS DERIVED FROM STANDARD CURVE DATA

Equation 1 Half Geometry $\mu\text{g F} = 0.22(\text{counts at } 1634 \text{ keV}) - 6.08$

Equation 2 Full Geometry $\mu\text{g F} = 0.18(\text{counts}_{1634} \text{ keV}) - 6.36$

Equation 3 Half Geometry $\mu\text{g Na} = 42.74 (\text{counts } 1634) - 1018.38$

Equation 4 Half Geometry $\mu\text{g Na} = 9.01 (\text{counts } 1368) - 541.89$

Equation 5 Half Geometry $\text{counts } 1634 = 0.21(\text{counts } 1368 \text{ keV}) + 11.15$

Equation 6 Full Geometry $\mu\text{g Na} = 30.30 (\text{counts } 1634) + 193.33$

Equation 7 Full Geometry $\mu\text{g Na} = 10.42 (\text{counts } 1368) - 606.88$

Equation 8 Full Geometry $\text{counts } 1634 \text{ keV} = 0.34 (\text{counts } 1368) - 26.41$

d) NAA ANIMAL DATA CONVERSION

1) Determination of F in animal samples

The kidney, GIT and tail samples were treated as Half Geometry samples and the liver and tumor samples as Full Geometry samples. The following is a sample calculation of a kidney sample taken 30 minutes post 5FU administration.

Mouse mass = 22.0 g
kidney mass = 0.405 g
mwt F = 19
mwt 5FU = 130
counts at 1634 keV = 163
counts at 1368 keV = 215

The total F, from all sources, in the sample is calculated with equation 1, since a Half Geometry sample is involved.

Equation 1 Half Geometry $\mu\text{g F} = 0.22(\text{counts at } 1634 \text{ keV}) - 6.08$

The counts at 1634 keV from Na interference is calculated with equation 5 and to save time is incorporated into equation 1 so that its solution would then be the net mass of F.

Equation 1 Half Geometry $\mu\text{g F} = 0.22(\text{counts } 1634 \text{ total} - 1634 \text{ Na}) - 6.08$

Equation 5 Half Geometry $\text{counts } 1634 = 0.21(\text{counts } 1368 \text{ keV}) + 11.15$
 $= 0.21(215) + 11.15$

$= 56.3$

$\mu\text{g F} = 0.22(163 - 56) - 6.08$

$= 17.46$

1 $\mu\text{g F}$ represents $130/19 = 6.842 \mu\text{g}$ of 5FU

$17.46 (6.842) = 119.46 \mu\text{g}$ of 5FU The initial dose administered was 0.2 mL of a 10 mg/mL solution.

$= 2 \text{ mg } 5\text{FU} = 2000 \mu\text{g}$ of 5FU

$\% \text{ injected dose per organ} = 119.46 \times 100/2000 = 5.97 \%$

The FUF samples were treated similarly, substituting the mwt of FUF for that of

5FU.

e) NAA CORRECTION FOR TAIL LOSS

To account for tail loss, the results were adjusted to account for a reduced administered dose. For the above sample 30.14% of the dose was detected in the tail.

This was applied as the reduced initial dose:

$$5.9 (1/1-.3014) = 8.2\%$$

B) APPENDIX 2. SYNTHESIS

i) SYNTHESIS OF FUCOSYL-5-FLUOROURACIL (V.J. Somayaji)

Synthesis of FUF was carried out by V.J. Somayaji and obtained very good yield by coupling the peracetylated fucose with 2,4-bis(trimethylsilyloxy)-5-fluorouracil in the presence of stannic chloride. The coupling reaction was carried out by standard procedure using Hilbert Johnson reaction to obtain pure compound (3), 1-(2',3',4'-tri-O-acetyl-β-L-fucopyranosyl)-5-fluorouracil (figure 40) with 83% yield. This was verified by TLC, melting point, ¹³C and proton NMR. The deblocking of compound (3) produced a 94% yield of compound (4), 1-(β-L-fucose)-5-fluorouracil (FUF), 645 mg.

This was characterized and verified with a melting point of 239-241⁰ C, TLC RF=0.22. Additional characterization included mass spectrum analysis(mass = 276.0754 for C₁₀H₁₃N₂O₆F, with a calculated value of 276.0757), ¹⁹F-NMR, ¹H-NMR, and ¹³C-NMR (Somayaji, 1989).

L-fucose-5-fluorouracil nucleoside was obtained in good yield by coupling the peracetylated fucose with 2,4-bis(trimethylsilyloxy) 5-fluoropyrimidine in the presence of stannic chloride. The solvents were distilled before use. These were dried by standard methods. TLC analysis was carried out on silica gel Whatman MK6F microplates using 4:6 ethyl acetate-toluene (solvent A) or 1:4:2 n-propanol-ethyl acetate-water (solvent B). Column chromatography was performed on silica gel powder

(60-200 mesh). All melting points are uncorrected. Proton, ^{13}C , and ^{19}F NMR spectra were recorded on a Bruker AM-300 spectrometer. Chemical shift (δ) values are given in ppm and coupling constant, J, in Hz. Low resolution mass spectra were measured on a Hewlet Packard 5995 mass spectrometer and exact mass spectra were measured on an AEI MS-50 mass spectrometer. Peracetylated fucose was prepared by adopting the standard procedure (Leaback, 1969). 5-FU was silylated using hexamethyl disilazane in the presence of small amount of ammonium sulfate (Beranek, 1978). Coupling reactions were carried out by standard procedures using Hilbert Johnson reaction.

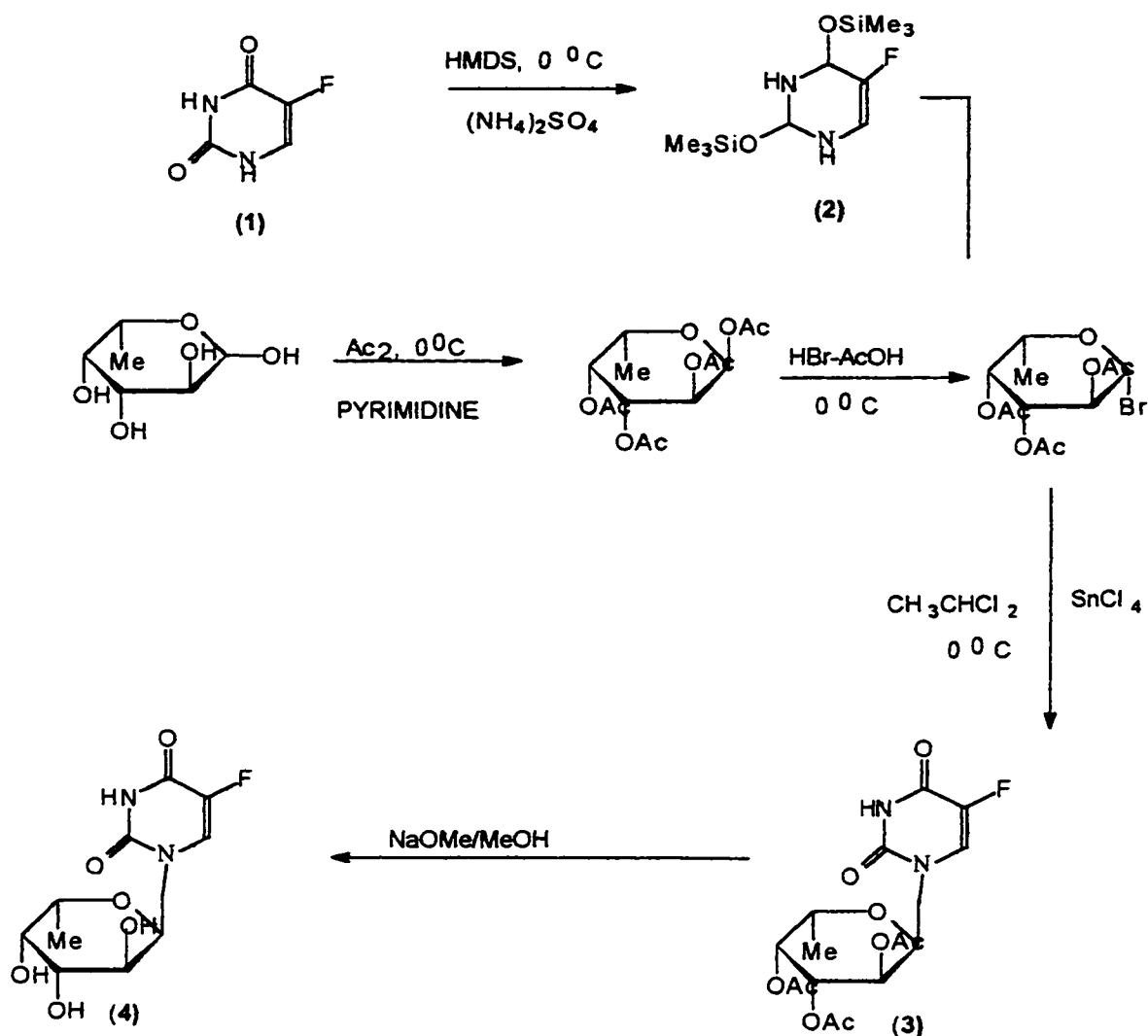


Figure 42 Synthesis of fucosyl-5-fluorouracil

1) 1-{2',3',4'-tri-O-acetyl-β-L-fucopyranosyl}-5-fluorouracil (3)

A solution of 2,4-bis(trimethylsilyloxy)-5-fluoropyrimidine (1.9 g, 7 mmol) was added to a stirred solution of peracetylated L-fucose (2.0 g, 6 mmol) in dry 1,2-dichlorostane (100 mL) and the mixture was cooled to 0 °C. Stannic chloride (0.82 mL, 7 mmol) in 1,2-dichloroethane (50 mL) was added to the reaction mixture with vigorous stirring, and the mixture allowed to come to room temperature. Stirring was continued for 12 hours. After this period, the reaction mixture was shaken with saturated sodium hydrogen carbonate solution and then with water. The organic layer was dried over

anhydrous sodium sulfate and solvent was evaporated. The residue obtained was purified on silica gel column using solvent A as an eluent and obtained pure compound (3) (2.0 g) in 83% yield. This was also verified by TCL, MS, and proton and ^{13}C NMR.

2) 1-(β -L-fucopyranosyl)-5-fluorouracil (4)

A solution of (3) (1 g, 2.5 mmol) in methanolic sodium methoxide (10 mL, 0.05M) was stored at room temperature for 2 days leading to direct crystallization of compound (4) (654 mg) in 94% yield. Chemical synthesis, characterization and analysis were done by V.J.Somayaji (Somayaji, 1989).

ii) RADIOLABELLED FUF SYNTHESIS

Radiolabelled FUF was also synthesized with the products possessing a different radiolabel on a major component of the molecule. One product possessing a ^3H radiolabel located on the base portion of FUF and the other having a ^{14}C radiolabel on the sugar portion. The synthesis procedures for the radiolabelled compound was the same as the procedure for the cold synthesis. The only variation was in that of the corresponding starting materials.

1) ^{14}C Labelled FUF

The starting materials for L-[1- ^{14}C]fucosyl-5-fluorouracil included a ^{14}C at the 1' position, L-[^{14}C]fucose (0.149mg, 50 mCi, 55 mCi/mmol), obtained from Amersham Canada Limited, Oakville, Ontario.

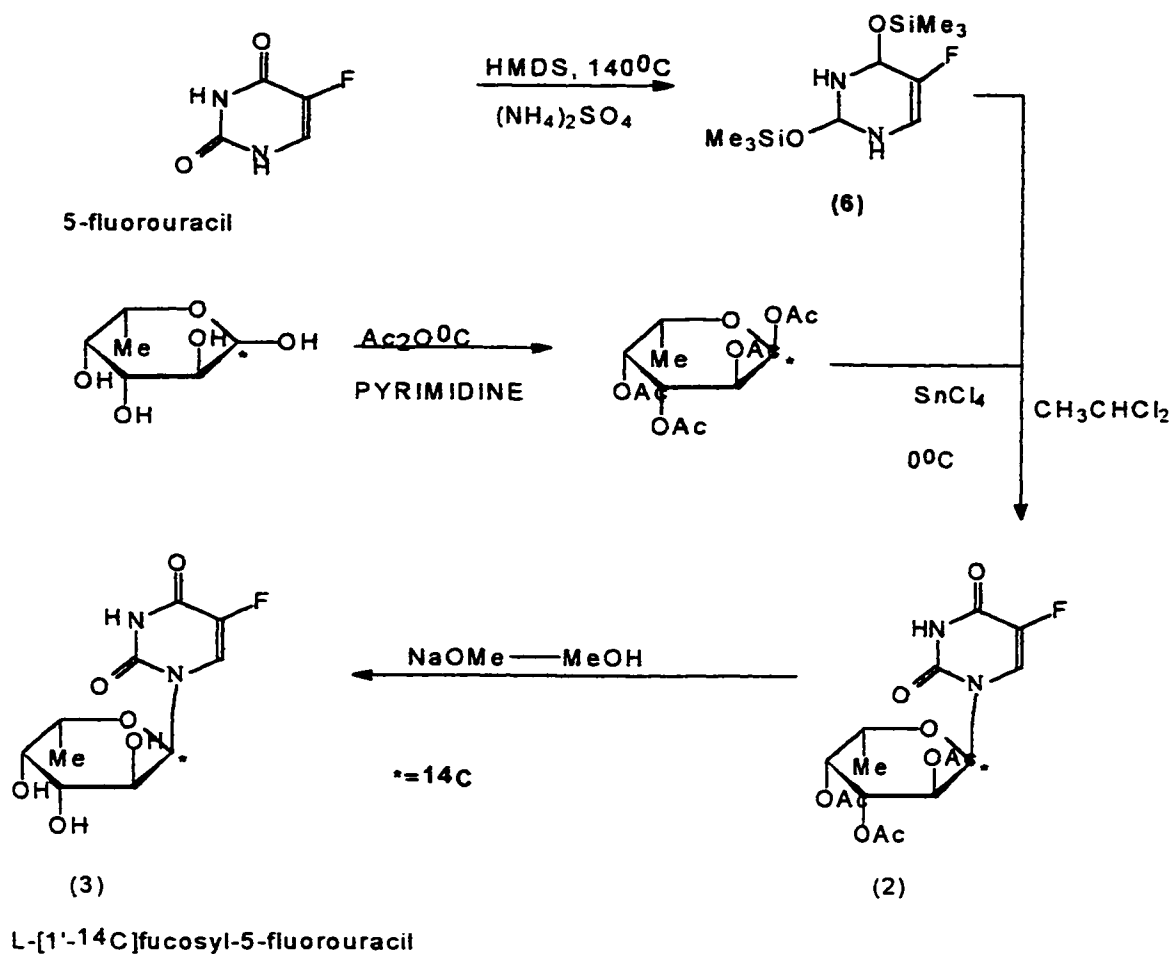


Figure 43 Synthesis of radiolabelled L-[1-¹⁴C]fucosyl-5-fluorouracil

This was mixed with 0.6 mg of cold L-fucose as part of the regular starting materials. The specific activity was decreased to 10.94 mCi/mmol. After the acetylation step 25 mCi of peracetylated L-[1'-¹⁴C]fucose (1) was obtained.

Using the labelled material, following the FUF synthesis procedure (figure 43), a ¹⁴C labelled product was obtained. The total activity of the product was determined to be 15.8 mCi with a specific activity of 10.38 mCi/mmol.

2) Tritium Labelled FUF

The same synthesis procedure as for cold FUF synthesis was followed with the exception of the 5FU starting material. In this case, 5FU (2.63 mg) is mixed with radiolabelled 5FU (1 mCi, 0.0066 mg, of 5-fluoro-[6-³H]-uracil) for a specific activity of 20 Ci/mmol, resulting in a starting material mixture of 5FU with a specific activity of 50 mCi/mmol.

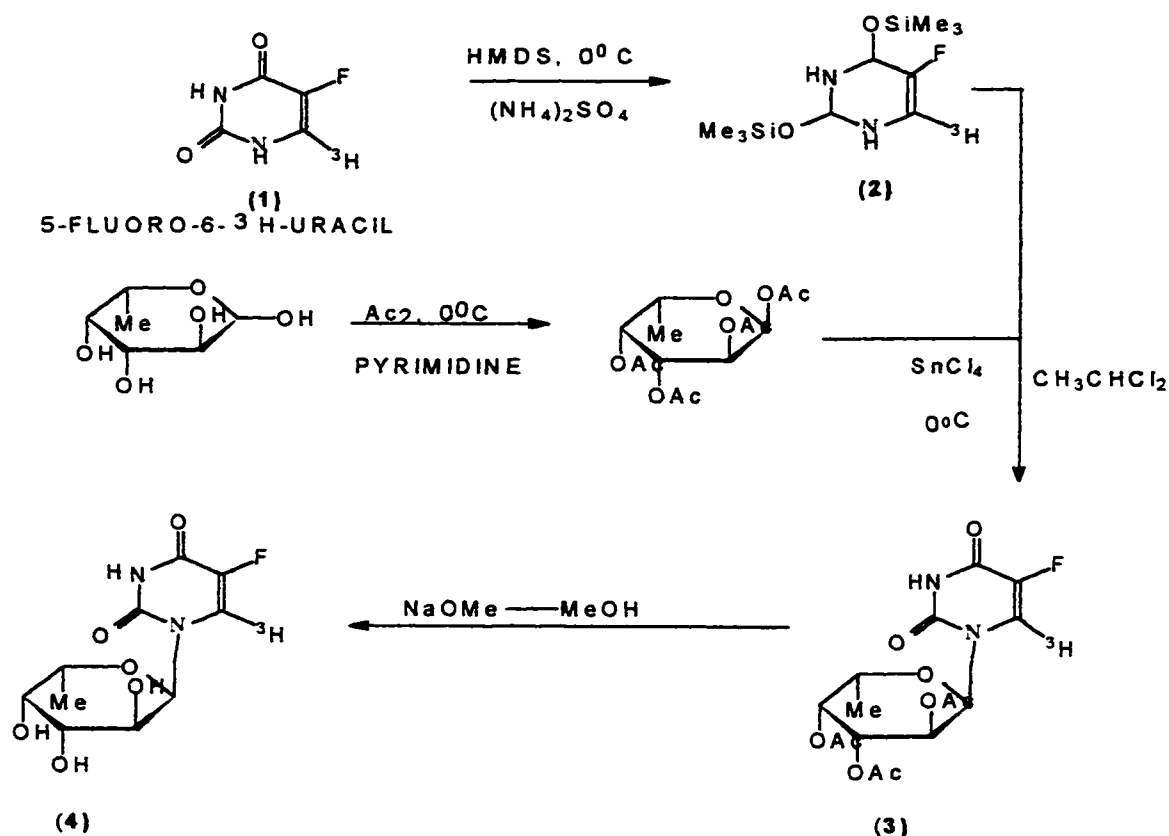


Figure 44 Synthesis of tritium labelled FUF

After drying the sample it was mixed with hexamethyldisilazane (1 mL) and 0.1 mg of ammonium sulfate and refluxed for 2 hours under nitrogen atmosphere. This produced the desired radiolabelled substrate, 2,4-bis(trimethylsiloxy)-5-fluoro-[6-³H]-uracil (2), that was then used in the same procedure as in the cold synthesis (see figure 44).

After reacting with the tetrahydrofucose, the mixture was washed and the organic phase was dried over anhydrous sodium sulfate and solvent evaporated under vacuum. The activity of the organic layer was 500 mCi, with the aqueous phase having an activity of 450 mCi. After purifying via TLC the pure product obtained (**3**) had an activity of 450 mCi. This product had an RF value of 0.19, under the same TLC conditions to that of the cold compound.

Product **3** was then deblocked via the same procedure as in the cold synthesis to obtain compound (**4**). After filtration and concentration, 2.45 mg of product **4** were obtained.

C) *APPENDIX 3* *DISTRIBUTION RESULTS*

i) *NAA STANDARD DATA RESULTS*

a) *Fluorine*

Table 6 Fluorine Standard Curve Data. Relating activity observed over time at 1634 keV for half and full geometry samples of incremental fluorine (μ F) mass samples.

μ g Fluorine	Counts HALF Geometry	Counts FULL Geometry
2	0	26
2	0	23
2	0	0
4	47	0
4	30	0
4	38	0
8	63	75
8	62	87
8	62	54
16	115	237
16	172	136
16	143	79
32	302	230

32	314	246
32	311	313
114		917
124		727
128	426	581
128	395	720
128	415	1095
197		1384
197		2036
197		1710
200		1821
256	1361	1367
256	1415	1080
256	1136	1305

b) Sodium

Table 7 Sodium Standard Curve Data. Relating activity observed at 1634 keV and 1368 keV for half and full geometry samples of incremental μ g of sodium over time.

μ g Na HALF	Counts 1634	Counts 1368	μ g Na FULL	Counts 1634	Counts 1368
180	21	39	180	0	28
360	0	71	180	0	39
360	20	64	360	0	33
360	57	59			
720	45	105	720	0	94
720	0	114			
720	0	122			
1440	0	349	1400	0	213
1440	58	191	1400	0	172
1440	81	184	1400	0	196
2000	114	323	2000	99	283

4000	184	635	4000	225	606
16000	598	1933	16000	596	1616
20000	321	2170	20000	573	1911

ii) 5FU ANIMAL DATA RESULTS

a) Liver

Table 8 Liver Results For 5FU. Counts at 1634 & 1368 keV, along with the liver mass, combined with known parameters is used to determine 5FU distribution to the liver expressed as % injected dose over time.

Minutes	Mouse g	Liver mg	Counts 1634	Counts 1368	% Injected Dose
30	22	1037	270	0	14.9
30	24	1049	430	163	21.1
30	25	1127	507	0	29.1
60	23	1002	205	153	7.8
60	25	1250	242	96	11.2
60	24	764	197	283	4.7
120	23	1142	215	336	4.6
120	24	1002	303	0	4.6
120	25	954	192	266	4.7
240	24	1270	0	240	3.2
240	27	1258	214	181	7.6
240	26	1195	148	286	1.6
1440	27	1102	168	281	2.9
1440	27	1041	99	0	4.6
1440	27	1125	151	217	3.3

Table 9 Kidney Results For 5FU. Counts at 1634 & 1368 keV, along with the kidney mass, combined with known parameters is used to determine 5FU distribution to the kidney expressed as % injected dose over time.

Minutes	Mouse g	Kidney mg	Counts 1634	Counts 1368	% Inj. Dose
---------	---------	-----------	-------------	-------------	----------------

30	22	405	163	215	5.9
30	24	390	155	248	4.9
30	25	453	218	247	9.5
60	23	401	169	201	6.6
60	25	485	560	142	6.1
60	24	316	160	238	5.4
120	23	438	135	202	4.2
120	24	346	137	225	4.1
120	25	400	127	350	1.4
240	24	399	111	234	2.1
240	27	418	97	269	0.5
240	26	456	88	213	0.7
1440	27	399	97	0	0
1440	27	458	114	298	1.3
1440	27	444	119	260	2.2

Table 10 Tumor Results For 5FU. Counts at 1634 & 1368 keV, along with the tumor mass, when combined with known parameters is used to determine 5FU distribution to the tumor expressed as % injected dose over time.

Minutes	Tumor mg	Counts 1634	Counts 11368	% Injected Dose
30	187	61	88	0.5
	290	93	134	1.5
	373	80	217	0
60	223	71	96	0.9
	631	154	222	3.3
	191	142	112	4.9
120	84	54	96	0
	825	205	298	4.8
	130	77	170	0
240	986	282	452	6.3
	633	174	433	0.2
	494	147	219	2.9

1440	210			0
	563	225	397	3.9
	489	159	346	1.1

Table 11 GIT Results For 5FU. Counts at 1634 & 1368 keV, along with the GIT mass, combined with known parameters is used to determine 5FU distribution to the GIT expressed as % injected dose over time.

Minutes	GIT mg	Counts 1634	Counts 1368	% Injected Dose
30	440	119	237	5.2
	753	123	281	5.9
	573	117	231	7.2
60	662	0	0	0.2
	650	148	200	0
	253	67	127	0.4
120	327	57	100	0
	275	62	135	1.4
	517	80	275	0
240	600	112	241	1.3
	727	170	304	0
	620	0	254	0
1440	668			3.1
	815	0	401	1.2
	620	124	324	3.9

Table 12 TAIL Results For 5FU Counts at 1634 & 1368 keV, along with the tail mass, combined with known parameters, is used to determine 5FU deposition to the tail expressed as % injected dose over time.

Minutes	Tail mg	Counts 1643	Counts 1368	% Injected
---------	---------	-------------	-------------	------------

				Dose
30	572	456	0	30.1
	605	660	280	40.5
	612	644	415	37.3
60	594	588	338	34.5
	668	613	279	37.2
	576	314	209	16.9
120	630	566	282	33.8
	562	642	319	38.6
	615	648	365	38.1
240	614	617	301	37.5
	676	615	317	37.1
	677	519	328	34.9
1440	623			
	679	356	220	17.2
	654	832	275	52.8

Table 13 % Injected Dose Of 5FU Per Organ Counts at 1634 & 1368 keV, along with the organ mass involved, combined with known parameters, used to determine 5FU distribution expressed as % injected dose over time.

Minutes	LIVER	KIDNEY	TUMOR	GIT	TAIL
30	14.9	5.9	0.5	5.2	
	21.1	4.9	1.5	5.9	
	29.1	9.5	0	7.2	
60	7.8	6.6	0.9	0.2	
	11.2	6.1	3.3	0	
	4.7	5.4	4.9	0.4	
120	4.6	4.2	0	0	
	4.6	4.1	4.8	1.4	
	4.7	1.4	0	0	

240	3.2	2.1	6.3	1.3
	7.8	0.5	0.2	0
	1.6	0.7	2.9	0
1440	2.9	4.5	0	3.1
	4.6	1.3	3.9	1.2
	3.3	2.2	1.1	3.9

Table 14 5FU data corrected for tail, % injected dose per organ Counts at 1634 & 1368 keV, along with the organ mass involved, shown here, when combined with known parameters can be used to determine 5FU distribution expressed as % injected dose over time.

MINUTES	LIVER	KIDNEY	TUMOR	GIT
30	21.3	8.2	0.7	7.4
30	35.5	8.2	2.5	9.8
30	46.4	15.2	0	11.4
60	11.9	10.1	1.4	0.3
60	17.8	9.7	5.2	0
60	5.7	6.5	5.9	0.5
120	7	6.3	0	0
120	7.5	6.6	7.8	2.3
120	7.6	2.3	0	0
240	5.1	3.4	10.1	2.1
240	12.4	0.8	0.3	0
240	2.5	1.1	4.5	0
1440	4.5	6.9	0	4.8
1440	5.6	1.6	4.7	1.5
1440	7	4.7	2.3	8.3

5-FLUOROURACIL
% INJECTED DOSE Vs TIME

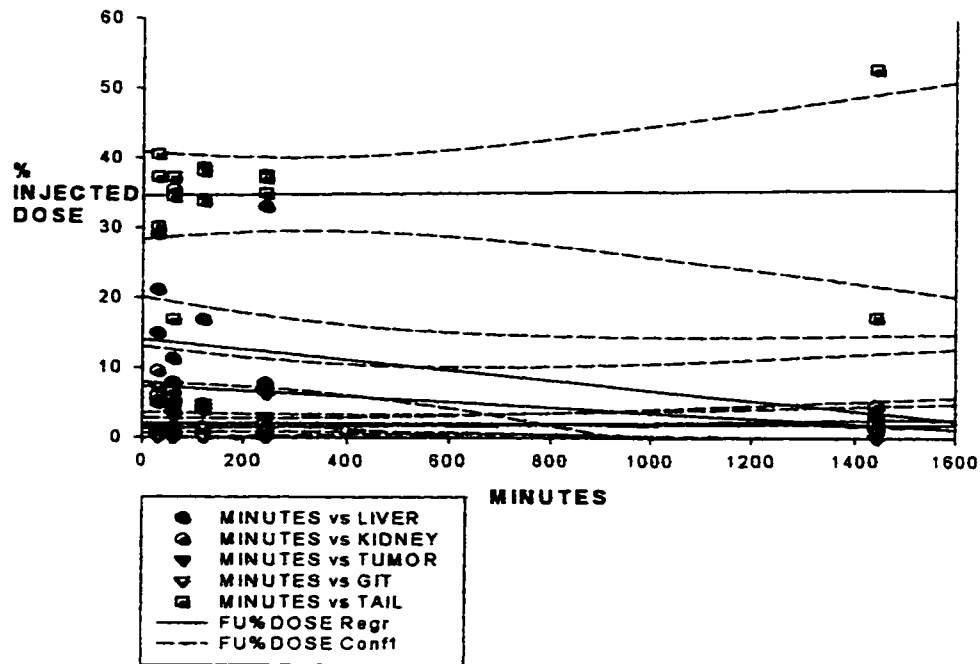


Figure 45 5-FU animal results expressed as % injected dose Vs time

iii) FUF NAA animal data results

Table 15 FUF NAA Animal Results For Tail Counts at 1634 & 1368 keV, along with the tail mass involved, shown here, when combined with known parameters can be used to determine FUF distribution to the tail expressed as % injected dose over time.

Minutes	Mouse g	Tail mg	Counts 1634	Counts 1368	% Injected Dose
30	29	649	346	283	18.1
	32	637	649	387	36.1
	28	606	320	277	16.3
60	30	614	597	352	34.9
	30	632	658	247	40.1
	28	651	826	329	51.6

120	28	601	762	495	44.5
	28	620	804	273	50.9
	32	650	888	385	55.2
240	32	637	535	186	32.9
	32	687	396	257	21.9
	32	684	489	302	28.7
2880	32	649	281	300	13.1
	29	650	600	137	38.4
	31	640	326	182	18.1

Table 16 FUF NAA Results For Liver Counts at 1634 & 1368 keV, along with the liver mass involved, shown here, when combined with known parameters can be used to determine FUF distribution to the liver expressed as % injected dose over time.

Minutes	Liver mg	Counts 1634	Counts 1368	% Injected Dose
30	1214	0	212	0
	1188	156	369	0.6
	871	0	311	0
60	1110	187	270	4.3
	1020	210	151	8.2
	980	0	245	0
120	983	0	183	0
	1224	0	315	0
	1130	131	260	1.2
240	1106	125	239	1.2
	1380	0	98	0
	1327	150	129	5.5
2880	1205	0	296	0
	1195	0	207	0
	1228	0	0	0

Table 17 NAA FUF GIT Data Counts at 1634 & 1368 keV, along with the GIT mass involved, shown here, when combined with known parameters can be used to determine FUF distribution to the GIT expressed as % injected dose over time.

Minutes	GIT mg	Counts 1634	Counts 1368	% Injected Dose
30	679	156	238	4.6
	317	84	262	3.6
	574	135	0	4.1
60	276	85	231	0
	258	86	172	0
	320	97	273	0.5
120	203	58	187	0
	430	115	290	1.4
	237	72	189	2.7
240	541	109	274	1.4
	543	61	183	0
	684	0	311	0
2880	679	134	272	2.9
	588	120	332	1.8
	673	135	216	3.2

Table 18 FUF NAA Tumor Data, Counts at 1634 & 1368 keV, along with the tumor mass involved, shown here, when combined with known parameters is used to determine FUF distribution to the tumor expressed as % injected dose over time.

Minutes	Tumor mg	Counts 1634	Counts 1368	% Injected Dose
30	428	83	152	0.5
	211	50	160	0
	383	116	286	0
60	375	148	333	0.7
	345	113	252	0.2
	313	108	284	0
120	477	109	335	0

	601	189	502	0
	788	232	455	3.2
240	599	0	404	0
	1177	134	365	0
	746	153	326	1.1
2880	606358	198	0	10.5
	582	64	272	0
		92	0	4.2

Table 19 FUF NAA Kidney Data. Counts at 1634 & 1368 keV, along with the kidney mass involved, shown here, when combined with known parameters used to determine FUF distribution to the kidney expressed as % injected dose over time.

Minutes	Kidney mg	Counts 1634	Counts 1368	% Injected Dose
30	474	143	277	3.6
	416			
	372	0	214	0
60	313	121	298	1.8
	330	551	206	33.8
	377	110	266	1.5
120	351	85	190	0.9
	368	111	290	1.2
	438			
240	407	83	262	0
	507	97	268	0.5
	519	335	305	16.9
2880	494	127	284	2.4
	461	0	293	0
	528	101	267	0.8

Table 20 FUF NAA Data Corrected For Tail Loss, % Injected Dose Per Organ Vs Time

Minutes	Liver	Kidney	Tumor	GIT
30	0	4.4	0.6	5.6
	0.9	0	0	5.8
	0	0	0	4.9
60	6.6	2.8	1.1	0
	13.9	57.3	0.3	0
	0	3.1	0	1
120	0	1.4	0	0
	0	2.4	0	2.8
	2.7	0	7.1	6
240	1.8	0	0	2.1
	0	0.6	0	0
	7.7	23.8	1.6	0
2880	0	2.8	12.2	3.3
	0	0	0	2.9
	0	0.9	5.1	3.9

iv) DUAL LABELLED ANIMAL STUDY RESULTS

Table 21 Dual Label Liver results. With % injected dose of ^3H representing fucosyl-5-fluoro-[6- ^3H]-uracil ($^3\text{HFUF}$) distribution to the liver over time. In addition, % injected dose ^{14}C representing [1'- ^{14}C]fucosyl-5-fluorouracil ($^{14}\text{CFUF}$) or the fucose portion of the molecule, to the liver over time.

Minutes	% Injected Dose ^3H	% Injected Dose ^{14}C
15	16.7	2.5
	35.8	0.1
	74.2	5.4
30	3.4	1.7
	60.5	6.3
	15.6	4

Table 22 Dual Label FUF Tumor results. With % injected dose of ^3H representing fucosyl-5-fluoro-[6- ^3H]-uracil ($^3\text{HFUF}$) distribution to the tumor over time. In addition, % injected dose ^{14}C representing [1'- ^{14}C]fucosyl-5-fluorouracil ($^{14}\text{CFUF}$) or the fucose portion of the molecule, to the tumor over time.

Minutes	% Injected Dose ^3H	% Injected Dose ^{14}C
15	13.7	4.4
	8.6	4.4
	7.4	3.7
30	2.9	2.5
	10.9	4.3
	4.9	2.4

Table 23 Dual Label FUF kidney results. With % injected dose of ^3H representing fucosyl-5-fluoro-[6- ^3H]-uracil ($^3\text{HFUF}$) distribution to the kidney over time. In addition, % injected dose ^{14}C representing [1'- ^{14}C]fucosyl-5-fluorouracil ($^{14}\text{CFUF}$) or the fucose portion of the molecule, to the kidney over time.

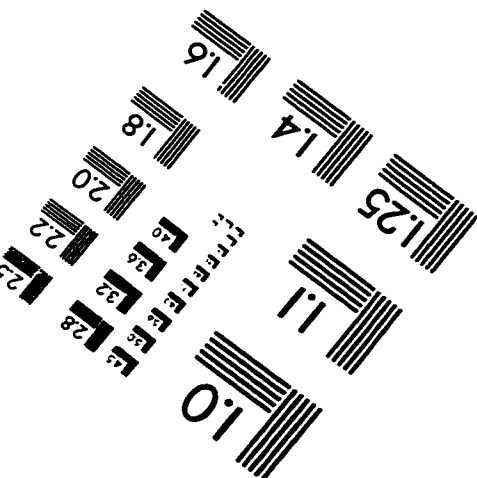
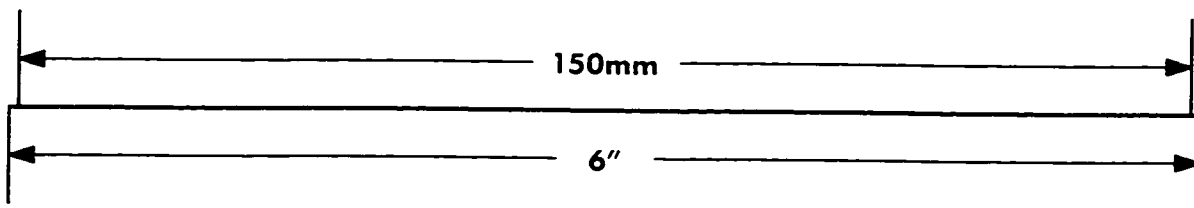
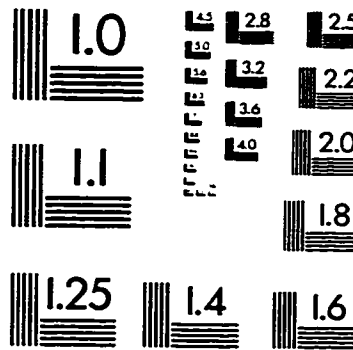
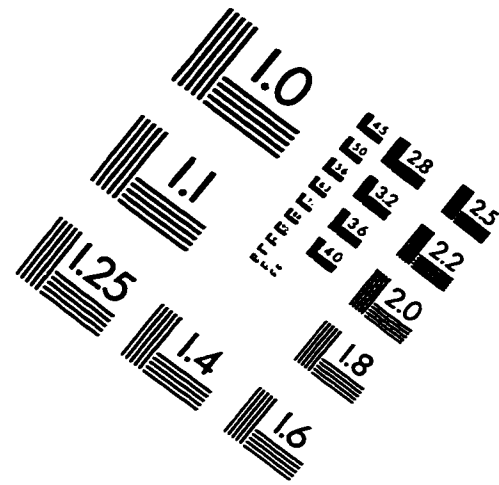
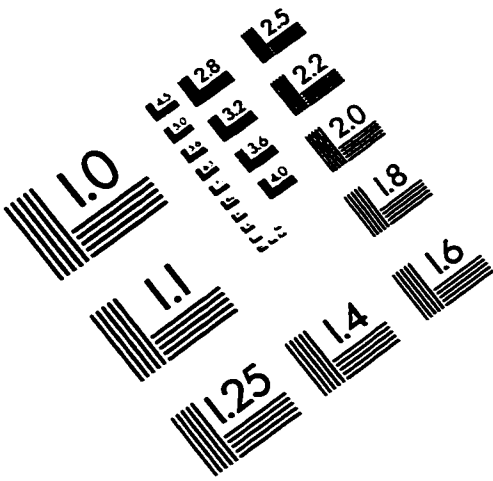
Minutes	% Injected Dose ^3H	% Injected Dose ^{14}C
15	34.7	34.1
	35.5	0
	29.8	0.1
30	14.8	6.1
	29.7	6.3
	42.1	9.2

Table 24 Dual Label Blood results. With % injected dose of ^3H representing fucosyl-5-fluoro-[6- ^3H]-uracil ($^3\text{HFUF}$) distribution in blood liver over time. In addition, % injected dose ^{14}C representing [1'- ^{14}C]fucosyl-5-fluorouracil ($^{14}\text{CFUF}$) or the fucose portion of the molecule, in blood over time

Minutes	% Injected Dose ^3H	% Injected Dose ^{14}C
---------	------------------------------	---------------------------------

15	0.9	2.2
	0.1	1.8
	0.4	0.1
30	0.9	1.1
	0.4	0.9
	0.3	0
60	0.5	0.4

IMAGE EVALUATION TEST TARGET (QA-3)



APPLIED IMAGE, Inc
1653 East Main Street
Rochester, NY 14609 USA
Phone: 716/482-0300
Fax: 716/288-5989

© 1993, Applied Image, Inc., All Rights Reserved

